Evaluating the Role of the COP9 Signalosome and Neddylation during Cytokinesis and in Response to DNA Damage

by

Dudley Chung

Submitted in partial fulfilment of the requirements
for the degree of Doctor of Philosophy

at

Dalhousie University
Halifax, Nova Scotia
December 2018

TABLE OF CONTENTS

LIST OF TABLES

LIST OF FIGURES

ABSTRACT

The covalent attachment of the ubiquitin-like protein NEDD8 via lysine residues on target proteins, termed neddylation, regulates the activity and stability of numerous proteins, particularly through regulating the activity of a key family of cellular enzymes known as the cullin E3 ubiquitin ligases. Neddylation is implicated in cell cycle regulation and DNA repair; however, the exact role and mechanism(s) are unclear. Here, two neddylation-regulated processes were investigated: control of cell division and response to DNA damage. The role of neddylation in cell division was evaluated using the neddylation inhibitor MLN4924, and by monitoring the localization of NEDD8, the subunits of the deneddylase COP9 signalosome (CSN) and cullin proteins during mitosis. Human HeLa cervical cancer cells treated with MLN4924 exhibited delayed physical separation of the daughter cells (abscission) and resulted in the appearance of multinucleated cells. Furthermore, treatment of mitotic cells with MLN4924 resulted in the earlier accumulation of the cytokinesis protein MKLP1 to the midbody. These results could provide a possible explanation for the ability of MLN4924 to increase the proportion of cells with >4N DNA content. The role of neddylation in response to DNA damage, induced by ultraviolet laser irradiation, was investigated using live-cell microscopy of DNA repair factors and CSN subunits. Laser-induced DNA damage in human U-2 OS osteosarcoma cells expressing fluorescently-tagged CSN3 and CSN4 subunits indicated that these CSN subunits accumulated in the nucleus following DNA damage, consistent with a possible role in the DNA damage response (DDR). Collectively, these findings indicate that neddylation and the CSN are linked to cytokinesis and the DDR.

LIST OF ABBREVIATIONS USED

a.u.	arbitrary units
AMP	adenosine monophosphate
APC/C	anaphase-promoting complex/cyclosome
ATM	ataxia telangiectasia mutated
ATP	adenosine triphosphate
bp	base pair
CDK	cyclin-dependent kinase
CDT1	chromatin licensing and DNA replication factor 1
cDNA	complementary DNA
CKI	cyclin-dependent kinase inhibitor
COP9	constitutive photomorphogenesis 9
CPC	chromosomal passenger complex
CRL	cullin-RING (ubiquitin) ligase
CSN	COP9 signalosome
Cul	cullin
DAPI	4',6-diamidino-2-phenylindole
DCUN1D	defective in cullin neddylation 1 domain
DDR	DNA damage response
DEN1	deneddylating enzyme 1
DIC	differential interference contrast
DMEM	Dulbecco's Modified Eagle Medium
DMSO	dimethyl sulfoxide
DNA	deoxyribonucleic acid
DSB	double-strand break
dsDNA	double-stranded DNA
EGFP	enhanced GFP
FBS	fetal bovine serum
FRAP	fluorescence recovery after photobleaching
FSC	forward scatter
GFP	green fluorescent protein
HDR	homology-directed repair
IR	ionizing radiation
iRFP	near-infrared red fluorescent protein
kDa	kilodalton
MKLP1	mitotic kinesin-like protein 1
MMEJ	microhomology-mediated end-joining
MPN	MPR1-PAD1-amino terminal
NA	numerical aperture
NAE	NEDD8 E1 activating enzyme
NEDD8	neural-precursor-cell-expressed, developmentally down-regulated 8
NHEJ	non-homologous end-joining
PCI	proteasome, COP9, initiation factor
PFA	paraformaldehyde

PI	propidium iodide
PPi	pyrophosphate
PTM	post-translational modification
RBX	RING box protein
RING	really interesting new gene
SCF	SKP-cullin-F-box
siRNA	small interfering ribonucleic acid
SKP	S-phase kinase-associated protein
SSA	single-strand annealing
SSC	side scatter
ssDNA	single-stranded DNA
STUbL	SUMO-targeted ubiquitin ligase
SUMO	small ubiquitin-like modifier
Ub	ubiquitin
UBE2F	ubiquitin-conjugating enzyme E2F
Ubl	ubiquitin-like
UV	ultraviolet
vs	versus

ACKNOWLEDGEMENTS

First, I would like to thank my supervisor, Dr. Graham Dellaire, for providing me the opportunity to train under his supervision. Not only was his guidance important to further developing my research capabilities, his enthusiasm in research meant that I was exposed to new ideas and techniques, and I was able to incorporate them in my work.

Second, I would also like to thank the members of my supervisory committee: Dr. Melanie Dobson, Dr. James Fawcett, and Dr. Paola Marcato. I appreciated their constructive feedback, which helped shape this project.

Third, I would like to acknowledge everyone in the Dellaire Lab, past and present, for all their help and advice.

Fourth, I would like to extend thanks to members of the Department of Pathology as well as to the Flow Cytometry Facility for helping when needed and for providing the opportunity and training to use their equipment.

Last, I would like to thank my family and friends for their support from beginning to end.

CHAPTER 1 INTRODUCTION

This chapter contains material originally published in:

Biomolecules, Vol 5(4), Chung D and Dellaire G, "The Role of the COP9 Signalosome and Neddylation in DNA Damage Signaling and Repair", 2388-2416, 2015. [1].

1.0 Introduction

The post-translational modification by a ubiquitin-like protein called NEDD8 via a process called neddylation, and removal of the NEDD8 modification by the protein complex COP9 signalosome (CSN) (deneddylation), can regulate multiple cellular processes. In this thesis, the roles of neddylation and the CSN in cell division, DNA damage response and DNA double-strand break repair are investigated. To understand the potential links between these processes, this chapter begins with an introduction to the ubiquitin-like proteins, NEDD8, the deneddylase CSN, and the neddylation pathway. The stages of the cell cycle, the events in mitosis, and cell cycle regulation are briefly reviewed, followed by an introduction to the DNA damage response (DDR), DNA repair of double-strand breaks, and its regulation. Notably, the position of the cell in the cell cycle can influence how DNA damage is repaired, and the presence of DNA damage can influence progression through the cell cycle; this inter-communication is regulated by neddylation and the CSN.

1.1 Post-translational Modification by Ubiquitin and Ubiquitin-like Proteins

The functional capability of eukaryotic proteins can be expanded beyond their amino acid composition by undergoing a form of chemical modification termed a post-translational modification (PTM). Different types of PTMs have been identified, from the attachment of small chemical groups and peptides, to structural modifications as a result of protease-mediated cleavage. One family of protein modifiers are the ubiquitin-like proteins (Ubls). Members of this family share structural similarity (β-grasp fold) and sequence similarity to the most characterised member, ubiquitin. Ubiquitin (Ub) is a 76 amino acid protein that primarily regulates protein function and degradation via different forms of mono- and polyubiquitylation [2]. For example, polyubiquitylation on the ubiquitin residue K43 is known to target proteins for degradation [3]. Polyubiquitylation of the ubiquitin lysine residue K11 (e.g. ubiquitylation during mitosis by the anaphase promoting complex/cyclosome (APC/C) ubiquitin ligase on the cell cycle regulator cyclin B [4] have also been implicated as a proteolytic signal, while other residues such as K63 are known for promoting protein recruitment [3]. Monoubiquitylation of substrates regulates cellular pathways as opposed to promoting protein degradation. For instance, upon DNA damage resulting in DNA inter-strand crosslinks, proper repair is facilitated by monoubiquitylation of Fanconi Anemia pathway proteins FANCD2 and FANCI [5].

The covalent attachment of ubiquitin is mediated by three types of enzymes: E1, E2, and E3. The Ub-activating enzyme (E1) and the Ub-conjugating enzyme (E2) prepare ubiquitin for conjugation onto substrates, while the Ub ligase (E3) recognizes specific protein substrates and allow the transfer of activated ubiquitin from the E2 onto substrates by covalently attaching the C-terminal glycine on ubiquitin to a lysine residue

on the substrate, or to lysines present in ubiquitin during ubiquitin chain formation [6]. The Ubl proteins use similar enzymatic mechanisms to covalently modify target substrates [7]. Ubls identified in eukaryotes include SUMO (Small ubiquitin-like modifier), ISG15, ATG8, and the focus of this study, NEDD8 (Neural-precursor-cell-expressed, Developmentally Down-regulated 8) (discussed in Section 1.2) [8].

1.2 Neddylation: An Overview

Neddylation is a form of reversible post-translational modification whereby the ubiquitin-like protein NEDD8 is conjugated to lysine residues in the target protein. Expression of the NEDD8 gene was initially identified to be downregulated during mouse brain development [9], and encodes an 81-amino acid protein that shows 60% identity and 80% similarity to ubiquitin [10, 11]. NEDD8 is also the Ubl with the highest structural similarity to ubiquitin [12].

1.2.1 The Neddylation Cascade: E1 and E2s

The neddylation pathway consists of E1, E2, and E3 enzymes, analogous to the ubiquitylation pathway (Figure 1.2.1). Precursor NEDD8 is processed at the C-terminal end (Gly76) to its mature form by deneddylating enzyme 1 (DEN1), also known as NEDP1 or SENP8 [13, 14, 15], and by ubiquitin C-terminal hydrolase isozyme 3 (UCHL3) [16]. Mature NEDD8, with its C-terminal glycine-glycine motif, is conjugated to the NEDD8 E1 activating enzyme (NAE), a heterodimer composed of amyloid-β precursor protein binding protein 1 (APPBP1, alternatively named NAE1) and ubiquitin-activating enzyme 3 (UBA3) [17, 18]. NAE then transfers NEDD8 to an E2, which in

metazoans are the ubiquitin-conjugating enzyme E2F (UBE2F) and ubiquitin-conjugating enzyme E2M (UBE2M, also known as UBC12) [19, 20]. UBE2F or UBE2M, with assistance from an E3, then transfers the NEDD8 onto the lysine of the target substrate.

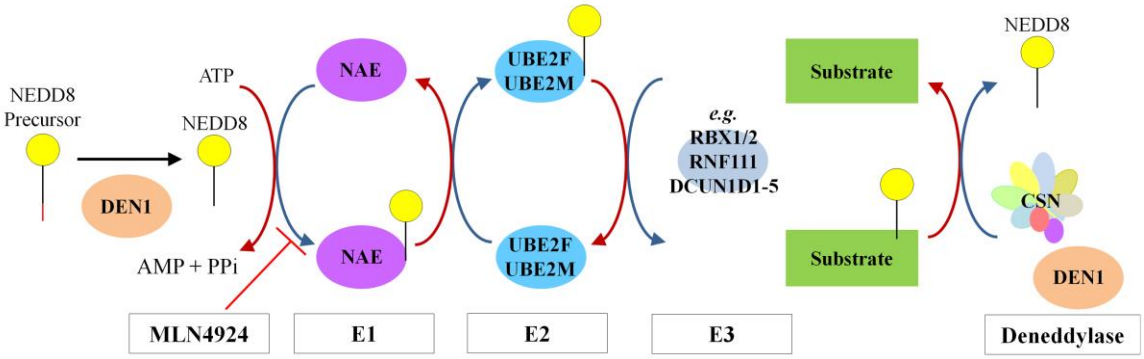

Figure 1.2.1. The neddylation cascade. A schematic representation of the main proteins in the neddylation cascade. Precursor NEDD8 is processed at the C-terminus to the activated form by DEN1. NEDD8 is conjugated to a lysine side chain of the target substrate through an E1 (NAE), and E2 (UBE2F or UBE2M), and an E3 (shown are RBX1/2, RNF111 and DCUN1D members). Deneddylation is achieved by the CSN or DEN1. The small molecule MLN4924 inhibits NAE, blocking the cascade.

1.2.2 The Neddylation Cascade: E3

Only a few E3s have been described to aid in neddylating targets [21]. RING box protein 1 (RBX1, also known as ROC1) interacting with UBE2M, and RBX2 (also known as ROC2 or RNF7) interacting with UBE2F, are E3s that target cullin-RING ubiquitin ligases for neddylation [22, 23, 24, 25]. Neddylation E3 activity has also been described for RING finger protein 111 (RNF111-Arkadia) [26], and defective-in-cullin neddylation-1-domain (DCUN1D)-containing proteins DCUN1D1-DCUN1D5 (SCCRO1-SCCRO5) [27, 28, 29, 30, 31]. While DCUN1D1 is not essential for neddylation *in vitro* [32], DCUN1D1 knockouts are lethal in yeast and *Caenorhabditis elegans* [28]. However, this is not the case in mice, possibly due to compensation by

other DCUN1D members [33]. Although it has been assumed that the DCUN1D proteins play similar roles in promoting neddylation, the case is not so clear for DCUN1D3 (SCCRO3). In one study, DCUN1D3 was shown to interact with UBE2M and promote cullin neddylation [30]. However, a later study found that DCUN1D3 does not have E3 activity and can inhibit DCUN1D1-mediated neddylation [33]. Additional proteins that exhibit NEDD8 E3 activity include murine double minute 2 (MDM2) [34], c-CBL [35, 36], yeast Tfb3 [37], tripartite motif containing 40 (TRIM40) [38], and SMAD-specific E3 ubiquitin protein ligase 1 (SMURF1) [39].

1.2.3 NEDD8 Deconjugating Proteins

Like ubiquitin and deubiquitylating enzymes, NEDD8 has a limited set of deneddylating enzymes that remove NEDD8 proteins from neddylated substrates by cleaving the isopeptide bond between the terminal glycine on NEDD8 and the ε-amino group of the lysine residue on the substrate protein [40]. They include deneddylating enzyme 1 (DEN1, also known as NEDP1 or SENP8), and the COP9 signalosome (CSN) (See Section 1.2.4). Although both CSN and DEN1 can theoretically deneddylate a given protein substrate, they in fact do not have extensively-overlapping protein targets [13, 41, 42]. DEN1 is more efficient in deconjugating hyperneddylated cullins to a mono-neddylated form *in vitro*, and DEN1 can deconjugate NEDD8 from non-cullin proteins *in vivo* in plants and humans [15, 43]. However, at least in plants, the CSN was found to be restricted to deconjugating mono-NEDD8 and did not appear to be efficient in processing precursor NEDD8 [15]. Furthermore, recent evidence suggests that the CSN can regulate human DEN1 and *Aspergillus nidulans* homolog DenA protein levels, but the exact

regulatory mechanism remains unknown [44]. Other deneddylases and their targets remain to be uncovered and fully characterized, for example ataxin-3, which *in vitro* data suggests has deneddylase activity [45].

1.2.4 The COP9 Signalosome

The COP9 Signalosome (CSN) is a multi-subunit protein complex that was identified in the 1990s in Arabidopsis as a repressor of photomorphogenesis [46], and was later found conserved in other unicellular and multicellular eukaryotes [47, 48, 49, 50, 51, 52]. In eukaryotes that have simpler CSN complexes such as yeast, several subunit deletions are viable [53, 54, 55]. However, null deletions in other organisms are lethal early in development [56, 57, 58], and conditional CSN5 knockouts in mouse livers show abnormal liver development and regeneration [59], suggesting an increase in functional complexity as the CSN evolved. The CSN deneddylates substrates, a key target being the cullin-RING E3 ubiquitin ligases (CRLs) in the ubiquitin proteasome pathway [22, 60]. In addition, early attempts to biochemically isolate and characterize the CSN protein complex found it promoted kinase activity [47], which the molecule curcumin was able to inhibit [61]. Later studies identified the kinases that interact with the CSN to impart the complex with associated kinase activity. Examples include protein kinase CK2 [62, 63], protein kinase D (PKD) [62], protein kinase B-Akt (Akt) [63], ataxia telangiectasia mutated (ATM) [64], and inositol 1,3,4-triphosphate 5/6 kinase [65]. These kinases modify the stability of ubiquitin-mediated proteasomal substrates.

1.2.5 COP9 Signalosome Architecture and Expression

The mammalian CSN holoenzyme consists of eight subunits (CSN1 to CSN8) [47, 49]. Six of the eight subunits (CSN1-4, and CSN7-8) contain a PCI (proteasome, COP9, initiation factor) domain, a feature shared with subunits of both the 19S proteasome regulatory complex and eIF3 (eukaryotic initiation factor 3) complex, suggesting a common evolutionary origin [61, 66]. Furthermore, studies suggest these complexes can interact with one another [49, 66, 67, 68]. CSN5, which is also called Jun activation domain-binding protein-1 (Jab1) [69], and CSN6 both contain an MPN (MPR1-PAD1-amino terminal) domain [41]. Unlike CSN6, the MPN domain in CSN5 contains a Zn^{2+} binding JAMM (JAB1/MPN/Mov34) motif, thus making it the sole catalytically active subunit in the CSN [55]. The metalloprotease JAMM/MPN motif possesses the His-x-His-x_{10}-Asp consensus sequence (where x indicates any amino acid residue) accompanied by a conserved glutamic acid upstream [41]. In addition, mammals express two forms of CSN7 (CSN7A and CSN7B) and CSN complexes likely contain either one or the other of these two isoforms [70].

Recent investigation of the individual subunits and of the CSN holoenzyme have provided new details to its organization [71, 72, 73, 74, 75, 76, 77] (Figure 1.2.5). Current understanding is that the winged-helix domains of the PCI domains (PCI ring) of CSN1-4 and CSN7-CSN8 are arranged as an open ring such that the N-terminal helical repeat domains of these subunits radiate out from it while the C-terminal helical tails form a bundle that anchors the complex [74, 76, 77, 78]. The MPN domains of the CSN5-CSN6 heterodimer rest on the helical bundle while their C-terminal helical tails are inserted into the helical bundle. Integration of CSN5 into the complex is abrogated by the

absence of CSN6, but deleting CSN1, 2, 4, or 7 can also disfavour CSN5 integration [77]. CSN4 and CSN6 appear to be the most important for stabilizing CSN5 and converting CSN5 into its active state, which was recently found to involve rearrangement within CSN5 to open the NEDD8-binding pocket [56, 77, 79], but full enzymatic activity *in vitro* requires the complete set of subunits [72]. The peripheral association of CSN5 with the complex is dynamic since free/monomeric CSN5 has been found in different organisms. However, evidence suggests that free CSN5 is essentially catalytically inactive [41, 56, 72, 79, 80, 81, 82]. Nonetheless, one cannot rule out any yet-to-be identified non-catalytic role for free CSN5 in the cell.

The CSN is catalytically active in both nuclear and cytoplasmic fractions [83, 84, 85, 86, 87]. Additionally, a small fraction of CSN is bound to chromatin [80, 88]. The CSN can be post-translationally modified, and indeed several subunits contain phosphorylation sites [61, 64, 80, 89, 90, 91, 92, 93, 94]. As a consequence, different cellular compartments can harbour different post-translationally modified forms of CSN, and much work remains to understand the regulation of CSN subunits through their phosphorylation [80].

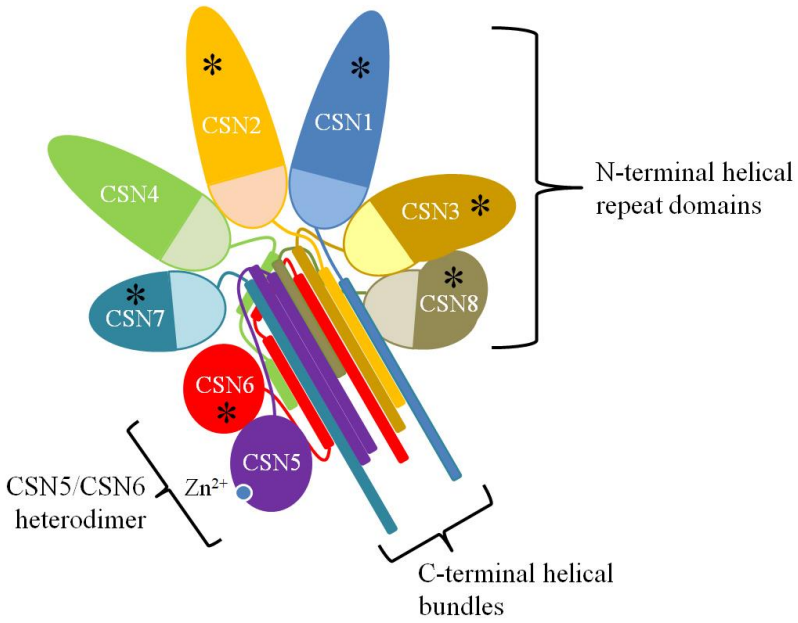

Figure 1.2.5. The CSN structure. A two-dimensional schematic representation of the three-dimensional structure of the CSN as determined by Lingaraju *et al.* [77]. The N-terminal repeat domains radiate out from the winged-helix domains of the PCI ring (lightly shaded half-circles). The C-terminal helical regions form a helical bundle that stabilizes the complex. The MPN domains of CSN5 and CSN6 rest on the helical bundle. Subunits reported as phosphorylation targets are marked with an asterisk (*).

1.3 Neddylation Targets: An Overview

Several neddylation substrates have been reported, but to varying degrees of characterization (Appendix I). Validation is a challenge since overexpression of exogenous NEDD8 can induce NEDD8 conjugation via ubiquitin ligases [95], and therefore alternate approaches such as deconjugation-resistant NEDD8 are being developed [96]. The most characterized group of neddylated substrates are the cullin-RING ubiquitin ligases, described in more detail below.

1.3.1 The Cullin-RING Ubiquitin Ligase: An Overview

Most proteins in the cell are targeted by different families of ubiquitin ligases that each can recognize different substrates. The multi-subunit cullin-RING ubiquitin ligases (CRLs) comprise the largest class of ligases [22]. The basic structure of the CRL is a heterodimer of a cullin protein and the RING-finger protein, the former bringing the substrate and substrate-specific adaptors in close proximity to the ubiquitin-carrying E2 protein which is recruited by the latter, therefore facilitating the transfer of ubiquitin onto the lysine residue on the target (Figure 1.3.1). CRLs are classed based on the cullin scaffold protein (CUL1-5, and CUL7), and specificity is defined by the cullin and a multitude of substrate adaptor proteins [22, 97]. All cullin groups described here are reportedly modified by NEDD8 [98, 99].

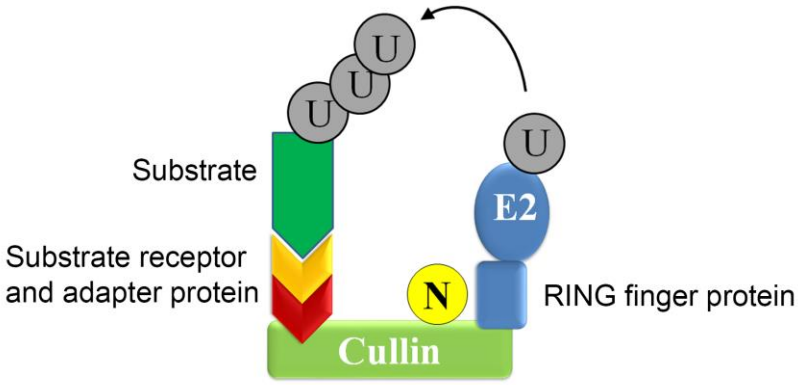

Figure 1.3.1. Schematic of a cullin-RING E3 ubiquitin ligase (CRL) ubiquitylating a substrate. The core structure of a CRL consists of the cullin protein and the RING finger protein. This heterodimer brings the substrate and substrate-specific adaptors to the ubiquitin-carrying E2 protein, which transfers ubiquitin (U) onto lysine residues in the target. NEDD8 (N) stabilizes the active conformation of CRLs.

1.3.2 Regulation of Cullin-RING Ubiquitin Ligases by Neddylation and De-neddylation

One of the known regulatory mechanisms that regulate CRL activity is through neddylation and CSN-mediated deneddylation. Activation of CRLs is understood to be through the covalent attachment of NEDD8 to cullins, which is mediated by RBX1 and DCUN1D1 members [24]. This causes a conformational change in the CRL architecture, promoting assembly, and enables substrate ubiquitylation [98]. For example, one study using $CUL5^{CTD}$-RBX1 found that neddylation led to a reorientation of the RING finger protein RBX1 [100]. Neddylation was shown to be critical for CRL ubiquitylation activity by using a drug called MLN4924 [101], a specific inhibitor of the neddylation E1 component APPBP1 (NAE1). This drug, which mimics the structure of AMP, forms an adduct with NEDD8 via NAE1 [102] (Figure 1.1.2), blocking the neddylation cascade. MLN4924 treatment led to a reduction in neddylated CRLs and CRL substrate accumulation in cells, demonstrating that neddylation strongly regulates CRL-mediated ubiquitylation and/or turnover of protein substrates [101].

The deneddylation of CRLs is achieved by the CSN, through its catalytic subunit CSN5. Initially the CSN holoenzyme was thought only transiently associate with the CRL to deneddylate cullins; however, a more complex picture of its role has begun to emerge. Structural analysis of the CSN-CRL association suggests that *in vitro* interaction with various cullins can further promote CSN5 activation [77, 103]. The deneddylated cullin is a substrate for the protein CAND1 (cullin-associated NEDD8-dissociated protein 1), which regulates CRL activity by sequestering deneddylated cullins [104, 105] (Figure 1.3.2 A). However, this interaction can be reversed depending on the levels of substrate

adaptor proteins. CAND1 regulation was shown to only affect deneddylated CRLs, since adding CAND1 to assembled CRLs containing neddylated cullin blocked substrate adaptor dissociation [106]. The current belief is that that CAND1 promotes exchange of the substrate adaptors to adapt to changing conditions in the cell [106, 107, 108, 109]. It should be noted that CAND1 does not associate to the same degree with the different cullin classes and may also display a preference to the exchange of particular substrate adaptors [107].

The CSN can also inhibit CRL activity independently of its deneddylase activity. The CSN can bind directly to CRLs and reduce ubiquitin ligase activity by sterically hindering interaction between the target substrate and the E2 (Figure 1.3.2 B) [103, 110]. It appears that this mode of regulation can be influenced by the levels of substrate, which can compete with the CSN for the cullin [103, 111]. This was evidenced in one study where there was a reduction of CSN-CRL association when preincubated CSN-CRL was placed in the presence of substrate [103, 110, 111]. Additionally, global mass spectrometry studies on the cullin proteins found that on average only 10-20% are associated with the CSN whereas the association with substrate adaptors was dominant, suggesting that substrate adaptor availability is important in regulating CRLs [79].

The CSN is able to associate with the cullin in both neddylated and unneddylated states. In a study focusing on the cullin 1 CRL, SCF-SKP2/CKS1, CSN2 and CSN4 appear to be important in the interaction with the cullin and RING finger protein, whereas the other subunits, such as CSN1 and CSN3, are oriented toward the substrate adaptors (Figure 1.3.2 C) [77, 103]. Association of the CSN to CRLs does not immediately lead to deneddylation. In a study that used o-ophenathroline to inhibit deneddylation after cell

lysis, up to half the CSN-associated cullins were also neddylated [107]. This may indicate that an additional signal is required to allow isopeptidase cleavage or that the CSN is inhibited by some unknown factor, such as a CRL architecture that disfavors CSN-mediated deneddylation.

In addition to direct deneddylation, and steric hindrance, the CSN can associate with the de-ubiquitylating enzyme USP15. For example, in the fission yeast *Schizosaccharomyces pombe*, the CSN associates with USP15 homolog Ubp12p [112] to inhibit ubiquitylation of substrates and autoubiquitylation of CRL components [113]. Therefore, it is thought that ubiquitylation takes place after the CSN is displaced from the CRL complex.

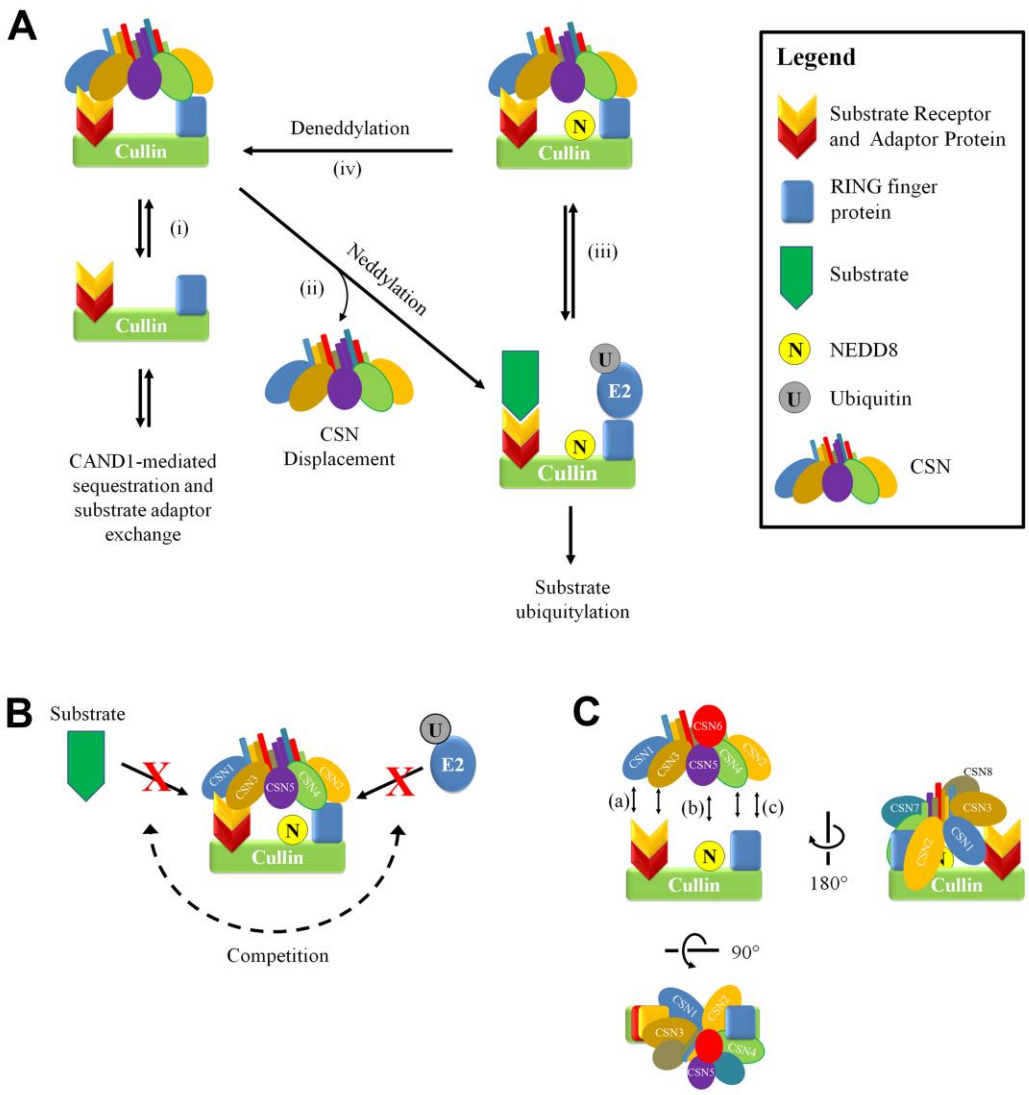

Figure 1.3.2 The regulation of cullin E3 ubiquitin ligase activity via neddylation and the CSN. **(A)** A schematic model for the neddylation-dependent regulation of CRLs by the CSN. The CSN can bind and inhibit substrate ubiquitylation in a neddylation-dependent manner. Deneddylated CRLs can be a substrate for CAND1-mediated cullin sequestration and substrate adaptor exchange (i) but can be activated through neddylation and CSN displacement to promote substrate and E2 binding, and subsequent substrate ubiquitylation (ii). Interaction between the CRL and the CSN (iii) position and activate CSN5 to allow deneddylation to occur (iv). **(B)** A schematic model of neddylation-independent regulation of CRLs by the CSN. The CSN interaction can inhibit CRLs in a neddylation-independent manner by competing with substrates and ubiquitin-E2s for binding sites. **(C)** The CSN and CRL interaction. The CSN-CRL association involves the interaction of CSN1 and CSN3 on the substrate receptor (a) and CSN2 and CSN4 on the RING finger protein and the C-terminal portion of the cullin (c) [93,117]. These interactions position and activate CSN5 to allow deneddylation to occur (b).

1.4 Cell Cycle: An Overview

When eukaryotic cells commit to growth and division, the process they take is tightly regulated by complex molecular checkpoints that control progression through the cell cycle (Figure 1.4). The cell cycle can be considered as a progression through distinct phases. G1 (gap 1) is a period of growth in which produced macromolecules accumulate until cells reach a size where they then commit to DNA synthesis. In S (synthetic) phase, DNA is faithfully replicated so that there are two identical copies of the genome distributed among a number of chromosomes that vary by species [114]. The two copies of each chromosome, referred to as sister chromatids, are held together by a protein complex called cohesin. Cells then progress into G2 (gap 2), which is a period of additional cell growth and biosynthesis in preparation for cell division. Successful cell division involves nuclear division (mitosis) and cytoplasmic division (cytokinesis) so that each daughter cell receives a complete set of chromosomes, organelles and cytoplasm. Mitosis (M-phase) consists of subphases that are visually seen. During prophase, the nuclear envelope breaks down and the replicated chromosomes become condensed. The mitotic spindle assembles from microtubules that are nucleated at the centrosomes or spindle poles. These spindle fibres become attached to protein complexes at the centromere known as kinetochores. The kinetochore on one sister chromatid is attached to microtubules from one spindle pole, while the kinetochore on the other sister chromatid is attached to microtubules from the opposite spindle pole [115]. The chromosomes align to the spindle assembly plate during metaphase. Sister chromatids separate during anaphase by cleavage of Cohesin by Separase [116], and segregate to opposite poles in a process driven by motor proteins belonging to the kinesin and dynein

families [117]. This is followed by decondensation of the chromosome and reformation of the nuclear lamina during telophase. In addition to the division of genetic material, during anaphase and telophase, cytoplasmic contents are also divided into the daughter cells, which together form a process termed cytokinesis (See Section 1.4.1). Two daughter cells are formed, and the cell cycle is completed. Depending on the tissue and developmental stage, cells may continue to progress through the cell cycle or exit and become quiescent (G0).

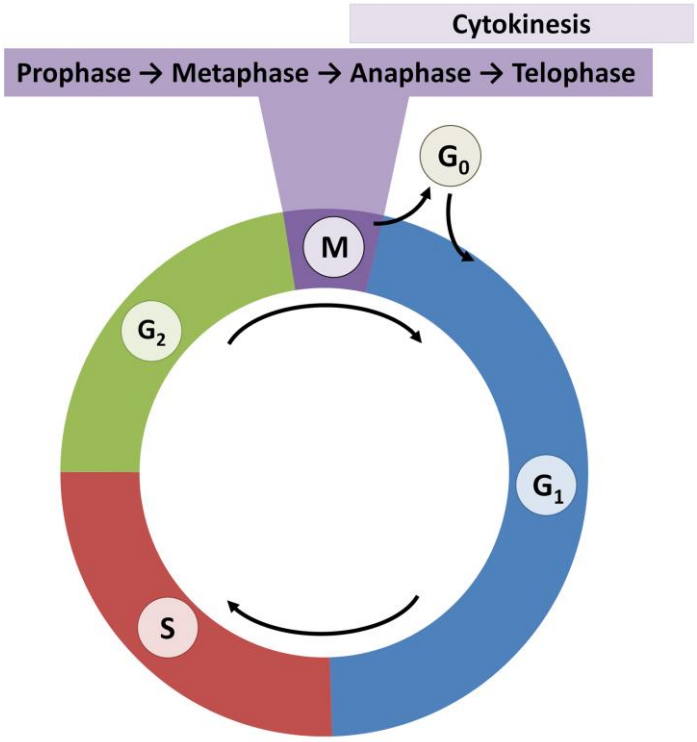

Figure 1.4. Schematic of the cell cycle in mammalian cells. The cell cycle is divided into four phases: G1, S, G2 and M. During M-phase (mitosis), the process can be subdivided into prophase, metaphase, anaphase, telophase, and culminating with division of cytoplasmic material (cytokinesis). Cells can also exit the cycle and enter a quiescent phase (G0).

1.4.1 Cytokinesis: An Overview

The final stage of the cell cycle, cytokinesis, is initiated by the formation of a cleavage furrow by the mitotic spindle. During the metaphase-to-anaphase transition, antiparallel non-kinetochore microtubules between separating chromosomes bundle together to form the spindle midzone, also referred to as the central spindle [118]. The spindle midzone is important for determining the position of the cleavage furrow in animal cells and serves as a platform to recruit proteins required for cytokinesis. Timing of midzone formation could depend on the kinases CDK1 or Plk1 regulating the anti-parallel microtubule bundling protein PRC1 [119]. Formation of the cleavage furrow in animal cells requires activation of the GTPase RhoA by the conserved guanine nucleotide exchange factor Ect2 [120]. Cleavage furrow ingression is powered by an actomyosin network known as the contractile ring. As the cleavage furrow ingresses, it constricts components of the midzone into a structure called the midbody (also referred to as a Flemming body [121]). Proteins involved in membrane tethering, fusion and fission accumulate around the intercellular bridge and midbody [122]. Finally, the contractile ring disassembles, and the plasma membranes resolve in a process called abscission to bring cytokinesis to completion.

The stability of the intercellular bridge is achieved by septin proteins. Septins are GTP-binding proteins that assemble into rod-shaped oligomeric complexes as well as higher-order filaments and bundles. Loss of septin activity usually causes cells to arrest during cytokinesis or produces binucleated cells due to failed abscission arising from an unstable cleavage furrow [123, 124, 125, 126, 127].

Abscission takes place close to the midbody. Abscission is mediated by the Endosomal Sorting Complex Required for Transport (ESCRT) machinery. In human cells, depletion of ESCRT and ESCRT-associated proteins, such as ALIX, TSG101 (ESCRT-I), and CHMP (ESCRT-III) proteins results in cytokinetic delay, abscission failure and binucleation [128].

Cytokinesis also depends on a protein complex called the chromosomal passenger complex (CPC) that associates with chromosomes and centromeres during early mitosis, then later re-locates to the spindle midzone and midbody during anaphase and cytokinesis [129]. The members of this complex, Aurora B kinase, INCENP (inner centromere protein), Survivin, and Borealin, are important for the spindle assembly checkpoint (Section 1.4.3). Loss of function of any of the CPC components results in defects in cytokinesis. Relocation of Aurora B to the spindle midzone was shown to be mediated by cullin E3 ubiquitin ligases CUL3-KLHL9-KLHL13 and CUL3-KLHL21 [130, 131].

Formation of the spindle midzone involves the centrospindlin motor protein, mitotic kinesin-like protein 1 (MKLP1; also known as KIF23). Phosphorylation of MKLP1 by Aurora B promotes clustering of MKLP1 and the GTPase-activating protein MgcRacGAP, to form the centrospindlin complex; the complex is required for microtubule-bundling activity, thereby stabilizing the central spindle [132]. Timing of the spindle midzone formation was shown to be regulated by Cyclin B-CDK1 phosphorylation of MKLP1 [133]. MKLP1 is also required for successful cytokinesis. Depletion of MKLP1 inhibited midbody formation and these cells failed to complete cytokinesis, and formed binucleated cells as a result [134].

1.4.2 Cell Cycle Regulation: An Overview

Whether or not a cell enters or exits the cell cycle depends on signals received from its surroundings. Most cells will proliferate when exposed to pro-growth factors, termed mitogens, a process mediated by mitogen-activated protein kinases (MAPKs) [135]. However, entry into the cell cycle can also be blocked in response to inhibitory factors such as DNA damage.

At each stage in the cell cycle, cyclin-dependent kinases (CDKs) regulate progression from one stage to the next, which are themselves regulated by reversible phosphorylation and ubiquitin-mediated degradation of their regulatory factors. For these kinases to function effectively, they must associate with a group of proteins called cyclins. Cyclins help to activate CDK enzymatic activity as well as to recognize substrates. This regulatory mechanism is highly conserved in eukaryotes with human CDK1 being able to successfully restore viability to yeast (*Schizosaccharomyces pombe*) with a mutant CDK1-homologous gene (Cdc2) [136].

The activities of different CDKs and their associated cyclins regulate the cell cycle at different time points (Figure 1.4.2). In G1, CDK4 and CDK6 activity are regulated by D-type cyclins. These cyclins are thought to be messengers between the outer environment and the cell as their levels are regulated by surface receptors via MAPK pathways [137]. Late in G1, E-type cyclins associate with CDK2, which phosphorylates substrates for entry into S-phase. In early S-phase, A-type cyclins displace E-type cyclins as the CDK2 partner. However, in late S-phase, the A-type cyclins replace CDK2 with CDK1 (also known as CDC2). In G2, B-type cyclins replace A-type cyclins as CDK1 partners and go on to initiate the events in mitosis.

Cyclin-CDK activity is further controlled by periodic expression of negative regulators known as CDK inhibitors (CKIs), whose function is to prevent aberrant cell cycle progression [138]. There are two major classes of CKIs. The first are members of the INK4 family (which include p15, p16, p18, and p19) [139]. They bind CDK4 and CDK6 to prevent association with D-type cyclins, thus inhibiting CDK4 and CDK6 activity. The second are members of the CIP/KIP family (which include p21, p27 and p57). They fit into the ATP-binding pocket of CDK1 and CDK2, thus inhibiting CDK1 and CDK2 activity [138].

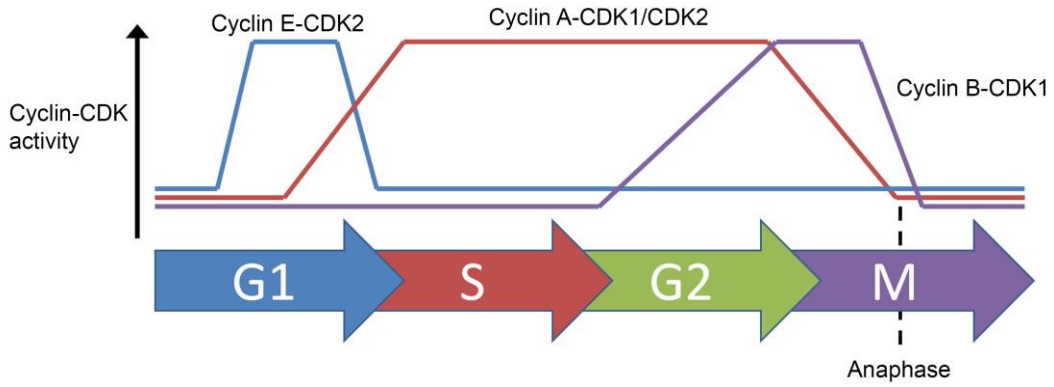

Figure 1.4.2. Schematic of cyclin and cyclin-dependent kinase activity during the cell cycle. In the classical model, D-type cyclins associate with CDK4 and CDK6 to initiate events in early G1 (not shown). In late G1, cyclin E-CDK2 activity phosphorylates substrates to begin DNA synthesis. During S-phase, E-type cyclins are exchanged with A-type cyclins as CDK2 binding partners. In late S-phase, A-type cyclins preferentially associate with CDK1. In G2, B-type cyclin levels increase, which displaces the A-type cyclins as binding partners to CDK1. Cyclin B-CDK1 remain active during early mitosis.

1.4.3 Cell Cycle Checkpoints: An Overview

The cell must be capable of successfully dividing. To mitigate malfunctioning of the machinery that drives the cell cycle, steps in the process are regulated at specific checkpoints such that progression into the next stage is halted until the previous stage has

been completed successfully (Figure 1.4.3). Throughout interphase, checkpoints are triggered if DNA becomes damaged or if there are insufficient nutrients to perform the next stage of the cell cycle. In the case of DNA damage, as described in more detail in section 1.5, there are sensors that activate downstream effector proteins that go on to prevent the activity of cyclin-CDKs, effectively halting progression.

In early G1, the transcription factors that promote entry into S-phase, the E2Fs (E2F1-3), are negatively inhibited by retinoblastoma (Rb) protein, p107 and p130 [140]. As progression through G1 continues, cyclin D levels increase, and the cyclin then complexes with CDK4 and CDK6, which go on to phosphorylate the inhibitory proteins. The phosphorylation releases them from the E2Fs, and results in the transcriptional activation of genes encoding downstream proteins, such as cyclin E [140]. Cyclin E levels increase and these complex with CDK2, while the removal of the inhibitory phosphates on CDK2 by the phosphatase CDC25A [141] promotes a positive feedback loop that commits the cell to enter S-phase.

The intra-S checkpoint ensures that errors that happen during DNA synthesis are repaired. Activation of this checkpoint can inhibit the firing of origins of DNA replication. One mechanism is through CDC25A degradation that leads to inhibition of CDK2 activity [142]. This prevents CDC45 from loading onto chromatin, thus DNA polymerase α cannot be recruited to pre-replication complexes. Additionally, the checkpoint protects stalled replication forks from collapsing and prevents lesions from becoming DNA breaks [142, 143].

If DNA replication is not complete and free of errors, a cell cannot proceed through G2 into M-phase. The G2/M checkpoint is based on the activity level of cyclin

B-CDK1. That is, a threshold in the amount of cyclin B, and therefore CDK1 activity, is required to enter mitosis. Various G2 proteins serve to activate cyclin B-CDK1. Cyclin A-CDK2 promotes the activation of CDC25 [144], an activator of cyclin B-CDK1 [145, 146]. A positive feedback loop is formed as the activated cyclin B-CDK1 phosphorylates and inactivates its inhibitor, WEE1. In late G2, PLK1 kinase, activated by Aurora A and Bora, phosphorylates WEE1 and is subsequently ubiquitylated by cullin-E3 ubiquitin ligase. Additionally, PLK1 (Polo-like Kinase 1) activates CDC25 (CDC25C) [147], which leads to the removal of inhibitory phosphorylation from CDC2. CDC2 can bind with Cyclin B to activate downstream targets that promote mitosis entry. Activation of the G2/M checkpoint results in the inhibition of CDC25 [148], and therefore CDC2 is prevented from complexing with cyclin B.

The process to divide the genome so that each daughter cell receives the full complement of genetic material (mitosis) is precise. Each chromosome must be properly attached to the mitotic spindle [149]. If they do not, the spindle assembly checkpoint (SAC) is triggered, with the signal cascade being activated by CDK1 and Aurora B phosphorylation of INCENP, a subunit of the chromosomal passenger complex (CPC). INCENP phosphorylation inhibits CPC association with the spindle midzone before anaphase. Subsequent de-phosphorylation of INCENP and relocation of the CPC during anaphase is believed to prevent re-activation of the SAC [150, 151, 152].

Once the cell passes the SAC, the anaphase-promoting complex/cyclosome (APC/C) becomes activated; it partners with CDC20 to ubiquitylate proteins for degradation. For example, APC/C targets the Separase inhibitor Securin, allowing

Separase to cleave Cohesin at the onset of anaphase [153]. APC/C targets cyclin B for degradation, which reduces CDK1 activity to allow mitotic exit [153, 154].

A final checkpoint regulates cytokinesis where the presence of lagging chromatin in the intercellular bridge or defects in nuclear pore reassembly activates the abscission checkpoint [155, 156, 157]. This checkpoint appears to require Aurora B activity. In higher eukaryotes, it is thought that phosphorylation of Shrb/CHMP4C in the ESCRT pathway by Aurora B, mediated by Borealin, can inhibit abscission [158, 159].

Figure 1.4.3. Schematic of the known checkpoints in relation to the cell cycle. The checkpoints are activated by unfavourable conditions, which include DNA damage and insufficient nutrients. Checkpoint activation halts progression into the next stage of the cell cycle until the previous stage has been completed successfully.

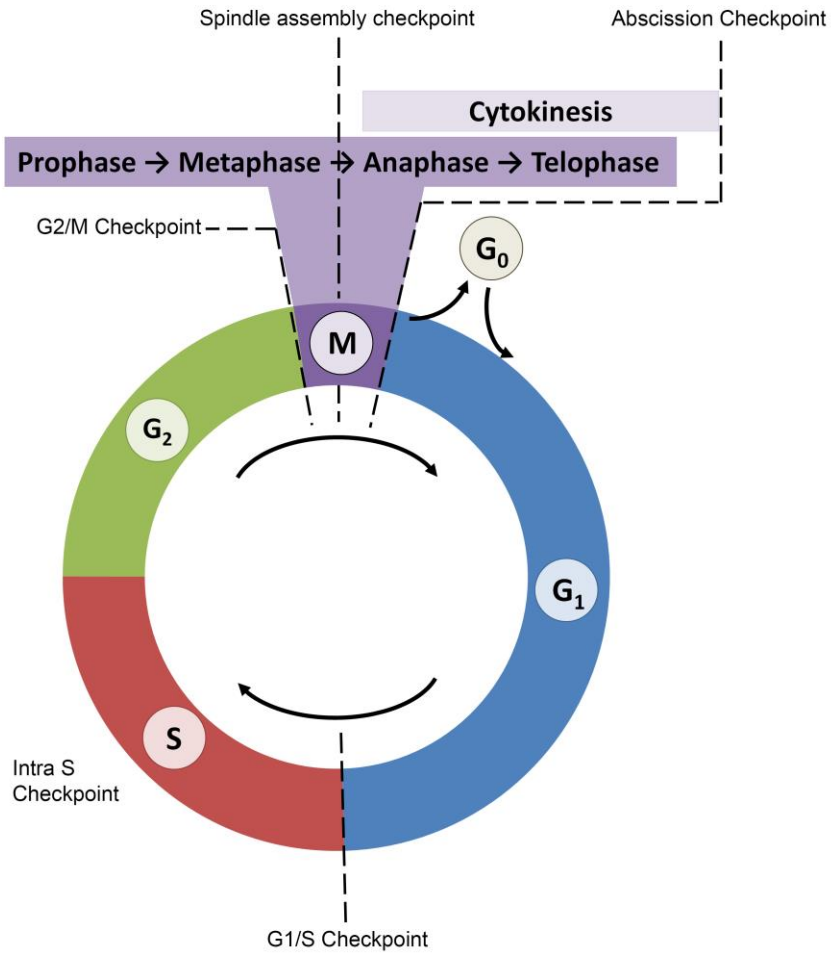

1.4.4 Regulation of Cell Cycle Proteins by Ubiquitin Ligases and Neddylation

Cell cycle-dependent changes in protein levels are triggered by ubiquitin-mediated proteasomal degradation. This helps to ensure directionality of cell cycle by preventing cells from revisiting the previous stage. The ubiquitin ligases play a large role in this process via two related complexes: the cullin E3 ligases, which include the SKP-cullin-F-box (SCF) complex, and the anaphase-promoting complex/cyclosome (APC/C) [160]. While it is known that cullin E3 ligases are neddylated, there are no reports that

APC/C subunits are neddylated, and therefore the role of neddylation in regulating the cell cycle is likely through the cullin E3 ligases.

Cullin E3 ligases are known to regulate G1/S transition, intra S-phase, and G2/M transition. In the G1/S transition, SCF-SKP2 targets CKIs such as p27 [161, 162], p21 and p57 [163] for degradation. CUL4A ubiquitin ligases have also been implicated in the degradation of p27 [164]. The CSN may also regulate this transition. When CSN deneddylase subunits CSN5 and CSN6 are ectopically expressed in cells, they were found to bind to p27 and p57, respectively [165, 166]. Subsequently, p27 and p57 were targeted for degradation [165, 166]. Degradation of p27 is preceded by its shuttling into the cytoplasm, which could be mediated by additional interaction with CSN6 and COP1 (constitutive photomorphogenic 1) proteins [167]. Additionally, CSN could promote phosphorylation of p27 by CK2 to signal p27 degradation [63]. Alongside CKIs, cyclin D levels in G1 are regulated by threonine-286 phosphorylation followed by SCF-FBX4 mediated ubiquitylation [168, 169].

In S-phase, SCF-SKP2, SCF-FBXW7, CUL3 and CUL4B ubiquitin ligases are known to target cyclin E for degradation, which allows cyclin A to associate with CDK2 [164, 170, 171, 172]. To exit S-phase or to pause after DNA damage, CUL4 in complex with the adapter DDB1 and substrate receptor CDT2 (also known as DCAF2), targets the replication licensing factor, CDT1 (Chromatin Licensing and DNA Replication Factor 1), for degradation [164, 173, 174, 175, 176]. Neddylation also regulates progression through this phase of the cell cycle. Cells treated with the neddylation inhibitor MLN4924 have altered S-phase progression due to inhibition of SCF-SKP2 and CUL4-CDT2, which stabilizes CDT1 leading to additional rounds of DNA replication [177, 178].

In response to genotoxic stress such as DNA damage in S-phase, SCF-β-TRCP promotes CDC25A degradation to pause the cell cycle [179, 180]. SCF-β-TRCP also functions in the transition from G2 to mitosis by ubiquitylating multiple targets. It promotes CDK1 activation by proteolysis of WEE1 [181], APC/C activation by targeting PLK1-phosphorylated EMI1 in prophase [182, 183], and de-represses mitotic checkpoint proteins by targeting REST (repressor-element-1-silencing transcription factor) for degradation [184]. Treatment of cells with MLN4924 was reported to stabilize WEE1 and CKIs including p21 and p27, resulting in G2 arrest [185, 186]. While not the focus of this thesis, the duplication of centrioles, which are components of eukaryotic centrosomes that organise the mitotic spindle, are also regulated by SCF-β-TRCP and its neddylation [187].

Given the role cullins have in the cell cycle, the results from studies on the cullin deneddylase, CSN, have given the CSN a similar biological role. For example, loss of CSN function suppresses CDT1 degradation during S-phase [188], which is similar to CUL4-DDB1 loss of function [188], and neddylation inhibition with MLN4924 [189]. Studies on other CSN subunits have reported that CSN8 regulates entry into S-phase, however the exact mechanism is unknown [82].

The role of cullin E3 ligases in cytokinesis is not as well studied. Depletion of CUL3 and CUL1 and their substrate adaptors have resulted in both failure to complete cytokinesis and multinucleated cells, suggesting that this group of E3 ligases have an important role in mitotic progression [130, 131, 190, 191]. Similarly, knockdown of the neddylation E3 protein DCUN1D1, and inhibition of neddylation with MLN4924 (see Chapter 3), resulted in a similar phenotype [192].

1.5 The Role of Neddylation in the DNA Damage Response

As mentioned before, DNA damage can cause cell cycle arrest. An emerging theme is the importance of ubiquitin and ubiquitin-like proteins and their corresponding E3 ligases, suggesting that the neddylation pathway could be important for regulating the DNA damage response (DDR). This section will touch on the different damage responses, but the discussion will focus mainly on the response to DNA double-strand breaks (DSBs). Special consideration is given to the current knowledge of how neddylation regulates the DDR and DSB repair.

1.5.1 Sources of DNA Damage

Organisms have evolved complex systems that form the DNA damage response (DDR) to protect their genome from unwanted damage. These pathways sense and recognize different types of damage and signal the activation of proteins for appropriate repair of DNA lesions. Since DNA damage comes in many forms, each type activates a unique repair response. Endogenous sources of DNA damage include hydrolysis (deamination, depurination, and depyrimidination), alkylation (6-O-Methylguanine) and oxidation (8-oxoG) by reactive oxygen species generated by respiration, and DNA mismatches during replication [193, 194]. Exogenous sources of DNA damage include physical (ionizing radiation (IR, e.g. X-rays), ultraviolet light (UV)) and chemical (chemotherapeutic drugs, environmental carcinogens such tobacco smoke) [194]. The type of damage can be covalent modifications, single-stranded DNA (ssDNA) breaks or double-stranded DNA breaks (DSBs).

1.5.2 Sensing DNA Damage

Regardless of the form of DNA damage and specific repair mechanism involved, all have a defined hierarchy of protein recruitment. The initial response begins with the recruitment of proteins that recognize the damage or alteration ("sensors"), followed by those that receive the signal from the sensors and transmit it downstream ("mediators/transducers"), ultimately recruiting proteins that repair the lesion ("effectors"). Cytologically, these proteins form observable nuclear foci, and the number of foci corresponds to the degree of DNA damage [195]. Depending on the severity of the damage, a number of cellular changes occur, which include reorganization of chromatin and changes to transcriptional activity, activation of checkpoints to delay or stop cell cycle progression, and to promote senescence and apoptosis [194].

A few DSB sensors have been identified in human cells. One is the MRN complex, composed of MRE11 (meiotic recombination 11), RAD50 and nibrin (NBN), which has DNA binding, exonuclease, and endouclease activity [196, 197, 198]. MRN, with retinoblastoma binding protein 8 (RBBP8, also known as CtIP), stabilizes the DNA ends and promotes initial DNA end-resection [199, 200]. Another DSB sensor is Ku (XRCC5), a heterodimer consisting of Ku70 and Ku80. Ku is a DNA-binding protein that quickly binds to free DNA ends and holds them close in space [201]. A third sensor is PARP, a family that includes PARP1 and PARP2, which recognizes single-strand and double-strand DNA breaks [202, 203, 204]. Each of these sensors, MRN, Ku, and PARP, direct a different repair pathway: homology-directed repair (HDR), non-homologous end-joining (NHEJ), and microhomology-mediated end joining (MMEJ), respectively. Why one sensor is preferentially recruited to a DSB site versus another (therefore promoting

one repair pathway over another) is poorly understood and under intense study, but cell cycle status, nuclear position, and chromatin structure play important roles in repair pathway choice [205, 206, 207].

1.5.3 Mediators/Transducers of the DNA Damage Response

The DNA damage response is mediated by proteins in the phosphatidylinositol 3-kinase-like protein kinase family (PIKKs), which include ATM, ATR, and DNA-PK, and by proteins in the poly(ADP-ribose) polymerase (PARP) family [208]. ATM and DNA-PK primarily respond to DSBs, the former through interacting with NBN in the MRN complex [209, 210], and the latter through Ku-mediated DNA binding [211]. ATR is activated by the ssDNA-binding protein RPA as a result of DNA end resection during DSB repair, or from replication stress [212]. PIKK members also phosphorylate effector proteins, which regulate cell cycle checkpoints, transcription, senescence, and apoptosis [212].

Another feature found early in DSB repair is the phosphorylation of histone variant H2AX on serine 139 (γH2AX). H2AX is phosphorylated by ATM in response to DSBs, but is also targeted by ATR and DNA-PK [213, 214], γH2AX signaling is sustained by the recruitment of mediator of DNA damage checkpoint protein 1 (MDC1), which amplifies the phosphorylation signal and prevents H2AX dephosphorylation [215]. γH2AX and MDC1 also recruit additional mediators, such as p53-binding protein 1 (53BP1), to the repair foci [212].

1.5.4 Effectors of the DNA Damage Response

The substrates of the mediator/transducer kinases and downstream kinases can be considered the "effectors". For example, ATM and ATR phosphorylate and activate checkpoint kinase 2 (CHK2), and checkpoint kinase 1 (CHK1) [216]. CHK2 phosphorylates CDC25A on serine 123 [147], which as described in section 1.4.3, removes the inhibitory phosphates from CDK2 in G1. The phosphorylation by CHK2 promotes the degradation of CDC25A. Without CDC25A, CDK2 is inactive and cells become arrested in G1 and S-phase [147]. CHK1 phosphorylates and inhibits the protein phosphatases CDC25A (on serine 178, serine 296 and threonine 507) and CDC25C (on serine 216), which are sequestered by 14-3-3 proteins [147, 148]. CDC25C removes the inhibitory phosphates on CDC2, and therefore its inhibition prevents CDC2 from complexing with cyclin B, thereby leading to G2 cell cycle arrest [217]. The negative regulation of PLK1 by ATM/ATR, which in turn results in the stabilization of WEE1 and MYT1, which can then phosphorylate and inhibit CDC2, also contributes to G2 arrest [212].

Aside from CHK1/2, another effector protein that becomes activated in response to DNA damage is p53, a protein phosphorylated by CHK1/2, ATM and DNA-PK [218, 219, 220]. One of the roles p53 performs following DNA damage is to upregulate the CDK inhibitor p21. Because p21 binds to CDK2 and inhibits its activity, the cell arrests at G1/S to prevent DNA replication until DNA damage is repaired [221]. DNA damage in G2 will also activate p53, which upregulates p21 and 14-3-3 proteins. p21 and 14-3-3 in turn inhibit cyclin B-CDC2 complexes through phosphorylation and cytoplasmic sequestering of CDC2 [222, 223]. In addition, the inactivation of CDC25 results in its

inability to dephosphorylate and activate CDC2 [217]. As described in more detail in the next section, p53 has a complex regulation that multiple studies have found involves neddylation and the deneddylase CSN.

1.5.5 Regulation of p53 through Neddylation and the CSN

Early investigations found that a specific phosphorylation (Thr155) of p53 promoted its degradation through its interaction with the E3 ubiquitin ligase MDM2 (mouse double minute 2). This phosphorylation appeared to be mediated by the p53 interaction with CSN5 in the CSN holoenzyme [65, 224]. In addition, MDM2 and CSN5 can regulate the export of p53 from the nucleus into the cytoplasm for degradation [225]. Similarly, it was found that over-expression of CSN6 can promote p53 degradation through inhibiting autoubiquitylation of MDM2, and mice that were heterozygous for a null version of *CSN6* were more susceptible to DNA damage [226]. HER2-Akt signaling may also promote p53 degradation by promoting the stability of CSN6 in addition to phosphorylation and stabilization of MDM2 [94, 227]. The p53 protein is also reported to be neddylated by MDM2 [34] and the SKP1-cullin-F-box (SCF) E3 ligase complex containing FBXO11 [228]. Currently, the biological role for p53 neddylation is not well characterized but is believed to impact p53 transcriptional activity [34, 228]. The p53 gene (*i.e. TP53)* itself is also indirectly regulated via neddylation of the ribosomal protein L11, which is found in the nucleolus conjugated to NEDD8 in unstressed cells [229]. DNA damage is able to disrupt the nucleolus, which releases L11 into the nucleoplasm [230, 231, 232]. Nucleoplasmic L11 is then deneddylated, possibly by DEN1, which allows L11 to be recruited to the p53 promoter [229, 230]. The localization of L11 was

also recently found to be regulated by the protein Myeloma overexpressed 2 (Myeov2). Myeov2 can sequester L11 in the nucleoplasm and promotes deneddylation of a host of proteins including L11, which in turn would impact *TP53* gene expression [229]. Interestingly Myeov2 also interacts with the CSN holoenzyme via interaction with CSN5, and while this interaction does not appear to affect L11 neddylation in the experimental conditions used, it raises the possibility for a neddylation-dependent role in either nucleolar maintenance and/or *TP53* gene regulation [229]. Finally, p53 transcriptional targets have also been shown to be regulated through neddylation. For example, the stability of the p53-regulated protein 14-3-3σ, a cell cycle regulator, appears to be regulated through interactions with CSN6 and COP1 [180].

1.6 DNA Double-strand Break Repair Pathways: An Overview

With the many alterations that can happen to DNA comes many ways to repair the damage. The focus of this section, however, is DNA double-strand break (DSB) repair. DSBs can arise through the action of enzymes such as topoisomerase II [233] that can break the DNA phosphodiester backbone, or those involved in normal antibody gene rearrangements and meiotic chromosome exchanges [201, 234]. Nucleolytic cleavage is also catalysed by enzymes that recognize specific DNA structures such as DNA inter-strand crosslinks, blocked DNA replication forks, and dsDNA/ssRNA hybrids (R-loops) [235, 236]. In addition, DSBs can occur through the action of endonucleases at defined DNA sequences, and small molecules and ionizing radiation that can break phosphodiester bonds [194, 237]. DSBs are repaired by pathways that generally fall under two broad branches, whose main difference is whether there is resection of DNA

ends to expose a single-stranded stretch that can pair with a homologous sequence (Figure 1.6). End resection is mainly mediated by CtIP [238], a protein activated by cyclin-CDK phosphorylation (Cdc28 in *S. cerevisiae*) [238, 239, 240]. There are indications that end-resection is suppressed in G1 [240], so that DSBs are likely repaired by (canonical) non-homologous end-joining (NHEJ). NHEJ is characterized by the ligation of two DSB ends since little to no sequence homology is used for repair [241]. This pathway involves the DNA damage sensor Ku holding the DNA ends in close proximity [201].

While NHEJ is active throughout the cell cycle [242], CtIP is not supressed during S and G2 [205, 243], and the repair pathways that depend on end resection can be used. In situations where 5' to 3' end resection produces short 3' end single-strand DNA overhangs, the overhangs can anneal to facilitate repair, termed microhomology-mediated end joining (MMEJ), also known as alternative end-joining (alt-EJ) [244, 245]. PARP, DNA polymerase theta and DNA ligase III are some proteins involved in this pathway [246, 247, 248]. If longer resection occurs at the break to expose enough homologous sequence flanking the DSB to facilitate annealing, the break is repaired by single-strand annealing (SSA). Annealing and processing the single-stranded ends are mediated by RAD52 and ERCC1 [249]. Both MMEJ and SSA are mutagenic because they lead to sequence deletion [250].

After the completion of DNA replication, findings by Johnson *et al.* [251] suggest that the presence of the sister chromatid favours homology-directed repair (HDR) to repair DSBs. In HDR the undamaged, identical sequence on the sister chromatid is employed as a template to repair the broken strand and is generally considered less error-

prone. HDR uses long homologous sequences and features more significant end processing [252]. RPA, which bind to and stabilizes exposed ssDNA, and RAD51, which facilitates strand invasion by the ssDNA to the homologous sequence in the sister chromatid, are members of this pathway [253]. While it is not discussed here, there are at least three known subtypes of HDR [254]. Despite what is currently known about DSB repair, precise mechanisms and all conditions that influence pathway choice remain unclear.

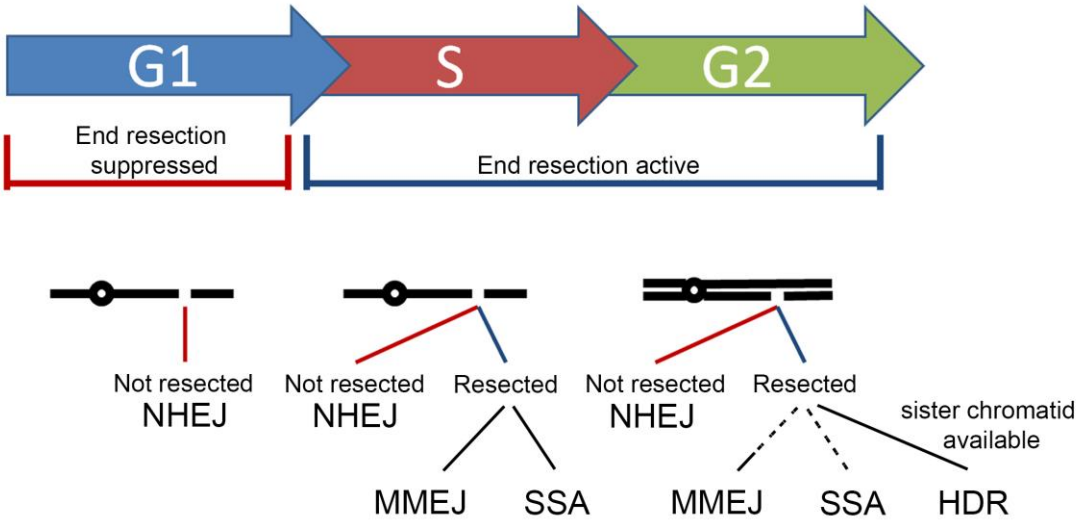

Figure 1.6. A model schematic of how the cell cycle influences DSB break repair pathways. CtIP-mediated end resection is suppressed in G1, promoting NHEJ (non-homologous end joining) to repair DSBs. CtIP is activated by CDK phosphorylation in S and G2, which allow the choice of end-resection-dependent repair pathways: microhomology-mediated end-joining (MMEJ), single-strand annealing (SSA), and homology-directed repair (HDR). Presence of the sister chromatid is thought to favour HDR over MMEJ or SSA (depicted as dashed lines), therefore DSBs arising in S-phase that are repaired before replication of the sister chromatid is complete could more likely be repaired by MMEJ or SSA [250].

1.6.1 The Role of Neddylation and the COP9 Signalosome in Double-strand Break Repair

There are many forms of DNA repair, but not all have been associated with neddylation. Nucleotide excision repair (NER) and double-strand break (DSB) repair have the most compelling data implicating neddylation in these mechanisms [1], however, only the latter will be described in this section.

A clear indication that neddylation is important for DSB repair is that inhibiting this pathway sensitizes cells to IR [255], and that NEDD8 localizes to DNA damage sites [26]. Preliminary studies suggest the possibility that the STUbL (SUMO-targeted ubiquitin ligase) RNF111 interacts with UBE2M to neddylate targets such as histone H4 at damage sites [26]. In addition, neddylated histone H4 is thought to be important for the recruitment of RNF168 to the site, which neddylates histone H2A to facilitate downstream recruitment of BRCA1 [256]. Nevertheless, the degree of neddylation may affect repair pathway choice. RNF111-mediated neddylation, according to Jimeno *et al*. [252], favoured the DNA ends undergoing end resection involving the BRCA1 binding partner CtIP [199, 257], therefore making HR less favourable. Inhibiting neddylation with MLN4924, or knockdown of UBE2M, led to the opposite effect by favouring HR as evidenced by an increase in RPA foci in the nucleus. However, the STUbL activity of RNF111 ubiquitylates SUMOylated proteins, suggesting RNF111-mediated post-translational modification in DDR is much more complex [258, 259]. What the neddylated targets are in this case will require additional studies. There is also indication that neddylation affects HR sub-pathways, such as single-strand annealing (SSA), however additional work is required to understand this effect [252]. Initial studies also

suggest that neddylation could be important for terminating DNA repair. One study found that inhibiting neddylation with MLN4924 delayed the release of NHEJ factors such as Ku from the break site after repair, possibly indicating that the dissolution of NHEJ factors from DNA breaks occurs through ubiquitylation by cullin E3 ligases [260].

The CSN appears to be important for regulating the response to DNA DSBs. Loss of CSN5 increased DSB defects and sensitized cells to DNA damage [261]. This was accompanied by increased γH2AX, and activation of cell cycle checkpoint proteins. In addition, both ATM- and ATR-mediated effects are increased in response to CSN5 knockdown [59, 262]. Since CSN5 harbours the deneddylase enzyme activity of the CSN complex, this data implies a possible role for deneddylation in DNA DSB repair. However, a non-catalytic role for free CSN5 cannot be fully discounted. There is also evidence that the CSN responds to DNA DSBs through changes in the localization and abundance of CSN subunits and/or coordination of the various repair pathways. For example, when treated with different doses of the DNA damage agent mitomycin C in HT29 cells, Feist *et al.* [90] noted a dose-dependent increase of CSN subunits. In addition, the CSN is recruited to DSB sites following IR, and the recruitment depends on neddylation [64, 260]. Currently it is unknown if the entire CSN complex, subcomplexes or individual subunits are mediating specific events during DNA DSB repair. However, CSN8 can interact with ATM kinase directly, and CSN3 is phosphorylated on S410 by ATM in response to DNA damage [64]. Mutation of CSN3 (*i.e.* S401A) to prevent its phosphorylation by ATM can increase radiosensitivity but did not affect the recruitment of CSN3 to DNA DSBs. CSN3 phosphorylation is also required for efficient RAD51 repair foci formation, suggesting a role for CSN3 in end resection and possibly HR [64].

However, despite evidence for neddylation and/or CSN subunits in promoting HR [64, 252], how the CSN might regulate DNA repair pathway choice between NHEJ and HR remains unclear. It has been speculated that repair pathway choice may depend on the degree of deneddylation following the initial round of neddylation [252]. Thus, echoing the role of ubiquitinylation in DNA repair, it appears that both neddylation and deneddylation are required for the regulation of DNA DSB repair.

1.7 Project Overview and Rationale for Study

Despite indications that neddylation is involved in cell division, DNA damage response, and double-strand break repair, few studies have addressed the role of neddylation in these processes. This project aimed to provide insight to the following: 1) Does neddylation and the deneddylase CSN play a role in cell division, specifically in cytokinesis? If cullins are found at midbodies during cytokinesis, is there evidence for the localization of NEDD8 and subunits of the CSN at the midbody? 2) How does inhibition of neddylation affect cytokinesis? 3) What role does the CSN have in response to DNA damage, and does the inhibition of neddylation affect sub-pathways of DNA double-strand break repair? Is there support for this in the form of altered localization of DNA repair proteins and CSN subunits in response to DSBs? The experimental results to these questions will help test the hypothesis that neddylation (and the CSN deneddylase) regulate cytokinesis and DNA DSB repair. The data is presented in two chapters: Chapter 3 focuses on the role of neddylation in cell division and Chapter 4 focuses on the role of neddylation in DNA damage response and DNA repair.

CHAPTER 2 MATERIALS AND METHODS

2.1 Chemical Reagents, DNA plasmids and Antibodies

MLN4924 was purchased from Active Biochemicals Co., Limited. (Cat# A-1139) and dissolved in DMSO.

Ribonuclease A (Sigma-Aldrich, Cat# 6513) powder was rehydrated in 1 mL of 0.01M sodium acetate, pH 5.2, and boiled for 15 minutes at 100 °C. The preparation was slowly cooled to room temperature before 0.1 volume of 1M Tris (Sigma-Aldrich, Cat# T1503), pH 7.6, was added.

pEGFP-C1-MKLP1 and pmCherry-C1-MKLP1 were gifts from Masanori Mishima (Addgene plasmid #70145 and #70154) [132, 263]. pLifeAct_mScarlet-i_N1 was a gift from Dorus Gadella (Addgene plasmid #85056) [264]. ES-FUCCI was a gift from Pierre Neveu (Addgene plasmid #62451) [265]. hprtSAGFP was a gift from Maria Jasin (Addgene plasmid #41594) [266]. piRFP670-N1 was a gift from Vladislav Verkhusha (Addgene plasmid #45457) [267]. pCMV-RAD52-GFP was a gift from Jean-Yves Masson. The CSN6 open reading frame (ORF) was subcloned from the plasmid pHA-CSN6, a gift from Brenda Tse (Dalhousie University). pEGFP-J1 and pmRuby2-J1 were gifts from Jordan Pinder (Dalhousie University), and pX330-LMNAgRNA1 and pCR2.1-CloverLMNA were published previously [268].

Antibodies used for Immunofluorescence (IF) or Western blotting (WB):

Santa-Cruz Biotechnology, Inc: Rabbit anti-MKLP1 (N-19) (Cat# SC-867) at 1/30 dilution (IF). Mouse anti-pericentrin (D-4) (Cat# SC-37611) at 1/50 dilution (IF).

Abcam: Rabbit anti-NEDD8 (Y297) (Cat# ab81264) at 1/100 (IF) or 1/1000 dilution (WB).

Invitrogen: Donkey anti-rabbit IgG secondary antibody with either Alexa Fluor 488 (Cat# A10042) or Alexa Fluor 568 (Cat# R37118) was used at 1/250 (IF) and 1/400 dilution (IF), respectively.

Sigma-Aldrich: Mouse anti-β-actin was used at 1/1000 (WB). HRP-conjugated secondary antibodies against mouse (Cat# A5906) and rabbit (Cat# AP307P) were used at 1/5000 dilution (WB).

2.2 Cell Lines and Tissue Culture

HeLa S3 (human adenocarcinoma) (ATCC® CCL-2.2) and U-2 OS (human osteosarcoma) cells (ATCC® HTB-96™) were maintained in DMEM containing 4.5 g/L D-Glucose, 110 mg/L sodium pyruvate and 584 mg/L L-glutamine (Gibco, Cat# 11995-065) that was supplemented with 10% (v/v) FBS (Gibco Cat# 12484-028), 1% (50,000 units) penicillin and 1% (50,000 μg/mL) streptomycin (Gibco Cat# 15140-122). Cells were cultured at 37°C in a humidified 5% CO_2 incubator.

To generate the HeLa ES-FUCCI (Fluorescent, Ubiquitination-based Cell Cycle Indicator [269]) cell line, HeLa S3 cells were transfected (Section 2.5) with linearized (BsaI restriction digest) and agarose gel-purified ES-FUCCI plasmid. Positive clones

were selected using 200 μg/mL hygomycin B (Invitrogen Cat# 10687010) 72 hours after transfection.

2.3 Plasmid Construction

To obtain cDNA encoding CSN subunits, HeLa cells were lysed with TRIzol ® Reagent (Invitrogen, Cat# 15596026) and the RNA extracted following the manufacturer's protocol. The total RNA was then reverse transcribed to cDNA and amplified using SuperScript® III One-Step RT-PCR with Platinum® Taq (Invitrogen, Cat# 12574-018) and custom-designed DNA primers specific for the coding region of each CSN subunit (see Appendix II). Flanking restriction sites were incorporated in primer sequences to allow cloning into expression plasmids.

The plasmid p2xNLS-iRFP670 was generated by PCR amplification of the iRFP670 ORF in piRFP670-N1 to introduce two nuclear localization signals (NLS) (See Appendix II). The primers designed to create 2xNLS-iRFP670 featured restriction sites suitable for cloning into expression plasmids.

Cloning reactions were performed using T4 DNA ligase (New England Biolabs) following manufacturer's protocol and 5 μL of the ligation was transformed into chemically competent *E. coli* (DH5α). Transformants were selected following standard protocols. Plasmid DNA was extracted from transformants and purified using a Miniprep or Midiprep kit (Qiagen) following manufacturer's protocol and the DNA was resuspended in either Elution Buffer (Miniprep) or sterile distilled water (Midiprep). Purified plasmids were assessed by enzymatic digestion and sequenced to verify correct inserts.

2.4 Cell Synchronization

To enrich for mitotic cells, an asynchronous population of cells was treated for 18 hours with 2 mM thymidine (Sigma-Aldrich, Cat# T9250), prepared in 1x DMEM containing 10% (v/v) FBS without antibiotics (antibiotic-free growth medium). High concentrations of thymidine have been shown to inhibit entry into S-phase [246]. Cells were released from thymidine-induced arrest by washing with sterile 1x PBS (pH 7.4) (Gibco, Cat# 10010-023) followed by incubation with antibiotic-free growth medium for nine hours. The same growth medium, containing 2 mM thymidine, was then applied to the cells and incubated for 15 hours. Cells were released from the second round of thymidine-induced arrest by washing with sterile 1x PBS followed by incubation with antibiotic-free growth medium for 8-9 hours before collecting.

2.5 Mitotic Shake-off

After visually confirming the presence of cells in mitosis, cells were gently washed once with 1x PBS. The aspirated vessel was subjected to three to four raps and the dislodged cells were collected by carefully applying and removing 2 mL of antibiotic-free growth medium. The medium containing dislodged cells was transferred to a pre-chilled polystyrene tube and held for a maximum of one hour on ice. When more cells were required, an additional round of collection was performed by adding growth medium to the vessel and returning it to the 37°C incubator for 30 minutes before repeating the procedure described above. Once enough cells have been collected, cells were collected by centrifugation at 300 x g for 5 minutes. The cell pellet was gently

resuspended in 1 mL live cell imaging medium (see Section 2.9) and transferred onto a poly-L-ornithine coated 35-mm glass bottom dish and allowed to settle for several minutes before imaging.

2.6 Transfection

2.6.1 Lipofection

The day before lipofection, cells were seeded at the amounts given in Appendix II. On the day of lipofection, plasmid DNA was mixed with Lipofectamine™ 2000 (ThermoFisher) at 1:2 in serum-free and antibiotic-free growth medium and allowed to incubate at room temperature for up to 15 minutes. The transfection mix was evenly distributed, and the cells were given fresh growth medium (volumes indicated in Appendix II). Cells were cultured at 37°C for 18-20 hours.

2.6.2 Electroporation

Harvested cells were gently resuspended in Buffer R to attain a concentration of 10^7 cells/mL. One hundred microlitres of the cell suspension was mixed with DNA and electroporated with the Neon ™ transfection system (Invitrogen, Cat# MPK10096) using the settings outlined in Table 2.6.2. Electroporated cells were seeded into growth medium with or without treatment and cultured at a 37°C.

Table 2.6.2 Neon™ Electroporation Settings for U-2 OS

Pulse voltage (v)	Pulse width (ms)	Pulse number
1230	10	4

2.7 Microscopy

All imaging work was performed using a Marianas spinning-disk confocal microscope system (Intelligent Imaging Innovations (3i)) based on a Zeiss Axio Cell Observer equipped with a Yokagawa CSU-M1 spinning-disk unit and 4 laser lines (405, 488, 560 and 640 nm). Cells were observed using a 40X or 63X objective (1.4 NA) lens and images were recorded using an Evolve 512 electron-multiplying CCD (EMCCD) (Photometrics). Both image acquisition and processing were performed using Slidebook 6.0 (3i). Immersol 518F immersion oil was purchased from Carl Zeiss (Cat# 4449600000000).

2.8 Immunofluorescence

No. 1.5 glass coverslips (Fisher Scientific, Cat #12-541-B) were briefly submerged in 95% ethanol and air dried. The dried coverslips were then set in 35-mm wells and seeded with cells. On the day of fixation, cells were washed twice with 1x PBS (five minutes each) and fixed with 4% (w/v) PFA (Electron Microscopy Services, Cat# 15710) prepared in PBS at room temperature for 20 minutes. Cells were washed twice with PBS (five minutes each) and permeabilized with PBS + 0.5% (8 mM) Triton X-100 (Sigma-Aldrich Cat# T8787) for 15 minutes at room temperature. Cells were washed three times with 1x PBS (five minutes each) and then incubated in blocking solution, consisting of 0.2 μm filtered 4% (w/v) BSA in 1x PBS, for 20 minutes at room temperature.

Coverslips were incubated in primary antibody for 1 hour at room temperature, or overnight at 4°C in a humidified chamber. Coverslips were washed 4x 5 minutes with

PBS, then incubated in fluorescent secondary antibody for 1 hour at room temperature, in darkness. Coverslips were washed with PBS then incubated with 5 μg/mL DAPI (Molecular Probes Cat# D1306) prepared in PBS for 10 minutes to label DNA. Excess moisture was carefully removed from the coverslips before placing onto microscope slides (Superfrost Plus, Fisher Scientific, Cat# 12-550-15) with Vectashield Antifade Mounting medium (Vector Laboratories, Cat# H-1000). Coverslips were allowed to settle overnight, protected from light, then tightly sealed with nail polish, and can be stored long-term at 4°C protected from light.

2.9 Live Cell Microscopy

Glass bottom 35-mm dishes (FluoroDish by World Precision Instruments, Cat# FD35-100) were coated with poly-L-ornithine to improve cell attachment to the glass surface (See Mitotic Shake-off). Dishes were coated at room temperature for one hour, then rinsed twice with sterilized water and allowed to dry overnight.

To image DNA over long periods, cells were labelled overnight with 1/1000 SiR-DNA (Cytoseleton, Inc., Cat# CY-SC007) following manufacturer instructions. Prior to imagining, the culture medium was replaced with CO_2 Independent Medium (Invitrogen, Cat# 18045-088) that was supplemented with 10% (v/v) FBS, L-alanyl-L-glutamine (Glutamax, Invitrogen, Cat# 35050061), and penicillin/streptomycin. Imaging was performed with the spinning-disk confocal microscope inside a heated stage (37°C). Using Slidebook 6.0 software (3i), captures were taken approximately every 4-5 minutes with reduced laser power of no greater than 20% to reduce phototoxicity. To account for drifting of the midbody in the Z plane while also keeping imaging time at each timepoint

as short as possible, a vertical stack of 10 μm was taken, with 0.7 μm separating each imaging plane.

2.10 Fluorescence Recovery after Photobleaching (FRAP)

Cells, cultured in 35-mm glass bottom dishes, were washed once in 1x PBS and given live cell imaging medium. The 488 nm laser was adjusted to the minimal power that is capable of photobleaching a spot on a test coverslip marked with green ink (generally 30-35% power) using the Vector Scan unit (3i). Midbodies were identified by mcherry-MKLP1 expression and a 1 μm x 1 μm region was set on Slidebook 6.0 (3i) to be photobleached. Captures were taken every five seconds for the duration of the session. In these experiments, the first three captures demonstrated the pre-photobleaching state. Photobleaching occurs between the third and fourth capture.

2.11 Micro-irradiation of Cells with a UV Laser to generate DNA Damage

UV-laser induced DNA damage was performed as described by Kruhlak *et al*., 2006 [250], using a Vector Scan unit (3i) and imaged concurrently by spinning-disk confocal microscopy. Briefly, 24 hours post-transfection, U-2 OS cells were photosensitized with 2 μM Hoechst 33342 (Thermo Fisher Scientific, Cat# H3570) for 10 minutes in the dark, then washed twice with PBS before incubation in Phenol Red-free DMEM, supplemented with 25 mM HEPES and 10% (v/v) FBS). The power on the 405 nm UV laser was adjusted by determining the amount required to photobleach a green coverslip. Images were captured every five seconds for the duration of the session.

2.12 Clover-Lamin A CRISPR/Cas9 Homology-directed Repair (HDR) Assay

U-2 OS cells (at ~60% confluency) were collected and washed with 1x PBS, then prepared for electroporation (See Section 2.6.2). The cell suspension was mixed with a 1.75:1 ratio of pX330-Lamin A gRNA and pCR2.1-CloverLamin, and a transfection efficiency marker (iRFP670-N1 or p2xNLS-iRFP670-N1). Twenty-four hours after electroporation, the spent media was replaced with fresh growth media, and cultured for an additional 48 hours before cells were harvested for flow cytometry (Section 2.14). If cells were cultured on coverslips, the coverslips were immersed in 4% paraformaldehyde (PFA) to fix the cells and the DNA was labeled by incubating the coverslips in PBS + DAPI (See Section 2.8). Random fields of view were captured by microscopy (See Section 2.7). To account for successfully transfected cells, only iRFP670-positive cells were selected for Clover-LMNA expression. Using this method, a minimum of 400 iRFP670-positive cells were manually counted for each assay sample.

2.13 SAGFP Single-strand Annealing (SSA) Reporter Assay

U-2 OS cells (at ~60% confluency) were collected and washed with 1x PBS, then prepared for electroporation (See Section 2.6.2). The cell suspension was mixed with a 1:1 ratio of hprtSAGFP and actin-SceI, and a transfection efficiency marker (p2xNLS-iRFP670-N1). Twenty-four hours after electroporation, the spent media was replaced with fresh growth media, and cultured for an additional 48 hours before cells were harvested for flow cytometry (Section 2.14). To account for successfully transfected cells, only iRFP670-positive cells were selected for Clover-LMNA expression.

2.14 Flow Cytometry

For cell cycle analysis, cells were harvested by 0.05% Trypsin-EDTA treatment (Gibco, Cat# 25300-062) and washed with 1x PBS. All centrifugation steps were performed at 300 x g for five minutes at room temperature. Cells were then fixed in 70% ethanol and stored at -20 °C overnight. On the day of analysis, samples were warmed to room temperature, centrifuged and washed once with 1x PBS. The cell pellets were resuspended with PBS-propidium iodide (PI) solution (0.1% (v/v) Triton X-100, 0.2 mg/mL RNaseA, 1 mg/mL PI), transferred into 5 mL polystyrene round-bottom tubes, and incubated at 37°C for 20-30 minutes in the dark. Following incubation, samples were kept on ice or at 4°C, protected from light, until data acquisition.

To prepare DNA repair reporter assay samples for data acquisition, cells were fixed in 2% paraformaldehyde for 20 minutes at room temperature, washed with 1x PBS, and resuspended in 1x PBS. All data acquisition was done with either the FACS Calibur or FACS Canto II (BD Biosciences). For each sample, a minimum of 10000 events was acquired.

2.15 Cell Viability using AlamarBlue®

Two thousand HeLa cells were plated in individual wells of a 96-well plate and allowed to adhere overnight. Cells were treated with a range of drug concentrations for 24 hours. At the 20th hour, alamarBlue® (Life Technologies, Cat# DAL1000) was applied to each well following the manufacturer's protocol. Fluorescence was measured using an Infinite M200 Pro plate reader (Tecan Group Ltd). For each treatment, data from the four technical replicates were averaged and normalised to the vehicle control.

2.16 Western Blotting

Protein lysates were quantified using the Bradford Protein Assay (Bio-Rad, Cat# 5000006) following manufacturer's instructions and concentrations calculated from the linear range of a BSA standard curve. Absorbance was measured using a BioPhotometer 6131 spectrophotometer (Eppendorf).

Cellular protein was extracted using 1x RIPA buffer (Sigma-Aldrich Cat# R0278) containing a protease inhibitor cocktail (Sigma-Aldrich, Cat# P8340), sodium orthovanadate (Sigma-Aldrich, Cat # 450243) (phosphotyrosyl phosphatase inhibitor), and sodium fluoride (Sigma-Aldrich, Cat# S1504) (phosphoseryl/phosphothreonyl phosphatase inhibitor). Protein samples were mixed with 1x Laemmli buffer and denatured at 95 °C. Proteins were separated by SDS-polyacrylamide gel electrophoresis (10% separating gel, 4% stacking gel) and transferred onto nitrocellulose membranes using wet transfer. PageRuler ^{TM} Prestained Protein Ladder (ThermoFisher, Cat# 26616) was loaded alongside the protein samples to estimate protein size. Blocking was performed using 5% (w/v) skim milk prepared in tris-buffered saline with 0.1% (v/v) Tween® 20 (TBS-T) (Sigma-Aldrich, Cat# P9416). Membranes were incubated with primary antibodies either overnight at 4°C, or 1 hour at room temperature, and then with secondary antibodies for 1 hour at room temperature. Signals were detected by chemiluminescence using Clarity Western ECL Substrate (Bio-Rad, Cat# 1705060) and exposure to autoradiography film (Santa Cruz Biotechnology, Cat# SC-201697).

2.17 Data and Statistical Analysis

mCherry-CDT1, Citrine-Geminin, and DAPI-stained DNA intensity, nuclear area, and signal intensity across specific cellular regions (*i.e.* the midbody) were quantified using Fiji (ImageJ 1.52b) software [71]. Colour channels were separated for each image, and a threshold was applied on the DAPI channel to highlight nuclei. Sub-nuclear objects were excluded by applying a minimum size cut-off. The threshold was then applied to the other channels. Nucleus area and integrated density was measured for each object. The product of the nucleus area and background fluorescence (mean gray value) was then subtracted from the integrated density measurement to obtain the corrected value. Plot profiles across representative midbodies was performed by line-scan across the midbody (over y/x) for each channel, and intensity values were combined to generate line graphs. Fluorescently-tagged proteins at the midbody were quantified using SlideBook 6.0 software (Intelligent Imaging Innovations). All dot plots, bar or line graphs and statistics were generated using GraphPad Prism software Ver. 5 and/or Excel (Microsoft). A Fisher's exact test or a two-tailed Student's t-test (with or without Welch's correction for non-equal variance, as indicated) was used for significance testing between treatment groups.

Cell profiles were determined from flow cytometry acquisitions using Flowing Software 2.5.1 (Perttu Terho, Turku Centre for Biotechnology). For flow cytometry analysis, debris and apoptotic cells were first gated out from the forward scatter (FSC) versus side scatter (SSC) dot plot. In the cell cycle experiments, single cells were gated from the FSC-height vs FSC-area and the PI-area vs PI-width dot plots. Cells that satisfied both conditions were then plotted on an PI-area histogram. Gates that separated

G0/G1, S, and G2/M populations were set on the untreated sample, and then applied to all other treatments (See Appendix III Figure A3.1). In the CRISPR Lamin A HDR reporter assay experiments, cells were displayed on a Clover versus iRFP670 plot, and a quadrant was then applied to delineate positive and negative populations (See Appendix III Figure A3.2). In the SAGFP reporter assay experiments, iRFP670-positive cells were first identified on an SSC-area vs iRFP670 plot. GFP-positive cells contained in the iRFP670-positive population were identified on an iRFP670 vs GFP plot.

CHAPTER 3 INVESTIGATING THE ROLE OF NEDDYLATION DURING CYTOKINESIS

3.1 MLN4924 Inhibits Neddylation in HeLa and U-2 OS Cells

To establish the inhibitory effect of MLN4924 on neddylation, HeLa and U-2 OS cells were treated with vehicle (DMSO) or MLN4924 (0.3 μM and 0.5 μM) for 24 hours and then harvested. Total protein was extracted and analyzed by western blotting to determine whether changes to global and cullin 1 (CUL1) neddylation were affected as previously reported [102, 255]. Treatment with 0.3 μM MLN4924 was able to reduce global neddylation (Figure 3.1 A) when compared to the vehicle control. The anti-CUL1 western showed depletion of a ~100 kDa species following MLN4924 treatment and enrichment of a ~90 kDa species, indicating that there was a depletion of neddylated CUL1 protein (Figure 3.1 B). The effect of neddylation on these two cell lines was also assayed by AlamarBlue® to determine cell viability. Cell viability decreased with increasing doses of MLN4924 with the effect being more pronounced for HeLa cells. The 0.3 μM MLN4924 treatment that was sufficient to reduce global neddylation (Figure 3.1 A) corresponded to a 20% and 5% decrease in cell viability in HeLa and U-2 OS, respectively (Figure 3.1 C).

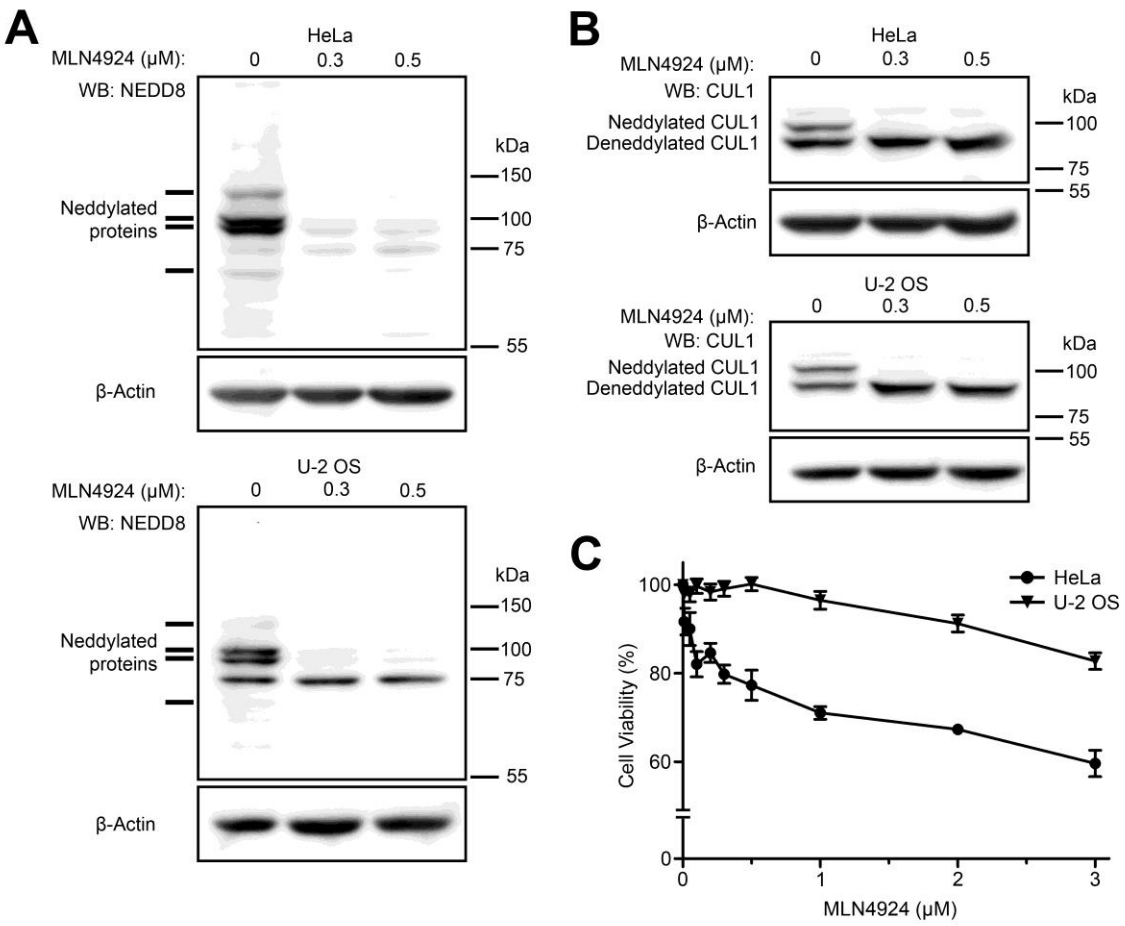

Figure 3.1. MLN4924 treatment alters neddylation status of proteins and cell viability in HeLa and U-2 OS cells. (**A, B**) HeLa and U-2 OS cells were treated with vehicle (DMSO), 0.3 μM and 0.5 μM MLN4924 for 24 hours. Cells were harvested then lysed. Total lysate (10 μg) from each sample was analyzed by immunoblotting with (**A**) anti-NEDD8, (**B**) anti-CUL1 and as a loading control, anti-β-actin antibody (**A**, **B** lower panel). (**C**) HeLa and U-2 OS cells were treated with vehicle (DMSO) or increasing concentrations (0.05, 0.1, 0.2, 0.3, 0.4, 0.5, 1.0, 2.0, and 3.0 μM) of MLN4924 for 24 hours before staining with alamarBlue to assay viability. Error bars indicate the standard error of the mean for three biological replicates. WB = western blot.

3.2 Inhibition of Neddylation with MLN4924 increased the Levels of Fluorescently-tagged CDT1 and Geminin

Following validation that the compound MLN4924 inhibits neddylation, the next step was to reassess the effects inhibiting neddylation on the cell cycle. The visualization of G1 and S/G2 cells can be achieved by having the cells express the ES-FUCCI (Fluorescent, Ubiquitination-based Cell Cycle Indicator [269]) reporter system [265]. The reporter consists of the fluorescently-tagged CRL substrate CDT1 (mcherry-CDT1), which is expressed in G1 and degraded in early S-phase, and the APC-CDH1 substrate Geminin (Citrine-Geminin), an inhibitor of CDT1, which is expressed in S-phase and degraded in mitosis (Figure 3.2 A). By employing this reporter, the progression from G1 through S and G2 can be followed. Because CDT1 is a CRL substrate, treatment with MLN4924 would be expected to alter its stability and impact cell cycle progression into, and through, S-phase [269].

Asynchronous HeLa cells containing the reporter were treated with 0.3 μM MLN4924 for 24 to 48 hours and then processed for microscopy. A significant increase in CDT1 protein levels was observed in MLN4924-treated cells over time as measured by the integrated fluorescent intensity of mCherry-CDT1 per cell ($p<0.0001$) (Figure 3.2 B and C), a result consistent with previous findings that MLN4924 treatment above 0.25 μM can strongly block neddylation and stabilize CDT1, leading to altered cell cycle progression [102, 270]. MLN4924 treatment for 48 hours also increased the levels of Citrine-Geminin, which is not a CRL substrate. This could be due to cells that were not initially arrested in G1/S had begun to accumulate in S/G2, and therefore the increase in Geminin protein levels was likely in response to elevated CDT1 levels.

Figure 3.2. Elevated fluorescent levels of the cell cycle-regulated proteins mCherry-CDT1 and Citrine-Geminin upon chemical inhibition of neddylation in asynchronous HeLa cells. Asynchronous HeLa cells stably expressing ES-FUCCI reporter were treated with vehicle (0.03% DMSO) or 0.3 μM MLN4924 for 24h and 48h. (**A**) A schematic of the abundance of DNA replication regulators CDT1 and Geminin in relation to phases of the cell cycle. The CRL substrate CDT1 is expressed in G1 and is degraded in S-phase. The APC-CDH1 substrate Geminin is expressed in S and is degraded in mitosis. The thickness of the outer circular border represents the protein levels of CDT1 (empty border) and Geminin (filled border). (**B**) Integrated fluorescent intensity per cell is shown for mCherry-CDT1 and Citrine-Geminin. Graphs are depicted as a box and whisker plot, where the mean, 9^{th} and 91^{st} percentile are depicted as horizontal bars, and the outliers beyond one standard deviation are plotted as individual points. Asterisks indicate degree of significance between means (*** = $p<0.0001$, ns = no significance). (**C**) Micrographs of mCherry-CDT1 and nuclei stained with DAPI are shown for cells treated with vehicle or 0.3 μM MLN4924 for 24h and 48 h.

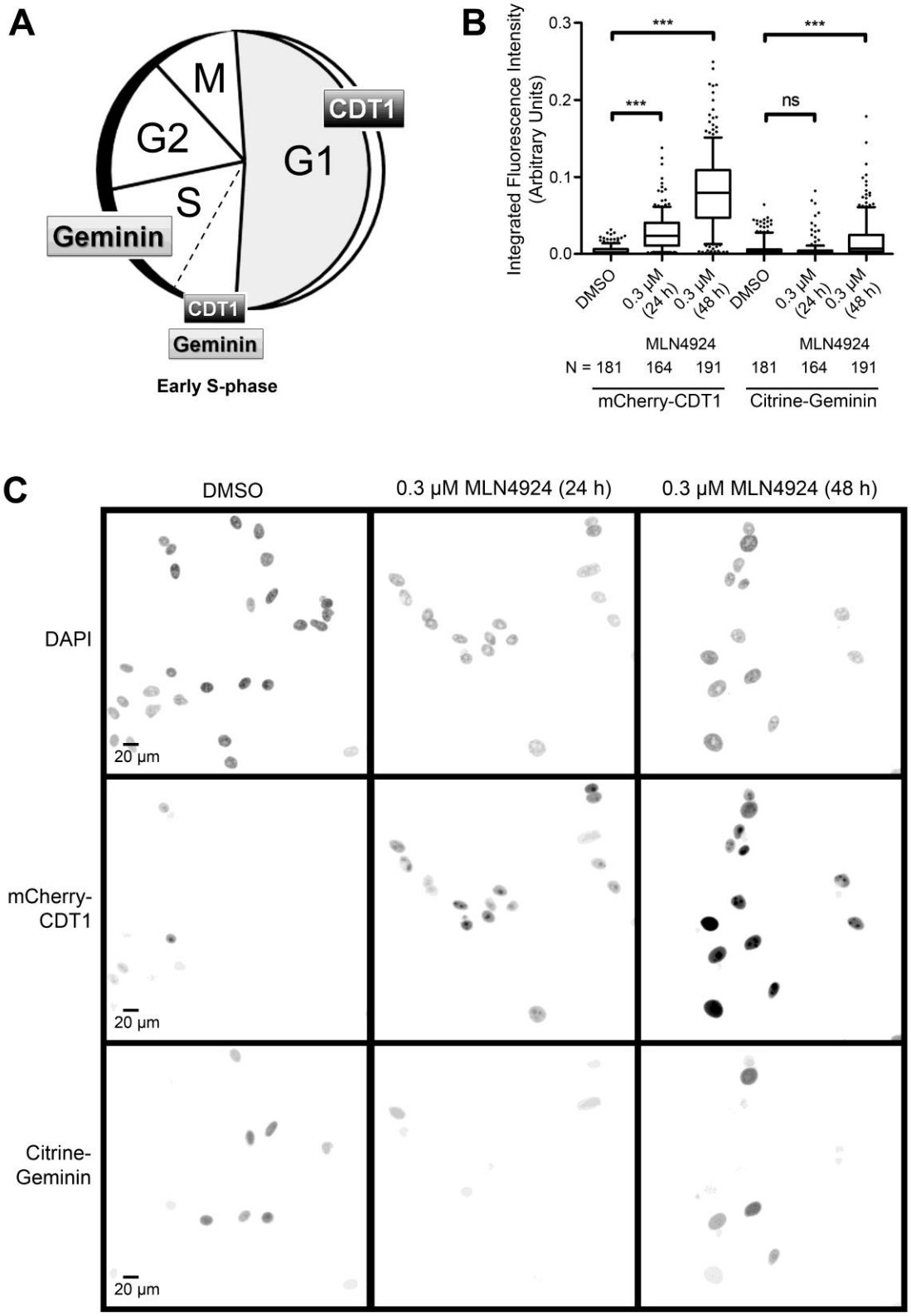
A
M
G2
G1
S
CDT1
Geminin
CDT1
Geminin
Early S-phase
B
Integrated Fluorescence Intensity (Arbitrary Units)
0.3
0.2
0.1
0.0
***
***
ns
DMSO
0.3 µM (24 h)
0.3 µM (48 h)
DMSO
0.3 µM (24 h)
0.3 µM (48 h)
MLN4924
MLN4924
N = 181 164 191 181 164 191
mCherry-CDT1
Citrine-Geminin
C
DMSO
0.3 µM MLN4924 (24 h)
0.3 µM MLN4924 (48 h)
DAPI
mCherry-CDT1
Citrine-Geminin
20 µm
20 µm
20 µm

3.3 Inhibition of Neddylation with MLN4924 alters the Cell Cycle Profile

Having established that the levels of two cell cycle-regulated proteins were affected by MLN4924 treatment using the ES-FUCCI cell cycle reporter, cell cycle distribution of vehicle (DMSO) and MLN4924-treated cells was then directly analyzed by flow cytometry (Figure 3.3 A, B). A trend was observed between 24 to 48 hours of decreasing numbers of cells in G1 ($p<0.01$ at 48 h) and increasing numbers of cells in G2/M with 4N DNA content ($p<0.05$ at 48 h), in addition to the accumulation of cells with >4N DNA content between drug-treated and vehicle (DMSO)-treated cells ($p<0.01$ at 48 h). Finally, G2 arrest in MLN4924-treated cells was observed that coincided with a significant increase in nuclear area overtime (Figure 3.3 C, $p<0.0001$). These results are consistent with previously reported G2 cell cycle arrest and the endoreplication of DNA in S-phase cells due to the accumulation of CDT1 in cells treated with MLN4924 [102].

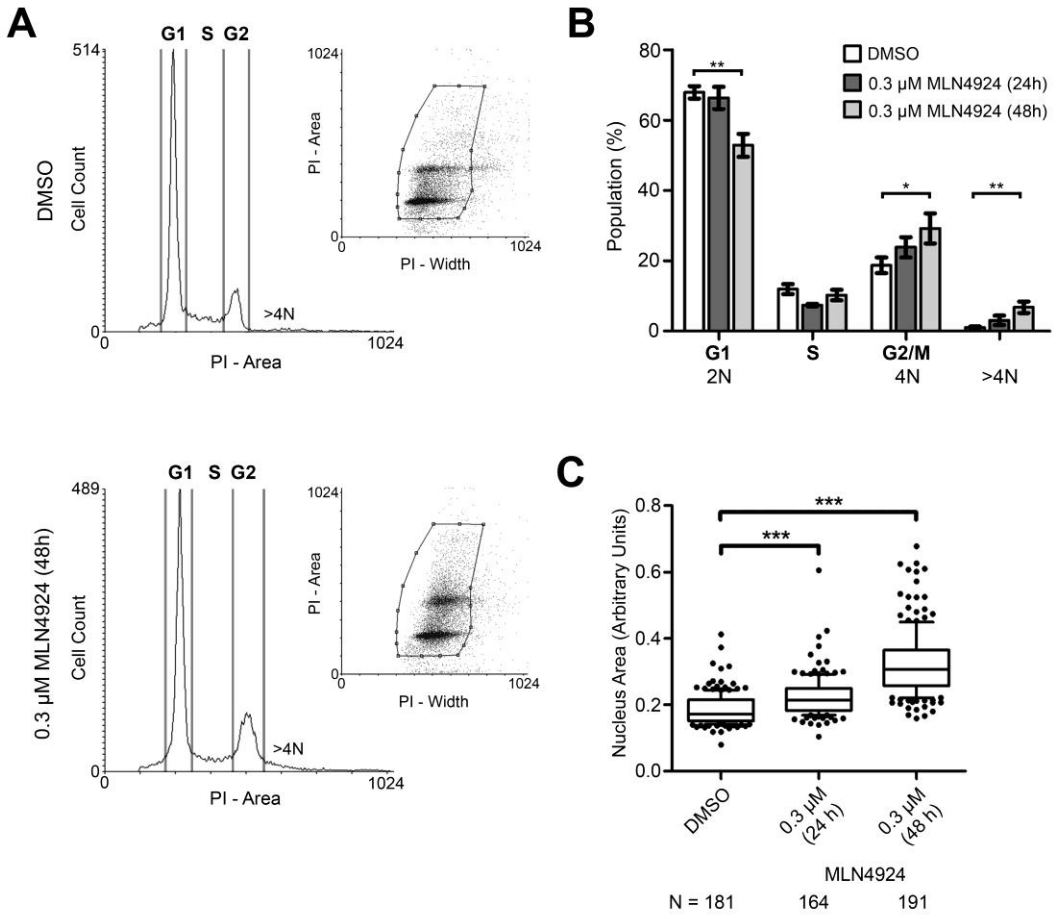

Figure 3.3. Cell cycle effects of chemical inhibition of neddylation on asynchronous HeLa cells. Asynchronous HeLa cells were treated with vehicle (0.03% DMSO) or 0.3 µM MLN4924 and analyzed 24h and 48h later by flow cytometry. (**A**) Representative histogram and dot plot of gated regions in untreated (top) and treated populations (bottom). Vertical lines in the histogram delineate populations according to cell cycle phase. (**B**) The mean percentage of cells in different cell cycle phases for four biological replicates of each treatment is shown. Error bars represent the standard error of the mean (**C**) Relative nuclear area (DNA stained with DAPI) was depicted as a box and whisker plot, where the mean, 9th and 91st percentile are depicted as horizontal bars, and the outliers beyond one standard deviation are plotted as individual points. (*** = $p<0.0001$, ** = $p<0.01$, * = $p<0.05$).

3.4 NEDD8 Localizes to the Cleavage Furrow and Midbody alongside Cullin 1, Cullin 3, and CSN4 during Cytokinesis

The presence of >4N cells after 48 hours of MLN4924 treatment (Figure 3.3) could arise by either DNA endoreplication, or by errors in cell division during mitosis that could contribute to aneuploidy [271]. Given that CRL E3 ubiquitin ligases are implicated in mitotic progression [130, 131, 190, 272], this prompted the question of whether neddylation is also involved in cytokinesis. To test this hypothesis, the localization of NEDD8, selected CRLs and subunits of the COP9 signalosome (CSN) was examined by immunofluorescence microscopy of endogenous proteins and those tagged with fluorescent proteins (Figure 3.4). Endogenous NEDD8 was detected on either side of the cleavage furrow (Figure 3.4 A), and then more centrally at the midbody (Figure 3.4 B and C), suggesting differential localization of neddylated proteins between early and late cytokinesis. The midbody localization of NEDD8 closely aligned with enhanced green fluorescent protein (EGFP)-CUL1 and endogenous CUL3, which are known neddylation substrates. Although both CUL1 and CUL3 have been previously identified as components of the midbody [130, 272], this is the first demonstration of NEDD8 localization at the cleavage furrow and midbody during cytokinesis.

Figure 3.4. NEDD8 localizes at the cleavage furrow and midbody alongside cullin proteins and CSN4. (**A**) Immunofluorescence detection of NEDD8 (green) at the cleavage furrow in untreated HeLa cells during cytokinesis. Magnified regions are indicated with white boxes, and the midbody is indicated (white arrowhead). DNA was stained with DAPI. (**B, C**) Co-immunofluorescence detection of NEDD8 (red) with EGFP-CUL1 (green) (Panel B), and NEDD8 (green) with CUL3 (red) and CSN4 (blue) (Panel C) at the midbody in untreated HeLa cells. Line scan plots of the signal intensity across the midbody (bounded by opposite facing arrowheads) are shown for each fluorescent channel.

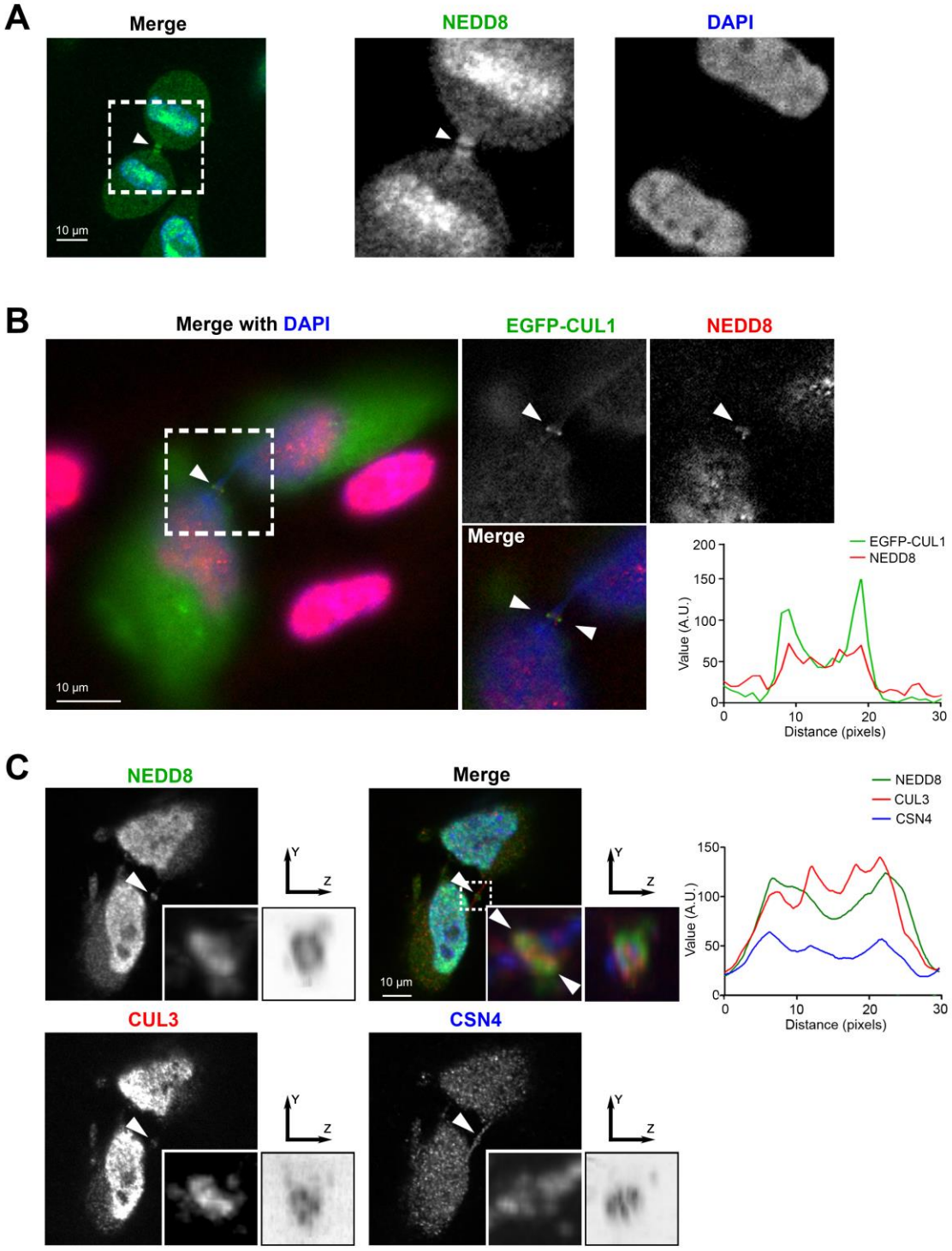
A
Merge
NEDD8
DAPI
10 μm
B
Merge with DAPI
EGFP-CUL1
NEDD8
Merge
10 μm
EGFP-CUL1
NEDD8
Value (A.U.)
Distance (pixels)
C
NEDD8
Merge
CUL3
CSN4
Y
Z
10 μm
NEDD8
CUL3
CSN4
Value (A.U.)
Distance (pixels)

3.5 CSN Subunits Localize to the Midbody during Cytokinesis

Localization of CSN4 to the intercellular bridge and the outer edges of the midbody (Figure 3.4 C) prompted a more thorough examination of the localization of the other CSN subunits, which together form the CSN holoenzyme [1]. This was accomplished by expressing CSN subunits fused to EGFP, which was necessary due to the paucity of antibodies available for this complex. Using DIC (differential interference contrast) and the MKLP1 protein to identify midbodies [134, 273, 274] within fluorescence micrographs, it was found that all subunits could be localized to the midbody, implying that the entire CSN complex is present there during cytokinesis (Figure 3.5, Figure A4). In agreement with CRL and NEDD8 localization at the midbody, most CSN subunits (expressed as EGFP or red fluorescent protein mRuby2 fusions) tended to be localized toward the outer edge of the midbody forming a ring-like structure (e.g. CSN4 and CSN6) or were found in both the centre and the edge of the midbody (e.g. CSN5) (Figure 3.5A). This contrasts with the faint localization of EGFP at the centre of the midbody, which is consistent with non-specific trapping of EGFP when not fused to a CSN subunit. Co-expressed pairs of CSN subunits also co-localized at midbodies in a ring pattern that overlapped with the immunofluorescence signal of endogenous MKLP1 (Figure 3.5 B). A redistribution of CSN5 from more diffuse localization throughout the midbody when co-expressed with CSN4 to a very distinct ring localization pattern with a central cavity when co-expressed with CSN6 was also observed, suggesting a specific recruitment of CSN5 to the contractile ring by CSN6 (Figure 3.5 B). Although signal intensity at the midbody imaged in the x/y dimension (with respect to the growth substrate) varied among the fluorescent protein-tagged CSN subunits, the mean

fluorescence of several of the subunits exhibited significantly higher fluorescent intensities than EGFP alone, specifically that of CSN4 ($p<0.01$), CSN6 ($p<0.01$), CSN7A ($p<0.001$), CSN7B ($p<0.01$) and CSN8 ($p<0.001$) (Figure 3.5 C). In addition, EGFP-CSN5 exhibited significantly lower fluorescent intensity at the midbody than EGFP alone ($p<0.001$; Figure 3.5 C), which could be because the CSN5 protein is more tightly regulated than compared to other CSN subunits.

Figure 3.5. CSN subunits localize at the midbody during cytokinesis.
(**A**) Representative images of EGFP tagged-CSN4, CSN5 and CSN6 localization at the midbody in untreated HeLa cells imaged by fluorescence microscopy. Midbodies are identified using differential interference contrast (DIC) (black arrows). Representative midbodies are magnified to highlight the expression pattern of CSN subunits. (**B**) Co-localization of transiently expressed EGFP-CSN5 (green) co-expressed with mRuby2-CSN4 or mRuby2-CSN6 (red) at midbodies, as identified with MKLP1 antibody staining (blue). Line scan plots of the signal intensity across the midbody (bounded by opposite facing arrowheads) are shown for each fluorescent channel. (**C**) Mean EGFP fluorescent signal intensity of all CSN subunits at midbodies was scored and compared with EGFP alone. Data is represented as vertical scatter plots with mean, SD and p-values indicated. (*** = $p<0.001$, ** = $p<0.01$, ns = not significant).

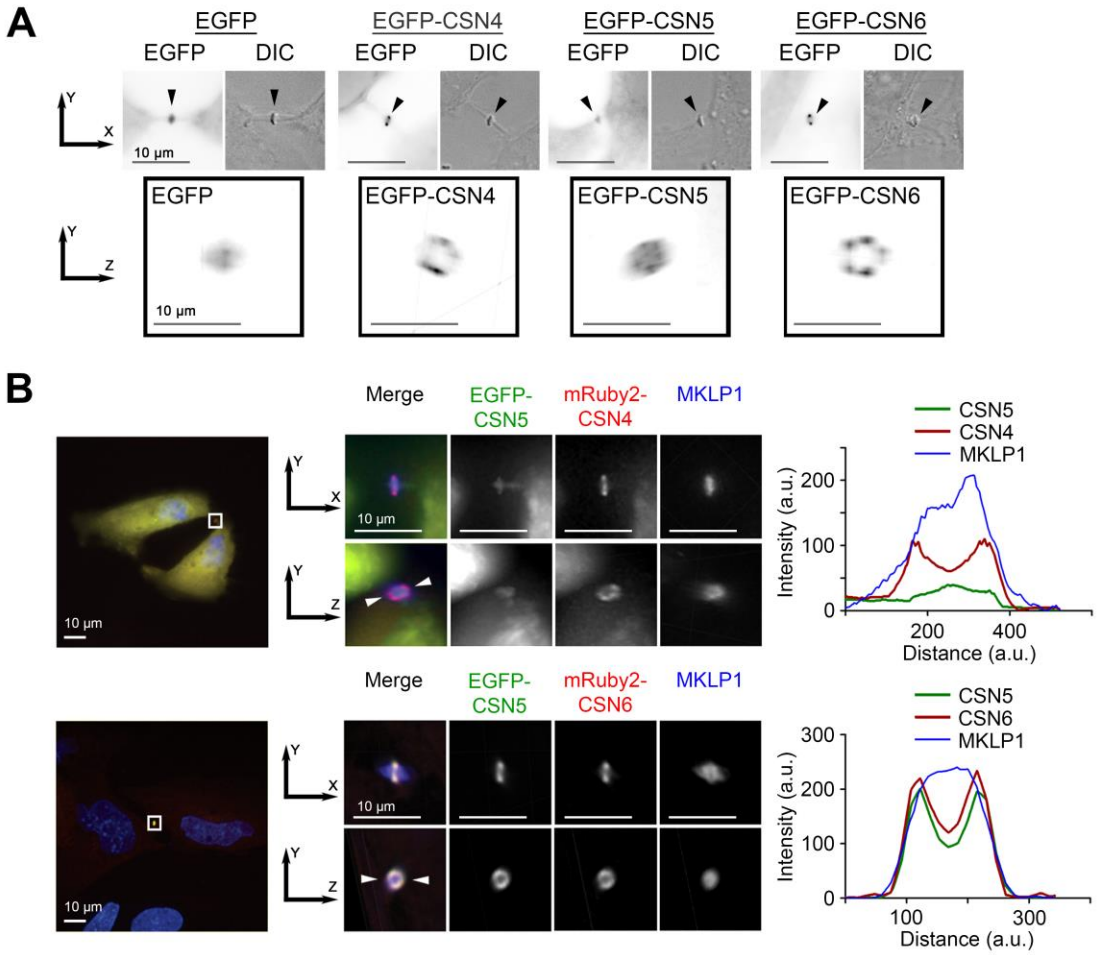
A
EGFP
EGFP-CSN4
EGFP-CSN5
EGFP-CSN6
EGFP DIC
EGFP DIC
EGFP DIC
EGFP DIC
Y X
10 µm
Y Z
EGFP
EGFP-CSN4
EGFP-CSN5
EGFP-CSN6
10 µm
B
Merge
EGFP-CSN5
mRuby2-CSN4
MKLP1
10 µm
Y X
Y Z
CSN5
CSN4
MKLP1
Intensity (a.u.)
200
100
0
200
400
Distance (a.u.)
Merge
EGFP-CSN5
mRuby2-CSN6
MKLP1
10 µm
CSN5
CSN6
MKLP1
Intensity (a.u.)
300
200
100
0
100
300
Distance (a.u.)
C
Normalized Mean EGFP Fluorescence Intensity (measured over X/Y)
10
8
6
4
2
0
***
**
***
**
***
**
ns
ns
ns
EGFP CSN1 CSN2 CSN3 CSN4 CSN5 CSN6 CSN7A CSN7B CSN8
N = 108 38 31 30 49 39 51 39 49 34

3.6 Measurement of CSN6 Recovery at the Midbody following Photobleaching Reveals that it is Relatively Immobile at the Midbody

Given the localization pattern and significantly higher fluorescence signal intensities of several of the fluorescent protein-tagged CSN subunits, it was hypothesized that the COP9 signalosome was likely associated with the actin-contractile ring at the midbody, and as such would exhibit restricted diffusion in comparison to a freely diffusing fluorescent protein such as EGFP alone. Therefore, to further characterize association of the CSN with the midbody, the localization and diffusion of EGFP-CSN6 as a marker of the COP9 signalosome in HeLa cells was examined by fluorescence recovery after photobleaching (FRAP) (Figure 3.6). In these bleaching experiments the localization of mCherry-tagged MKLP1 was used as a fiduciary for the position of the midbody and a high intensity 488 nm laser was employed to simultaneously bleach mCherry-MKLP1 and EGFP-CSN6 (or EGFP) at the midbody (Figure 3.6 A). Fluorescence recovery of EGFP was very rapid, while EGFP-CSN6 and mCherry-MKLP1 only recovered partially over the 5-minute time period observed (Figure 3.6 B). By plotting the mean intensity of the fluorescent signal for EGFP and EGFP-CSN6, and the recovery curves fitted using a non-linear regression and the exponential one-phase association model [275], it was found that CSN6 has a larger immobile fraction than EGFP (Fig. 3.6 C); a result consistent with a strong association with substructures within the midbody such as the contractile ring.

Figure 3.6. Measurement of CSN6 recovery following bleaching reveals that it is relatively immobile at the midbody. (**A**) Representative images of EGFP-CSN6 and midbody protein mCherry-MKLP1 before and after photobleaching. (**B**) The mean normalized fluorescence intensity is shown in the recovery curve, and the vertical bars show standard error of the mean. Data was collected for up to 5 minutes post bleach event. A fitted curve (green line) was used to determine the mobile and immobile fraction (indicated as F_M and F_I, respectively) and the recovery half-life ($\tau_{1/2}$).

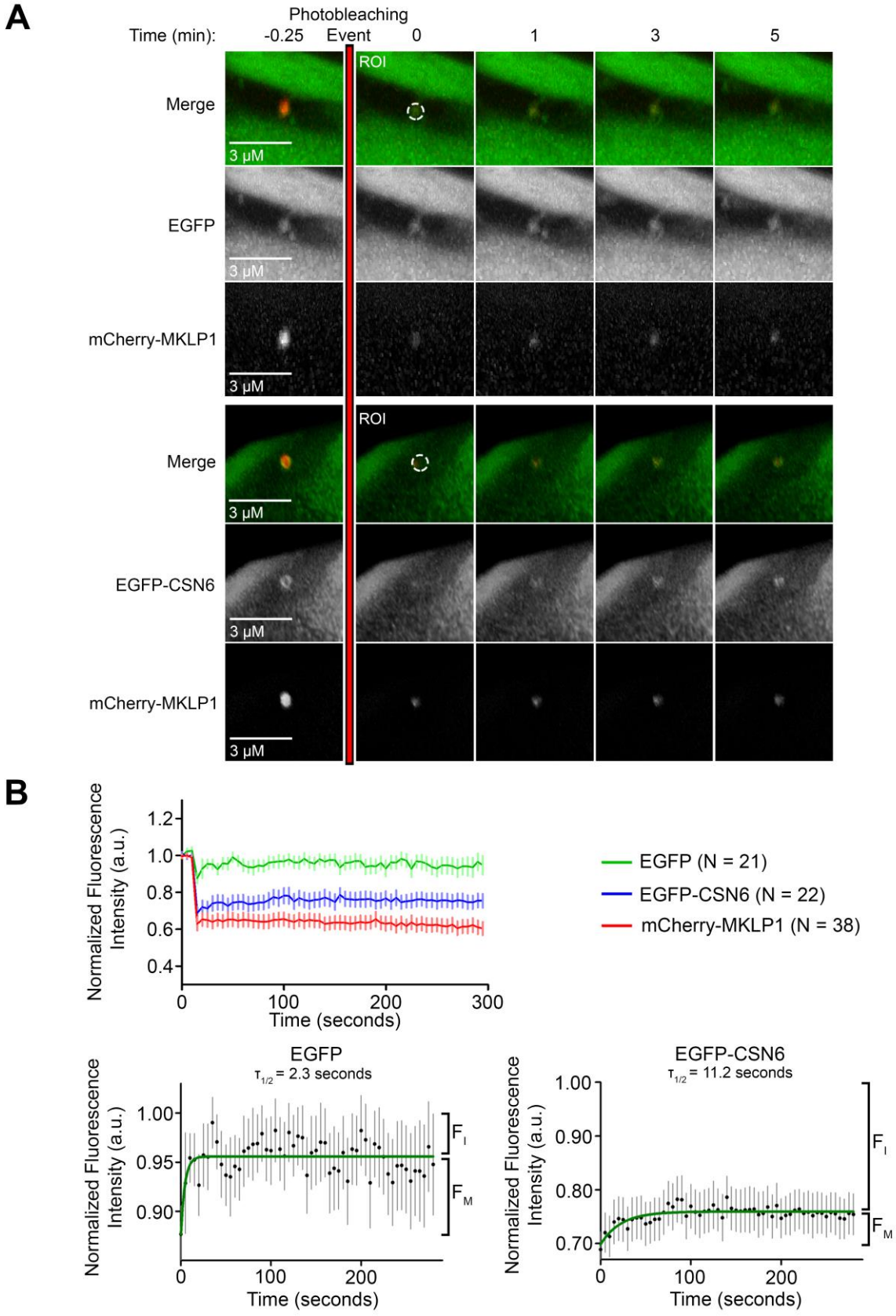
A
Photobleaching
Time (min):
-0.25
Event
0
1
3
5
Merge
EGFP
mCherry-MKLP1
Merge
EGFP-CSN6
mCherry-MKLP1
ROI
ROI
3 µM
B
Normalized Fluorescence Intensity (a.u.)
Time (seconds)
EGFP (N = 21)
EGFP-CSN6 (N = 22)
mCherry-MKLP1 (N = 38)
EGFP
τ1/2 = 2.3 seconds
EGFP-CSN6
τ1/2 = 11.2 seconds
FI
FM

3.7 Inhibiting Neddylation with MLN4924 causes Aberrant Mitosis

Treatment of asynchronous HeLa cells with the neddylation inhibitor MLN4924 produced a small subset of cells with greater than 4N DNA content (Figure 3.2). Given the data demonstrating neddylated substrates such as the cullins (*i.e.* CUL 1 and 3; Figure 3.4) and the CSN deneddylase complex are localized to the midbody during cytokinesis (Figure 3.5), the next step was to determine if aberrant mitosis might partly explain changes in DNA content per cell. Microscopic analysis of cell morphology revealed that cells treated with the neddylation inhibitor MLN4924 for 48 hours had a significant increase in abnormal mitotic events compared to the control (Figure 3.7). These abnormal mitotic events included lagging chromosomes, chromosome bridges, asymmetric cell division and binucleated cells. NEDD8 was also detected by immunofluorescence in MLN4924-treated cells at the midbody; a result that could indicate either the presence of unconjugated NEDD8 at the midbody and/or that of yet-to-be identified protein(s) in this structure that remains stably neddylated despite treatment.

Figure 3.7. Chemical inhibition of neddylation in HeLa cells increases abnormal mitotic events. (**A**) Representative images of HeLa cells treated with vehicle (0.03% DMSO) or 0.3 μM MLN4924 for 48h. The midbody was identified with NEDD8 antibody staining (white arrowhead) and DNA was detected using DAPI staining. Abnormal mitosis, including binucleated cells (*) lagging chromosomes (**) are indicated with white asterisks. (**B**) The number of normal and abnormal cell division, defined as whether there was asymmetric cell division (resulting in binucleated cells), lagging chromosomes or presence of chromosomal bridges, was quantified and statistical significance determined by Fisher's exact test. Asterisks indicate degree of significance between means (** = $p<0.01$).

A

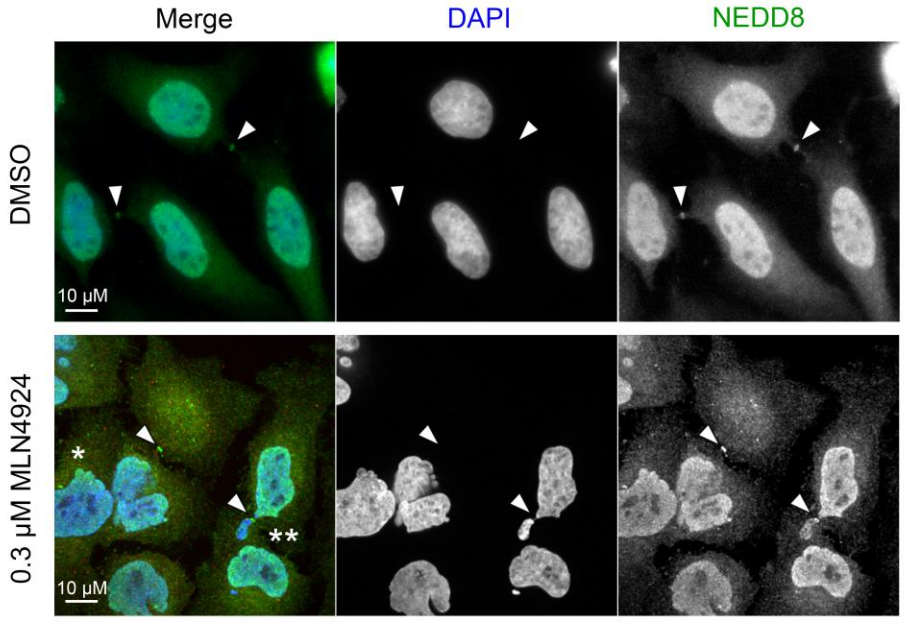

B

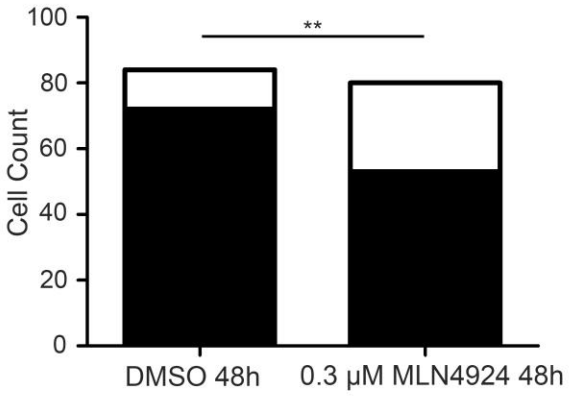

Cell Division

Normal

Abnormal

	Normal	Abnormal
DMSO	72	12
0.3 μM MLN4924	53	27

Odds ratio	3.06
95% CI	1.42 to 6.58
P value	0.006

3.8 Inhibiting Neddylation with MLN4924 causes an Early Accumulation of the Midbody Protein MKLP1

These observed mitotic abnormalities could be related to the accumulation of cullin E3 ubiquitin ligase substrates during extended treatment of cells with MLN4924. Thus, to gain additional insight into the role of neddylation specifically in mitosis, HeLa cells, synchronized by mitotic shake-off, were treated with MLN4924 and then followed as they entered cytokinesis by live-cell spinning-disk confocal microscopy (Figure 3.8). To facilitate live-cell imaging, GFP-MKLP1 was transiently expressed to mark the midbody, mScarlet-i-LifeAct to label the actin cytoskeleton and to identify the cleavage furrow, and DNA was stained with the viable far-red dye SiR-DNA (Figure 3.8 A). MKLP1 was observed to accumulate at the cleavage furrow and midbody in MLN4924-treated cells significantly earlier after the onset of anaphase (18.3 ± 1.4 min, 95% CI: 15.4 to 21.2 min) than in vehicle-treated cells (26.7 ± 3.5 min, 95% CI: 19.3 to 34.1 min) ($p<0.05$; Figure 3.8 B).

Figure 3.8. Chemical inhibition of neddylation in HeLa cells during metaphase leads to earlier MKLP1 accumulation to the midbody. (**A**) Mitotic HeLa cells expressing mScarlet-i-LifeAct were treated with vehicle (0.03% DMSO) or 0.3 μM MLN4924 and followed over time by live-cell spinning disk confocal microscopy. DNA was stained with the far-red dye SiR-DNA and the actin cytoskeleton was visualized by mScarlet-i-LifeAct. MKLP1 accumulation at the midbody is indicated with a black arrowhead. (**B**) A horizontal scatter plot of the timing (in minutes) of MKLP1 accumulation at the cleavage furrow (and midbody) after the onset of anaphase is shown, where each dot represents one dividing cell and the mean length of time and standard error are indicated (* = $p<0.05$).

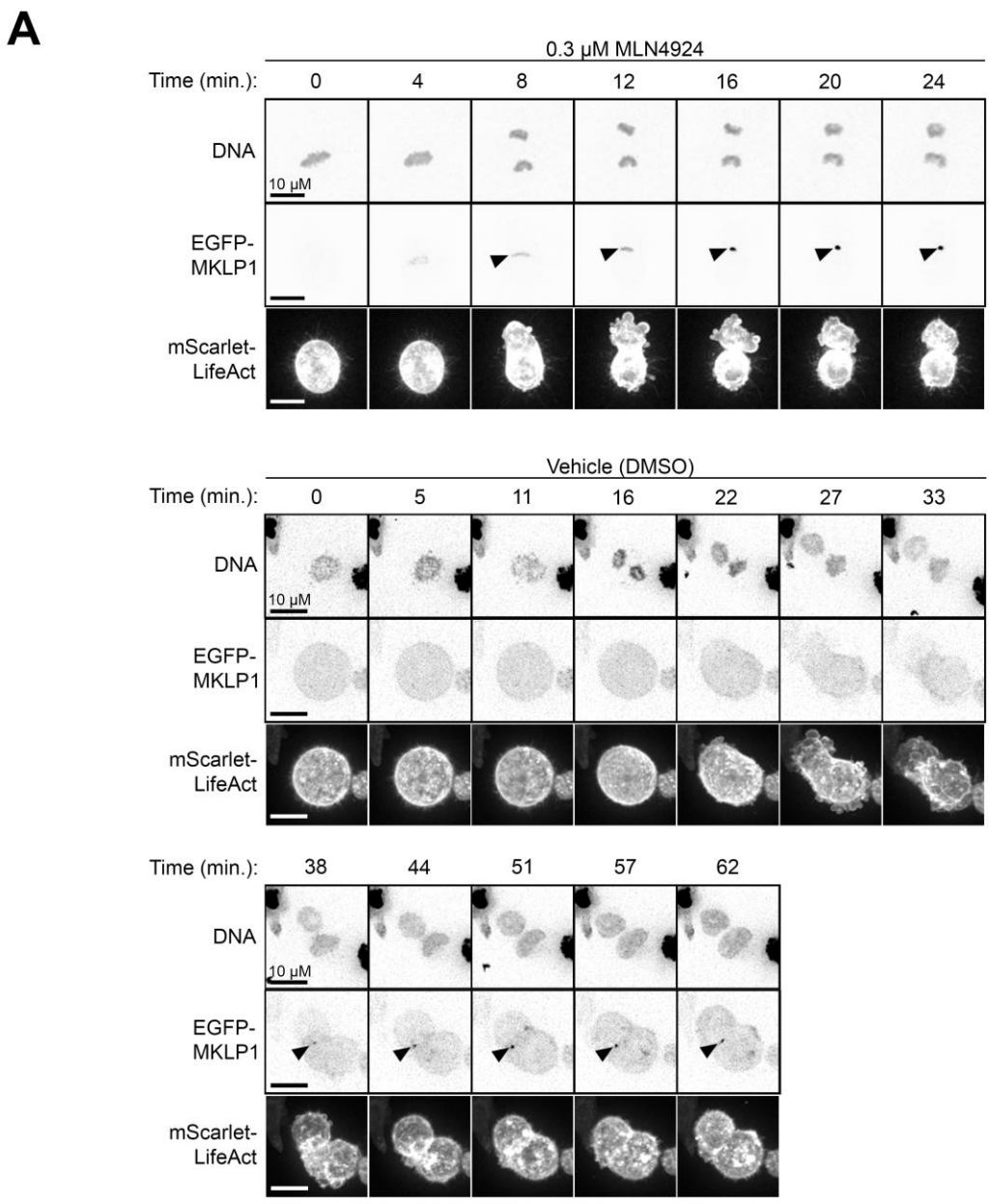
A
0.3 μM MLN4924
Time (min.):
0
4
8
12
16
20
24
DNA
10 μM
EGFP-MKLP1
mScarlet-LifeAct
Vehicle (DMSO)
Time (min.):
0
5
11
16
22
27
33
DNA
10 μM
EGFP-MKLP1
mScarlet-LifeAct
Time (min.):
38
44
51
57
62
DNA
10 μM
EGFP-MKLP1
mScarlet-LifeAct

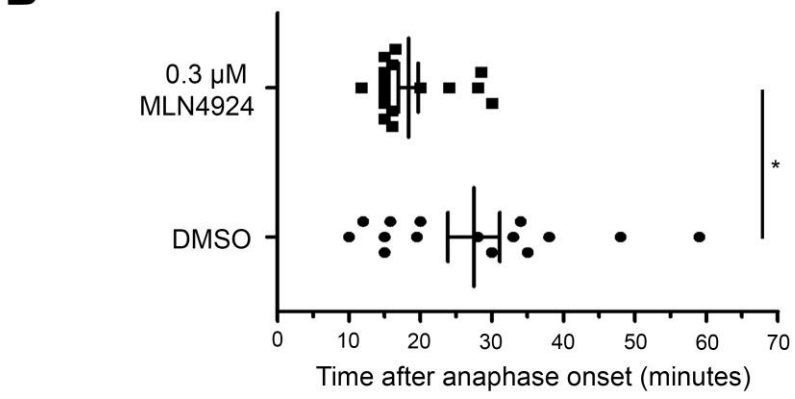
B
0.3 μM MLN4924
DMSO
*
0
10
20
30
40
50
60
70
Time after anaphase onset (minutes)

3.9 Inhibiting Neddylation with MLN4924 causes Delayed or Failed Abscission

In addition to observing earlier MKLP1 accumulation at the midbody in MLN4924-treated cells, when the cells were followed over a time course of eight hours, a significant number of cells was observed with delayed or failed abscission as compared to those treated with vehicle ($p<0.0001$; Figure 3.9 A and B). MKLP1 localization at the midbody became fragmented between 90 min and 180 min after the onset of anaphase in a subset of MLN4924-treated cells as they entered late telophase, which was concomitant with abscission delay (Figure 3.9 C). This indicates that ongoing neddylation in mitosis plays a role in regulating the accumulation of MKLP1 at the midbody and is required for efficient and timely abscission during cytokinesis.

Figure 3.9. Chemical inhibition of neddylation in HeLa cells undergoing mitosis results in delayed abscission or abscission failure. (**A**) Representative images of HeLa cells expressing an actin cytoskeleton marker mScarlet-i-LifeAct and midbody marker EGFP-MKLP1 were stained with viable DNA dye SiR-DNA and treated with vehicle (0.03% DMSO) or 0.3 μM MLN4924 during metaphase, and then followed for 8 hours. The asterisk (*) indicates cellular debris captured in the field of view. (**B**) The number of cells completing cytokinesis (separated) versus the number of cells remaining joined by a cellular bridge with delayed or failed abscission marked by binucleated cells (unseparated) was quantified and depicted as a stacked histogram. Significance between the number of delayed/failed abscission events occurring in vehicle versus drug treated cells was determined by Fisher's exact test (*** = $p<0.0001$). (**C**) Representative images of EGFP-MKLP1 localization at the midbody becoming fragmented between anaphase and late telophase in a subset of MLN4924-treated cells, concomitant with abscission failure. White arrowheads indicate position of MKLP1 at the midbody, and red is the actin cytoskeleton marker mScarlet-i-LifeAct.

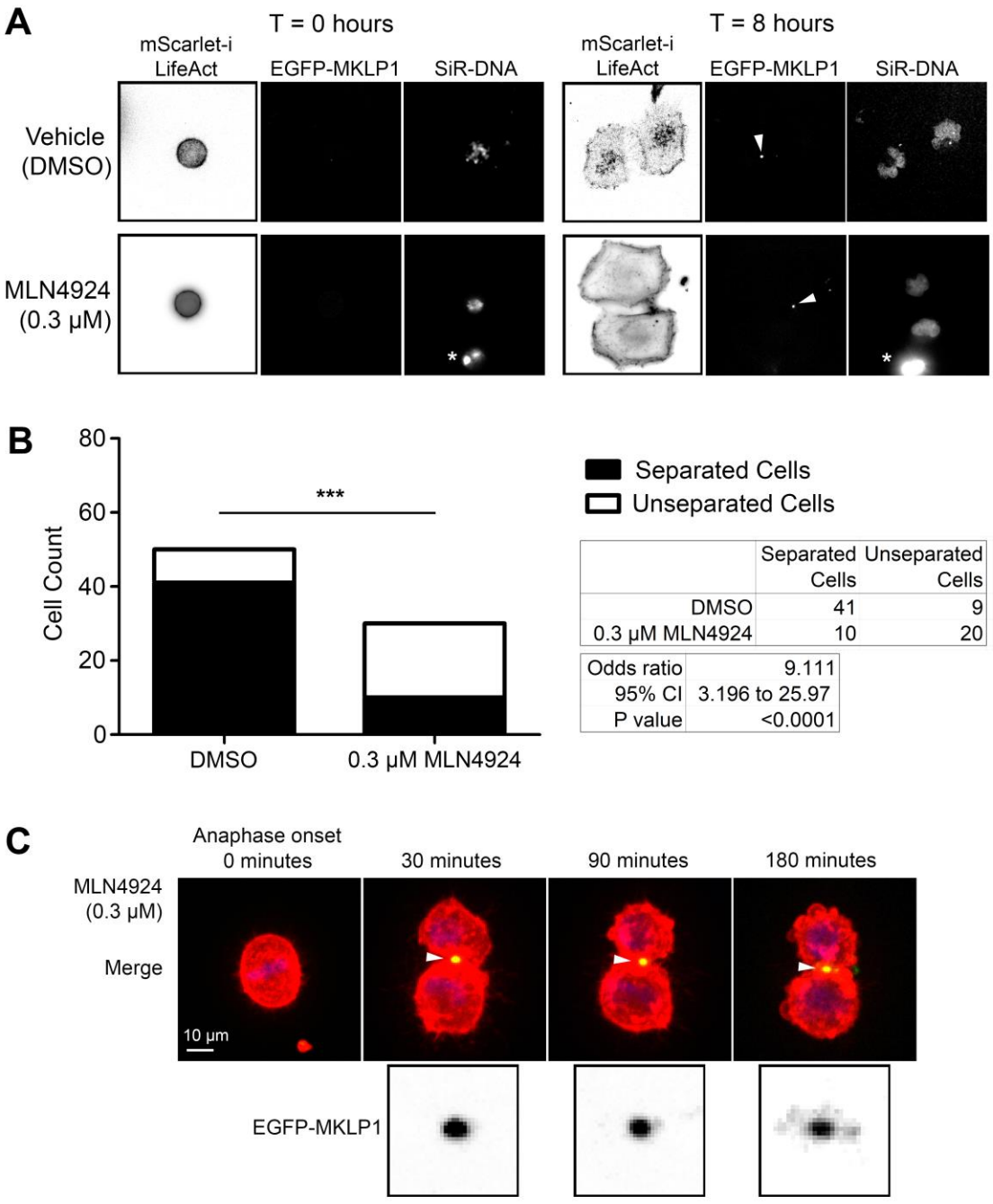
A
T = 0 hours
T = 8 hours
mScarlet-i LifeAct
EGFP-MKLP1
SiR-DNA
mScarlet-i LifeAct
EGFP-MKLP1
SiR-DNA
Vehicle (DMSO)
MLN4924 (0.3 μM)
B
Cell Count
80
60
40
20
0
***
DMSO
0.3 μM MLN4924
Separated Cells
Unseparated Cells
Separated Cells
Unseparated Cells
DMSO 41 9
0.3 μM MLN4924 10 20
Odds ratio 9.111
95% CI 3.196 to 25.97
P value <0.0001
C
Anaphase onset
0 minutes
30 minutes
90 minutes
180 minutes
MLN4924 (0.3 μM)
Merge
10 μm
EGFP-MKLP1

3.10 Summary

Every stage of the cell cycle is intricately controlled by various extracellular and intracellular signals. One level of control is through the post-translational modification with NEDD8 through a process known as neddylation. Neddylation is known to regulate cullin E3 ligase activity, which in turn regulates ubiquitylation of cell cycle proteins such as CDT1. However, the effects of neddylation have not been well studied in cell division, particularly during cytokinesis. In this chapter, the role of neddylation during cytokinesis was investigated using fluorescently-tagged protein expression and with the neddylation inhibitor MLN4924. After first validating the cell cycle effects of treating cells with MLN4924 using flow cytometry, the cell cycle reporter ES-FUCCI, and western blotting, the inhibitor MLN4924 was used to treat HeLa cells and the frequency of abnormal cell division events was measured. After MLN4924 treatment, abnormal cytokinesis was increased, as indicated by an increase in cells with intercellular bridges and multi-nucleated cells. Furthermore, treatment of HeLa cells in metaphase with MLN4924 led to an early accumulation of the cytokinesis protein MKLP1, a protein important for abscission. With the finding that neddylation affected cytokinesis, localization of neddylation pathway components to the midbody was examined. Immunofluorescence revealed that both NEDD8 and CSN4 localized to the midbody, along with fluorescently-tagged CUL1, CUL3 and CSN subunits. Taken together, the data supports an important role for neddylation in regulating cytokinesis.

CHAPTER 4 INVESTIGATING THE ROLE OF NEDDYLATION AND THE CSN IN THE DNA DAMAGE RESPONSE AND IN DNA DOUBLE-STRAND BREAK REPAIR

Figure 4.2 (panel B) in this chapter contains material originally published in:

Molecular Cell, Vol 69, Baranes-Bacher K, Levy-Barda A, Oehler J, Reid DA, Soria-Bretones I, Voss TC, Chung D, Park Y, Liu C, Yoon J-B, Li W, Dellaire G, Misteli T, Huertas P, Rothernberg E, Ramadan K, Ziv Y and Shiloh Y, "The Ubiquitin E3/E4 Ligase UBE4A Adjusts Protein Ubiquitylation and Accumulation at Sites of DNA Damage, Facilitating Double-Strand Break Repair", 866-878, 2018. [276].
The figure was used with permission from Elsevier.

4.1 CSN3 and CSN4 Subunit Protein Levels Increase in the Nucleus following Laser-induced DNA Damage

Neddylation and the CSN have a role in the DNA damage response [1], and studies have shown that CSN subunits respond to DNA double-strand breaks (DSBs) [64, 90]. For example, GFP-CSN3 and GFP-CSN5 have both been shown to be recruited to laser-induced DSBs within 5 minutes [64, 260]. From this observation, it was hypothesized that other CSN subunits are also recruited to DSBs. To test this, EGFP-CSN3 and EGFP-CSN4 expressing U-2 OS cells were subjected to 405 nm UV laser microirradiation to generate DSBs and followed over time (Figure 4.1). Contrary to what was previously shown, EGFP-CSN3 was not recruited to DSBs to form a "stripe", and

the increase in nuclear-to-cytoplasmic signal ratio (N:C) was similar to that of EGFP alone (Figure 4.1 A and B). However, unlike EGFP, EGFP-CSN3 N:C signal ratio did surpass the initial fluorescence intensity 200 seconds after microirradiation. The N:C signal ratio also increased faster for EGFP-CSN4 than it did for EGFP (surpassing initial fluorescence intensity 100 seconds after microirradiation), although, as with EGFP-CSN3, EGFP-CSN4 also did not form a characteristic stripe. This suggests that CSN4 responded to DNA damage more strongly than CSN3; however, it does not rule out a response by CSN3 as the initial increase in N:C fluorescence ratio after UV laser irradiation in EGFP-CSN3 expressing cells was of greater magnitude than for EGFP alone. To demonstrate that DSBs were being induced in my experiments, U-2 OS cells expressing the DNA binding protein, Ku80 [201] (as a mRuby2 fusion), were irradiated and mRuby2-Ku80 formed a "stripe" phenotype along the laser track in under 10 seconds.

Figure 4.1. Laser-induced DNA DSBs does not lead to CSN3 and CSN4 recruitment at sites of DNA damage but cause an increase in CSN3 and CSN4 subunit signal in the nucleus. (**A**) Representative images of EGFP, EGFP-CSN3, EGFP-CSN4 and mRuby2-Ku80 expressing U-2 OS cells responding to DNA DSBs. The path through the nucleus that was irradiated by the 405 nm laser is bounded by white triangles. (**B**) Signal intensity in the nucleus and cytoplasm was measured, then normalized to the initial timepoint measurement, and the nuclear-to-cytoplasmic signal ratio (N:C) at each timepoint was plotted. The timepoint when microirradiation occurred is indicated by the blue arrow.

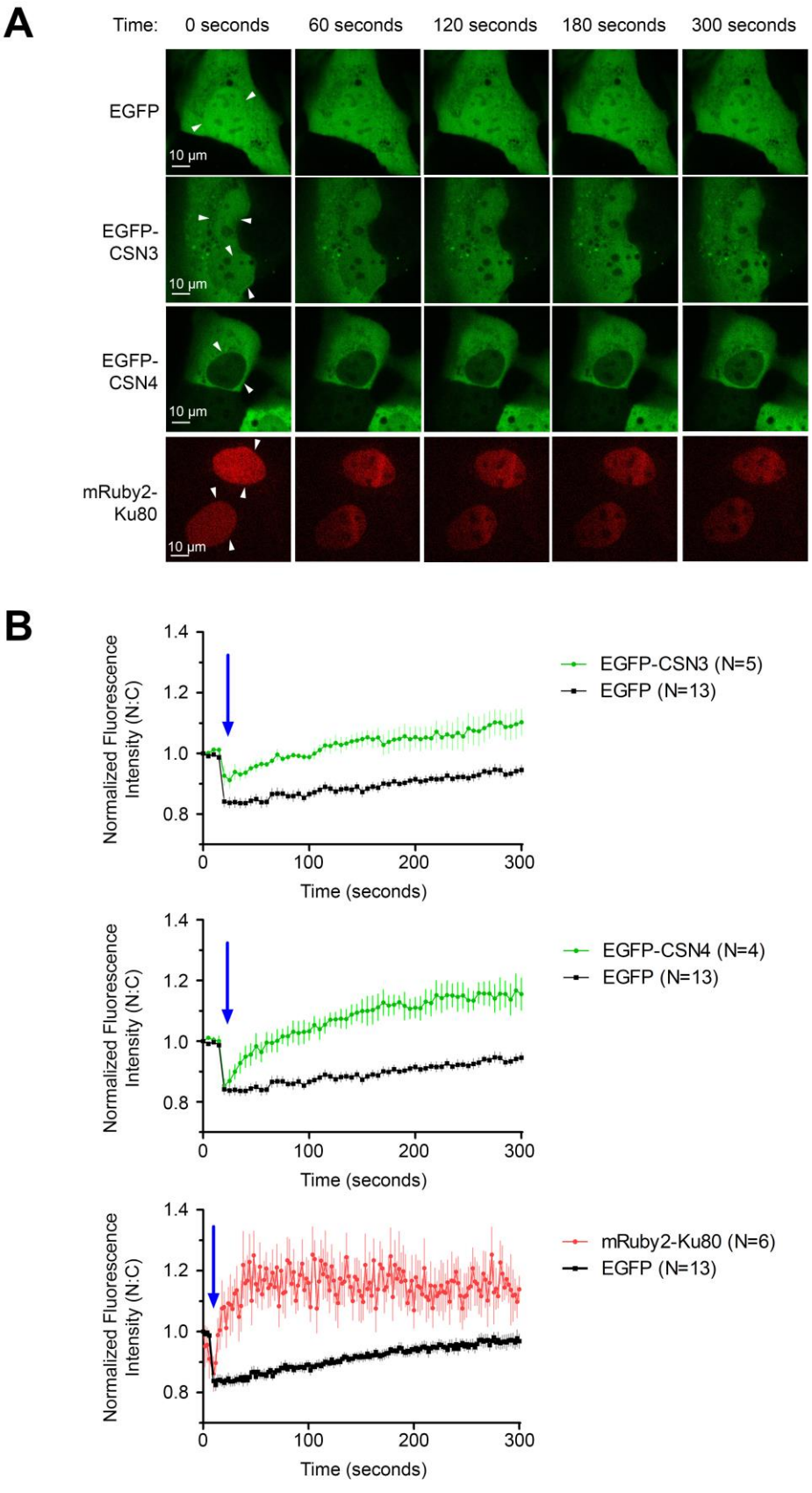
A
Time:
0 seconds
60 seconds
120 seconds
180 seconds
300 seconds
EGFP
EGFP-CSN3
EGFP-CSN4
mRuby2-Ku80
10 µm
B
Normalized Fluorescence Intensity (N:C)
Time (seconds)
EGFP-CSN3 (N=5)
EGFP (N=13)
EGFP-CSN4 (N=4)
EGFP (N=13)
mRuby2-Ku80 (N=6)
EGFP (N=13)

4.2 MLN4924 does not affect Homology-directed Repair (HDR) using the CRISPR/Cas9 Clover-LMNA Reporter Assay

A role for the CSN in the DDR is also supported by the finding that CSN1 and CSN5 depletion by siRNA increased the ratio of non-homologous end-joining (NHEJ) to homology-directed repair (HR), assayed using the SeeSaw 2.0 reporter system [64, 277]. Because the CSN is a deneddylase and knockdown implies suppression of deneddylase activity, this prompted the question of whether inhibiting deneddylation with MLN4924 would affect DNA DSB repair pathway choice. As the SeeSaw reporter measures the relative ratio of these two modes of repair, it remained unclear whether the difference is because of increased NHEJ, decreased HDR, or an increase/decrease of both but to different degrees. To answer whether inhibiting neddylation affects individual DSB repair pathways differently, I employed DNA repair pathway reporters, including a novel assay developed by the Dellaire laboratory that measures HDR by CRISPR/Cas9-induced DNA DSBs.

Briefly, CRISPR (clustered regularly interspaced short palindromic repeats)/Cas9 is an engineered system based on the bacterial endonuclease Cas9 that can generate a DNA DSB at a targeted site determined by a short single-stranded guide RNA expressed in the cells along with Cas9 [278, 279]. The cell can repair the CRISPR/Cas9-induced DSB by HDR if a homology-containing donor sequence is supplied. For this assay, a guide RNA directed the DSB to occur at the Lamin A gene (*LMNA*), and a LMNA-homology-containing donor sequence was supplied in the cells that would to insert the 720-nucleotide sequence encoding the green fluorescent protein Clover [280] into *LMNA*, if repair occurred by the HDR pathway. Repaired cells express a green fluorescent

nuclear lamina that can in turn be enumerated as a read-out for HDR efficiency (Figure 4.2 A) [268]. This assay has successfully been used in a collaboration to confirm that the HDR protein RAD51, and the ubiquitin ligase UBE4A, were positive regulators of HDR (Figure 4.2 B) [276]. Using the assay in U-2 OS cells treated with 0.3 μM MLN4924 for 24 hours immediately following transfection, it was found that inhibiting neddylation did not significantly change the percentage of clover-positive cells compared to vehicle (DMSO) treatment, however the mean gene-targeting efficiency was increased slightly (Figure 4.2 C-E). Together, this indicates that inhibiting neddylation does not significantly affect HDR.

Figure 4.2. Homology-directed repair is not affected by MLN4924.
(**A**) Schematic representation of the CRISPR-LMNA HDR assay. Cas9 is targeted to *LMNA* by the target-specific gRNA (sgRNA) to create a DSB in exon 1. The donor template contains the green fluorescent protein mClover inserted in-frame to the 5' end of exon 1. Repair of the Cas9-induced DSB using the donor template by HDR results in the insertion of mClover into the locus. (**B**) Using the CRISPR-LMNA HDR assay, it was shown that HDR is reduced by depleting cells of either the ubiquitin ligase UBE4A or the known HDR protein RAD51 by siRNA, as reported in Baranes-Bachar *et al.* [276]. Depletion of UBE4A or RAD51 was verified by western blotting (lower panels). (**C, D**) Gene-targeting efficiency (%) of U-2 OS cells treated with MLN4924 and normalized to DMSO was assayed by using either microscopy (panel C) or flow cytometry (panel D) to quantify the fraction of fluorescent cells. Positively-transfected cells were identified by iRFP670 expression. Each dot represents the mean LMNA gene-targeting efficiency for each biological replicate (N >400 iRFP670-positive cells in panel C; N >10000 iRFP670-positive cells in panel D). Bars represent the mean and standard error from the three biological replicates. (**E**) Representative images of the U-2 OS cells treated with DMSO or 0.3 μM MLN4924 for 24 hours. (** = $p<0.01$, *** = $p<0.001$, ns = not significant).

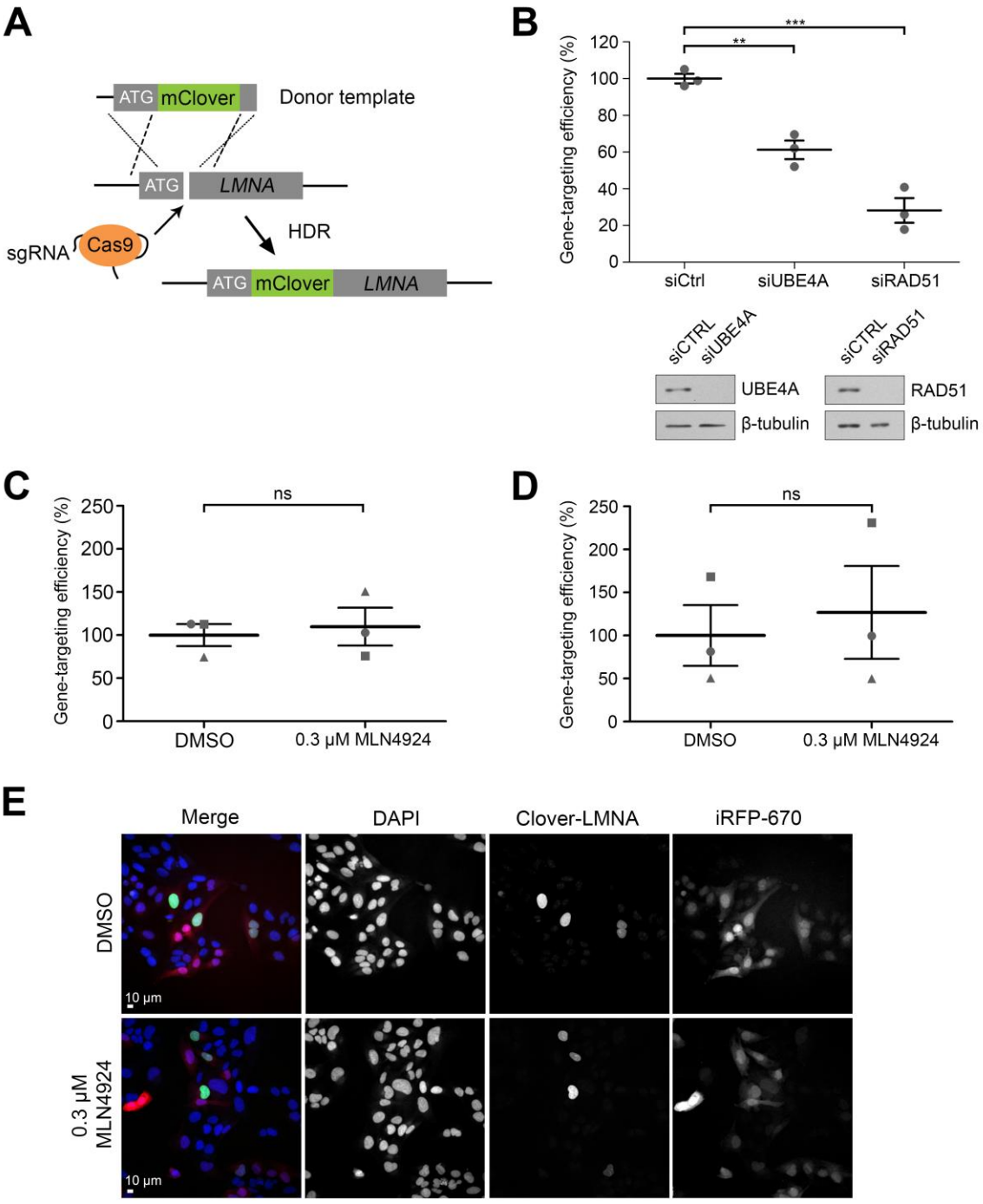
A
ATG mClover
Donor template
ATG LMNA
sgRNA
Cas9
HDR
ATG mClover LMNA
B
Gene-targeting efficiency (%)
120
100
80
60
40
20
0
***
**
siCtrl
siUBE4A
siRAD51
siCTRL
siUBE4A
siCTRL
siRAD51
UBE4A
β-tubulin
RAD51
β-tubulin
C
Gene-targeting efficiency (%)
250
200
150
100
50
0
ns
DMSO
0.3 μM MLN4924
D
Gene-targeting efficiency (%)
250
200
150
100
50
0
ns
DMSO
0.3 μM MLN4924
E
Merge
DAPI
Clover-LMNA
iRFP-670
DMSO
0.3 μM MLN4924
10 μm
10 μm

4.3 Neddylation regulates the Persistence of Single-strand Annealing Protein RAD52 at Laser-induced DNA Damage Sites

With the finding that inhibiting neddylation does not significantly affect HDR (Section 4.2), I investigated whether the sub-pathway of homology repair called single-strand annealing (SSA) might be affected by observing the DNA damage-dependent localization of the protein RAD52, a key factor in SSA [250]. U-2 OS cells expressing RAD52-GFP were microirradiated with the 405 nm UV laser to generate DSBs. Cells pre-treated with either DMSO or with 0.3 μM MLN4924 overnight exhibited rapid recruitment of RAD52-GFP to the laser track within one minute after DNA damage, possibly indicating SSA repair at the UV laser-induced DNA damage. In both vehicle and MLN4924-treated cells RAD52-GFP, once recruited to the break, was then released over the next 3 minutes (~210 seconds) post-irradiation. However, starting at ~4 minutes post-irradiation, the MLN4924-treated cells showed an accumulation of RAD52-GFP at the site of DNA damage that persisted over the following 20 minutes, suggesting aberrant RAD52-mediated DNA repair (Figure 4.3). This increase in RAD52 accumulation was not seen with DMSO treatment. Interestingly, the RAD52-GFP signal became more unevenly concentrated (punctate) along the laser track at later timepoints in MLN4924-treated cells.

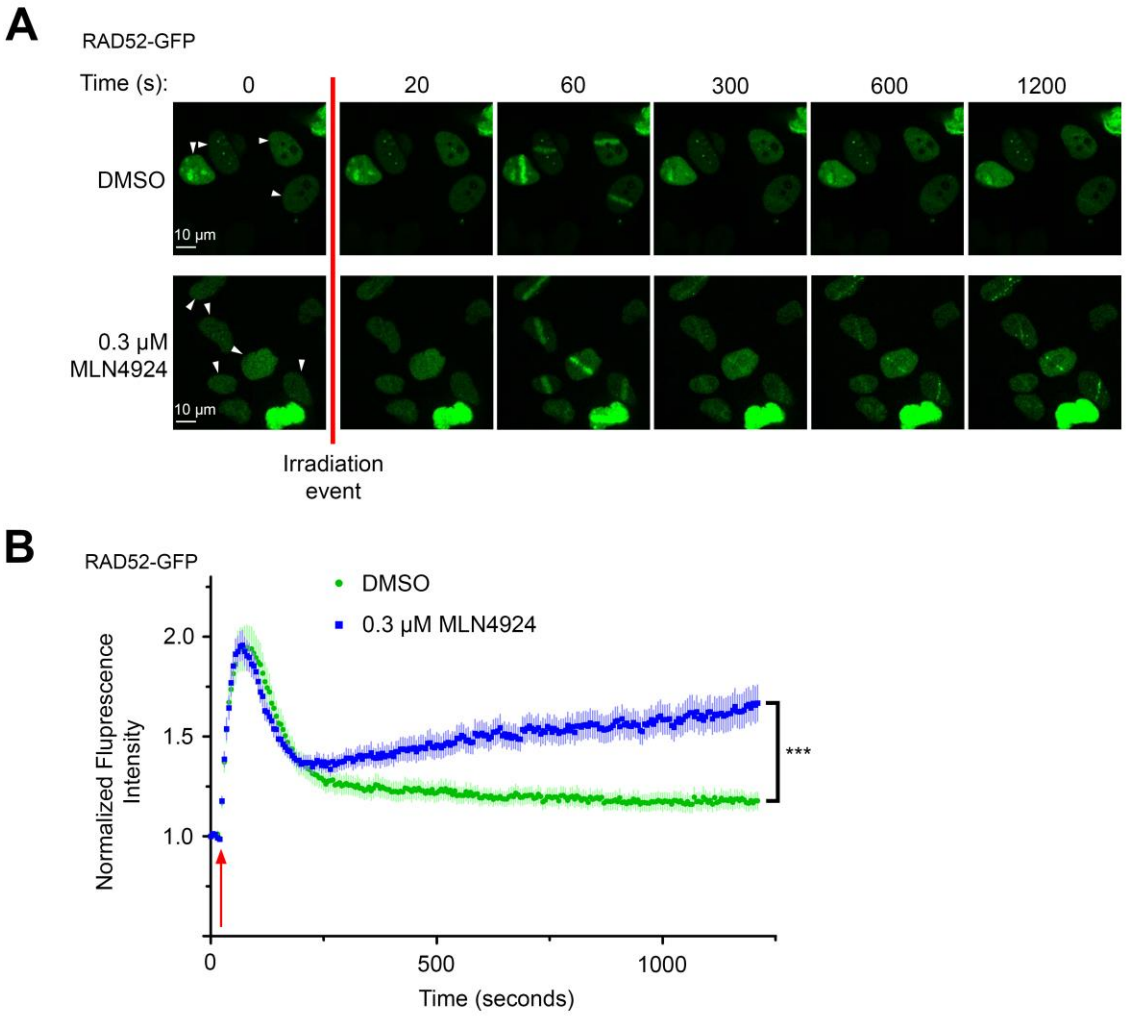

Figure 4.3. MLN4924 causes accumulation of the single-strand annealing protein RAD52 at sites of UV laser-induced DNA damage. U-2 OS cells were treated with DMSO (N = 26) or 0.3 µM MLN4924 (N = 45) for 18 hours and irradiated. (**A**) Representative frames showing the recruitment of RAD52-GFP to DNA damage sites over time. Irradiation occurred between captures and is indicated with a red vertical line (**B**) Changes to the mean of the normalized fluorescence signal for the vehicle (DMSO) and MLN4924 treatment groups throughout the capture session. Light-coloured bars represent the standard error. The red arrow indicates when the irradiation event occurred. (*** = $p<0.001$).

4.4 Preliminary Results suggest that Single-strand Annealing is Increased in Cells after Neddylation Inhibition by MLN4924

The altered RAD52 recruitment (or persistence) at later timepoints after MLN4924 treatment prompted an investigation into whether SSA repair is altered after neddylation inhibition by using the SAGFP reporter assay [266]. The reporter consists of a 5'GFP gene fragment and a 3'GFP gene fragment (SceGFP3'), which have 266 bp of homology (Figure 4.4 A). The 3'GFP fragment is disrupted by the insertion of an 18-bp sequence that is recognized by the rare-cutting endonuclease I-SceI. Repair of a DSB generated by I-SceI by the SSA pathway yields a functional GFP gene. U-2 OS cells electroporated with the reporter and I-SceI expression plasmids were treated with vehicle (DMSO) or 0.3 μM MLN4924 for 24 hours immediately following electroporation. An apparent increase in the percentage of GFP-positive (GFP+) cells was observed for the MLN4924-treated cells compared to DMSO-treated cells, which indicates MLN4924 treatment favours the repair of DNA DSBs by SSA (Figure 4.4). Due to mechanical issues only two biological replicates were performed. Due to time constraints, an integrated reporter cell line could not be used. Having an integrated reporter in U-2 OS would likely provide a better transfection yield and reduce background signal in the negative controls.

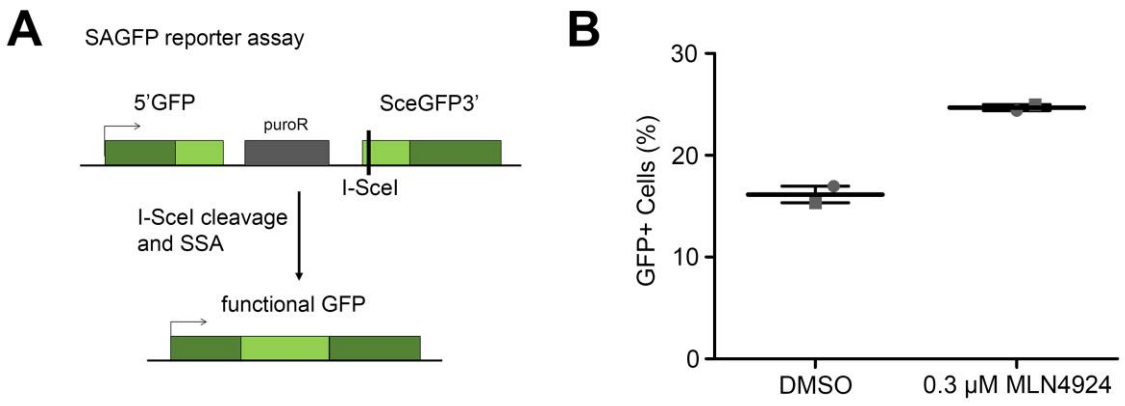

Figure 4.4. Single-strand annealing is increased in MLN4924-treated cells.
(**A**) Schematic representation of the SAGFP reporter assay. Expression of the endonuclease I-SceI generates a DSB at the I-SceI recognition sequence located at the 3'GFP gene fragment (SceGFP3'). Repair of the DSB by SSA using a 266 bp homology sequence (light green) creates a functional GFP gene. (**B**) U-2 OS cells transfected with the SAGFP reporter plasmid were treated with DMSO or MLN4924, and the percentage of GFP-positive cells using the SAGFP reporter was determined. Each dot represents the mean percent GFP-positive cells (adjusted by subtracting out background signal) for each biological replicate. Bars represent the mean and standard error from two replicates.

4.5 Summary

While previous reports have indicated a role for neddylation and the CSN in the DNA damage response and repair of DNA double-strand breaks (DSBs), a closer investigation of individual repair pathways had not been done. An attempt was made to determine if CSN subunits (other than CSN3 and CSN5) responded to UV laser-induced DNA DSBs, and while the CSN4 subunit did respond to DNA damage as evidenced by the increase in nuclear fluorescence signal over cytoplasmic signal, I did not observe the recruitment of CSN subunits to the site of DNA damage as previously reported [64, 260]. While inhibiting neddylation with MLN4924 did not change the relative amount of homology-directed repair events in cells, it was observed that inhibiting neddylation resulted in RAD52 persisting at DSB sites for far longer post-irradiation than in untreated cells, and that single-strand annealing (SSA) repair was increased according to the

SAGFP SSA reporter assay. Collectively, the data indicates a role for neddylation in SSA.

CHAPTER 5 DISCUSSION AND CONCLUSION

5.1 General Overview

Protein neddylation is involved in many cellular processes by regulating the activity of cullin-RING E3 ubiquitin ligases (CRLs), which are responsible for ubiquitylating substrates that regulate diverse cellular functions including epithelial-to-mesenchymal transition [281], autophagy [282], and senescence [177, 283]. A subset of the CRL substrates are also involved cell cycle regulation and the DNA damage response. Furthermore, the neddylation status of CRLs is regulated by the deneddylase COP9 signalosome (CSN), which removes NEDD8 from cullins and obstructs the formation of the active CRL complex.

In this thesis, the role of neddylation and the CSN in the context of cytokinesis and in the DNA damage response was evaluated. Consistent with previous reports in other cell types [102], the neddylation inhibitor MLN4924 affected cell cycle progression in HeLa cells, as shown by the accumulation of mCherry-CDT1 and Citrine-Geminin protein expression and increased nuclear size (Figure 3.2). Treatment with MLN4924 increased the proportion of cells with 4N (G2 phase) and >4N DNA content (Figure 3.3). These effects are attributed to reduced neddylation of CRLs resulting in reduced CRL activity and the accumulation of CDT1 and other substrates, and indeed a reduction in bulk protein neddylation and a reduction in cullin 1 (CUL1) protein neddylation was observed (Figure 3.1). However, the previous studies did not distinctly characterize the mitotic effects of MLN4924, nor has the CSN been localized to the cleavage furrow structure, the midbody, during cytokinesis. This study was able to demonstrate for the

first time that NEDD8 and CSN subunits colocalize with CUL1 and cullin 3 (CUL3) at the cleavage furrow and midbody (Figures 3.4 to 3.6, Figure 5.1 A), and provide evidence supporting a role for on-going neddylation during cytokinesis. Specifically, inhibition of neddylation by MLN4924 induced mitotic defects in asynchronously growing cells (Figure 3.7, Figure 5.1 B), and that treatment of metaphase cells with MLN4924 resulted in the early accumulation of MKLP1 at the midbody concomitant with abscission delay (or failure) and ultimately resulted in chromosome segregation defects including lagging chromosomes and binucleated cells (Figure 3.8, 3.9). Thus, the increase in DNA content measured by flow cytometry seen with prolonged MLN4924 treatment arises not only from endoreplication of DNA but also from mitotic defects elicited by inhibition of neddylation.

Figure 5.1 Summary of important findings regarding the role of neddylation during cytokinesis. (A) The neddylation pathway components NEDD8 and the CSN subunits, along with neddylation substrates the cullin proteins, localized at the midbody during cytokinesis. **(B)** Treatment using the neddylation inhibitor MLN4924 on mitotic cells before anaphase lead to earlier MKLP1 accumulation at the cleavage furrow/midbody, and a delay or failure in abscission.

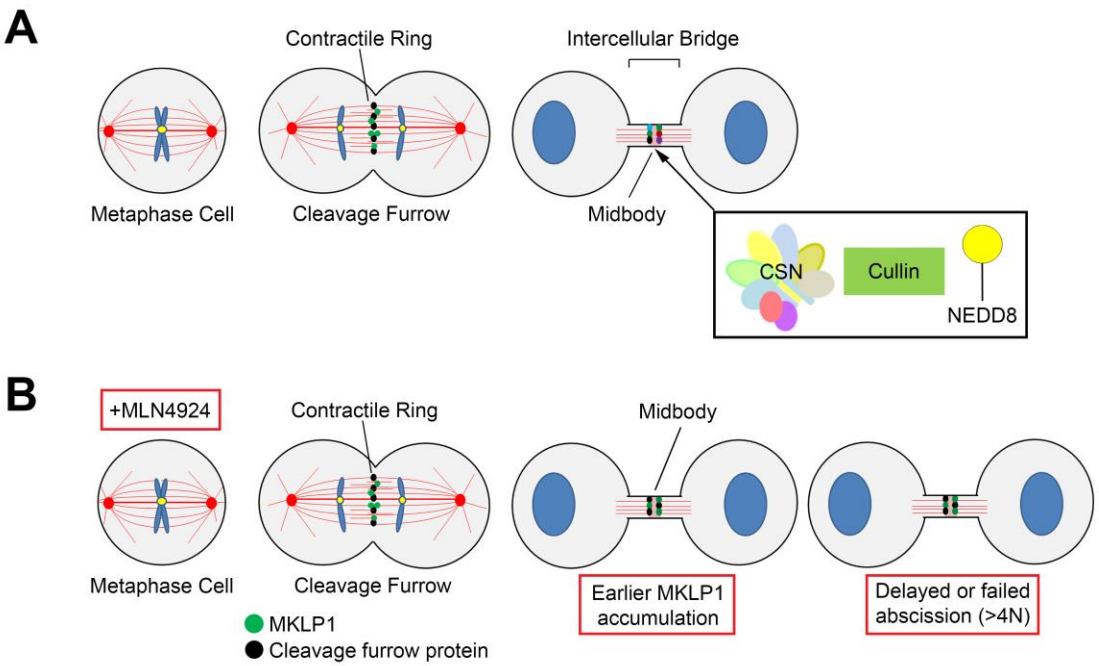

Finally, the role of the CSN in the DNA damage response and neddylation on DNA double-strand break repair, namely homology-directed repair and RAD52 recruitment, was examined. It was found that individual CSN subunits CSN3 and CSN4 responded after laser-induced DNA damage (Figure 4.1), indicated by an increase in nuclear to cytoplasmic signal, however they did not localize to the site of DNA damage within the UV laser "stripe". In addition, it was determined that inhibiting neddylation with MLN4924 did not alter the efficiency of homology-directed repair (HDR) in an asynchronous cell population (Figure 4.2), however treatment of cells with MLN4924 altered RAD52 accumulation at UV laser-induced DNA break sites (Figure 4.3) and appeared to increase single-strand annealing (Figure 4.4).

5.2 The Role of Neddylation and the CSN in Cytokinesis

As described in Chapter 3, chemical inhibition of neddylation with MLN4924 can affect the timing of the accumulation of the key cytokinesis protein MKLP1 to the cleavage furrow. How neddylation regulates mitosis could be through its regulation of the cullin-RING ubiquitin ligases (CRLs). One important finding is that the SKP-cullin-F box (SCF) ubiquitin ligase complex is known to associate at the centrosome, which organizes the mitotic spindle that segregates chromosomes in mitosis [272]. During later stages of mitosis, SCF and CUL3 complexes relocate to the midbody to regulate cytokinesis [130, 190, 192, 272]. Certain inner centromere proteins could be their substrates. For example, the chromosomal passenger complex (CPC) member Aurora B kinase was reported to be targeted by two cullin complexes, SCF-FBXL2 and CUL3, but they target Aurora B at different times during mitosis (Figure 5.2). Before anaphase, Aurora B is localized at chromosomes, but re-localizes to the spindle midzone during anaphase and then to the midbody. Aurora B release from the chromosome is possibly due to CUL3-KLHL9/KLHL13 or CUL3-KLHL21 ubiquitylation [130, 131, 192]. However, in this situation it is likely that the ubiquitylation of Aurora B is not a signal for its degradation. CUL3 has also been observed at the midbody, which suggests that there could be other roles for CUL3 ubiquitin ligases, possibly though interacting with additional substrate adaptors. Aurora B at the midbody is likely targeted by SCF-FBXL2 for proteasomal degradation [190].

Under this model, it is possible that inhibition of CUL3 ubiquitin ligase activity by MLN4924 may alter the localization of midbody-associated proteins. Recent studies have supported this notion since both knockout of the neddylation E3 ligase DCUN1D1

in mouse embryonic fibroblasts and inhibiting neddylation using MLN4924 resulted in altered Aurora B recruitment to the cleavage furrow [192]. Both Aurora B and the CPC protein INCENP have been reported to recruit MKLP1 to the midbody and regulate its activity by phosphorylation [134, 273, 284]. Given that MKLP1 was observed to accumulate at the midbody earlier (Figure 3.8), and its localization at the midbody appeared fragmented at later timepoints (Figure 3.9) after MLN4924 treatment, it is possible that CUL1 and CUL3 neddylation and thus ubiquitin ligase activity could alter Aurora B and INCENP accumulation at the midbody; an event that could in turn alter MKLP1 accumulation. Another candidate protein involved in cytokinesis that is also a substrate of CUL3 is KATNA1 (also known as p60/Katanin in mammals and MEI-1 in *C. elegans*), which localizes to the mitotic spindle during mitosis and is responsible for severing microtubules [285, 286]. KATNA1 localizes to the spindle midzone in anaphase and knock-down of CUL3 by siRNA results in accumulation of KATNA1, which is speculated to alter microtubule integrity and contribute to mitotic defects [286], defects that may also contribute to altered localization of MKLP1. Finally, it was reported that MKLP1 recruits the protein BRUCE to the midbody to aid in abscission [287], raising the possibility that BRUCE localization at the midbody may also be dependent on CRL activity and/or neddylation.

While the most likely targets of neddylation during cytokinesis are CRLs, it is very possible other substrates become neddylated, which impacts their function during cytokinesis. For example, MKLP1 ubiquitylation, mediated by UBPY (also known as USP8) (monoubiquitylation) [287] and TRAF6 (possibly polyubiquitylation) [274], could be altered directly by MKLP1 neddylation on acceptor lysines used for ubiquitylation; a

possibility that is supported by recent evidence that MKLP1 may be neddylated [96]. However, the early accumulation of MKLP1 at the midbody when cells were treated with MLN4924 to inhibit *de novo* neddylation during mitosis is more consistent with the stabilization of MKLP1 in early anaphase rather than increased degradation, which would be the outcome if *de novo* neddylation of MKLP1 during mitosis served to block its ubiquitylation.

In addition to on-going neddylation playing a role in mitosis and cytokinesis, the localization of the CSN at the midbody also implicates protein deneddylation at the cleavage furrow and midbody during cytokinesis. Previous studies have potentially implicated the CSN complex in mitosis through the localization of CSN subunits at centrosomes in human cells [288], which are known to play a role in mitotic spindle formation [289], and the mitotic spindle defects seen in *C. elegans* embryos during the first mitotic cell division after siRNA knock-down of CSN subunits [285]. However, this study is the first to demonstrate that the CSN can also localize to the midbody, and together with previous findings the results indicate that the CSN may be considered an additional "chromosomal passenger protein" complex that localizes progressively from the centrosome to the cleavage furrow, presumably to regulate the activity of cullins as cells progress through mitosis and ultimately cytokinesis. In addition, given the mitotic defects induced by the inhibition of neddylation specifically in mitosis, and the detection of the CSN at the midbody, it could be that cycle(s) of neddylation/deneddylation of cullins (or other protein substrates) may be critical to ensure the tight regulation of the protein stability of cullin substrates during cytokinesis.

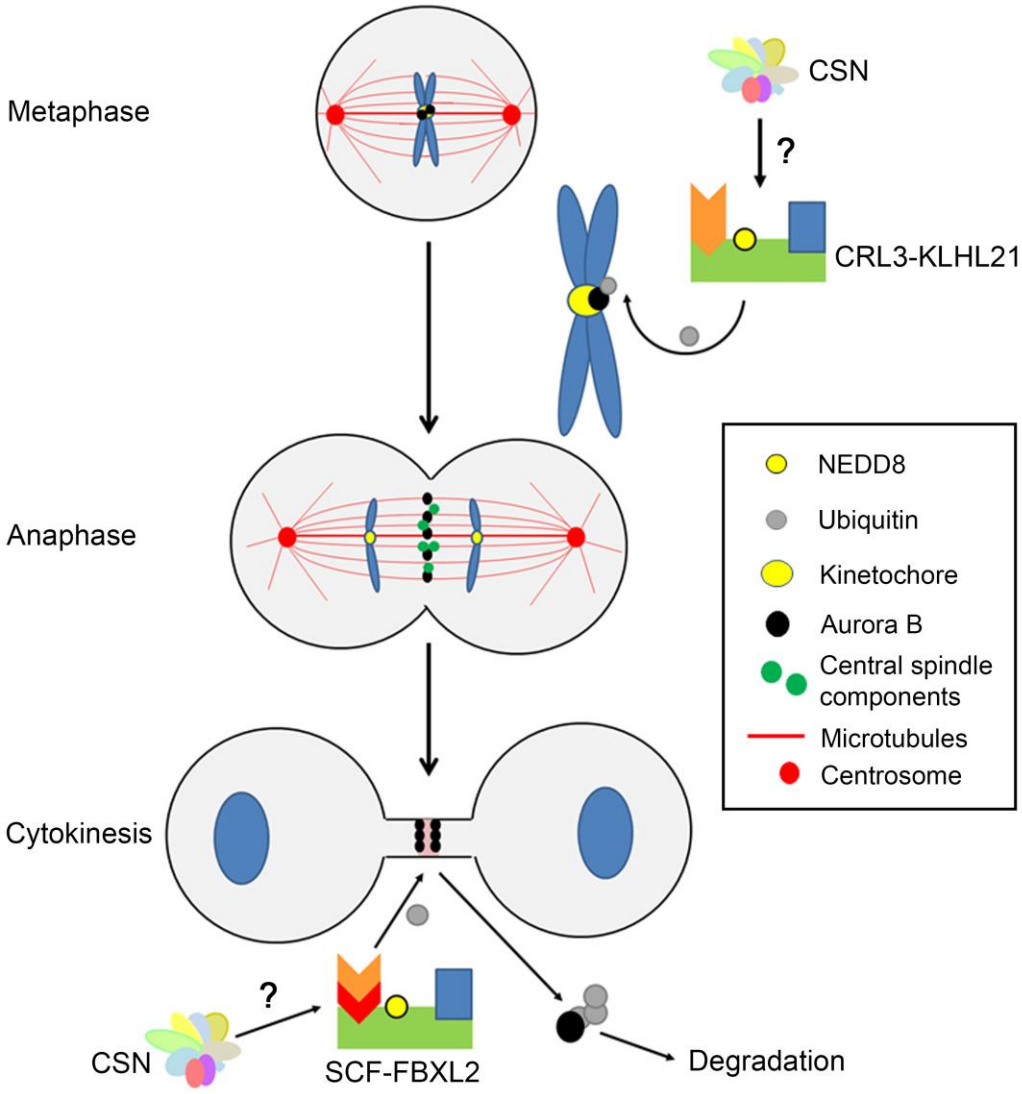

Figure 5.2. Aurora B localization during mitosis and cytokinesis is regulated by cullin-RING E3 ubiquitin ligases. Monoubiquitylation of Aurora B by CRL3-KLHL21 promotes relocation from chromosomes to the spindle midzone during anaphase and later accumulates at the midbody during cytokinesis. Ubiquitylation of Aurora B by the midbody-localized SCF-FBXL2 may promote its degradation. Neddylation and the deneddylase CSN may regulate Aurora B localization and degradation through regulating the CRLs that ubiquitylate Aurora B.

5.2.1 Experimental Limitations

Thus far, the investigation on the role of neddylation during cytokinesis has relied on the use of HeLa cells. HeLa contains sequences from the human papilloma virus 18 (HPV18) and expresses HPV proteins [290, 291]. A consequence of expressing HPV proteins is that HeLa cells, while having a wild-type p53 allele, express the HPV protein E6 that promotes p53 protein degradation, rendering HeLa cells deficient in p53 activity [291]. While not focused on in this study, p53 is active when a cell cycle checkpoint is triggered. For instance, activated p53 following DNA damage regulates CDK activity as well as inducing apoptosis if the damage is too severe [292]. Therefore, HeLa cells are unsuitable for studying p53 regulated processes. The loss of p53 has been reported to increase tetraploidy [293], however that could be due to dysregulated cell cycle checkpoints allowing genomically unstable cells to go through the cell cycle. This could be one explanation for the presence of abnormal mitoses in untreated HeLa cells (Figure 3.7). While p53 activity is so far not linked directly to the abscission checkpoint, wildtype cells that fail to complete cytokinesis (resulting in tetraploidy) do activate p53 and those cells arrest in G1 [294]. Nevertheless, the results found in HeLa cells will have to be verified using a different cell line, such as p53-expressing U-2 OS osteosarcoma cells. To study cellular processes in a normal (diploid) line, another option is the hTERT RPE-1 epithelial cells, which are immortalized by expressing telomerase [295].

Given that many proteins are directly or indirectly regulated by neddylation, the use of MLN4924 to study cellular processes is limited to being used as a broad tool to understand neddylation. An approach to investigating the specific impacts of neddylation on a specific protein may require identifying and modifying the lysine acceptor site(s) on

the substrate. For instance, to validate that MKLP1 is modified by NEDD8, the lysine residue can be mutated to an arginine to remove the potential NEDD8 conjugation site [96]. Wildtype and NEDD8-deficient MKLP1, when expressed in cells as a fusion protein with an immuno-precipitatable epitope, can be assayed for the presence of NEDD8 by western blotting.

5.3 The Role of Neddylation in the DNA Damage Response and DNA Double-strand Break Repair

The DNA damage response (DDR) is tightly controlled by reversible post-translational protein modifications that include the modification with the ubiquitin-like (Ubl) protein NEDD8 (neddylation). Neddylation is a primary regulator of cullin E3 ubiquitin ligase (CRL) activity, which is a family of enzymes that target many DDR proteins. The CSN deneddylase complex has previously been reported to be involved in nucleotide excision repair (NER) by regulating CRL activity including cullin 4 ubiquitin ligases (CRL4) [110, 296, 297]. One of the objectives in this study was to investigate whether CSN subunits respond to UV-laser-induced DNA breaks. Although CSN subunits CSN3 and CSN4 accumulated in the nucleus after DNA damage (Figure 4.1), I did not observe specific recruitment to DNA damage sites as previously reported for CSN3 [64] and CSN5 [260]. It is possible that culturing conditions at the time were not optimized to allow me to see this effect. Damage over the whole nucleus was shown to affect the abundance of CSN subunits in the nucleus, at least in the context of UV-C damage (200-280 nm) [80, 298]. In that study, the cytosolic and nuclear fractions of UV-C-treated cells were obtained and CSN protein abundance was detected by western

blotting. In agreement with my observations using a 405 nm UV laser, they report that CSN subunit protein transiently increased in the nucleus because of redistribution of the total CSN protein pool [80]. While I did not investigate NEDD8 and CRLs in the context of DSBs, it has been reported that NEDD8 and the cullin 4 protein (CUL4A) are recruited to DSBs [64, 260]. It could be that the CSN is brought in to mobilize the DDR through modulating CRL4 activity. A likely outcome of CSN regulation is in the choice of repair pathway for DSBs since it was reported that the depletion of CSN1 by siRNA reduced the extent of end-resection following a DSB [64]. Whether NEDD8 is involved in end-resection specifically is currently unknown and proteins that are involved in this step will have to be analyzed for potential neddylation sites.

This modulation of CRL4 activity by the CSN could be through post-translational modifications to CSN subunits themselves, which would add an additional layer of complexity. Potential phosphorylation sites have been identified in many of the subunits using mass spectrometry [80], however the functional significance of these modifications remains to be determined. A recent mass spectrometry screen in UV-damaged cells identified CSN3 and CSN7A as phosphorylation substrates of ATM [64, 93]. Phosphorylation of CSN3 is functionally significant since the loss of CSN3 phosphorylation was observed to impact the accumulation of the DNA-binding protein RAD51 in IR-treated cells [64]. These ATM-dependent phosphorylation sites on CSN3 and CSN7A map to the C-terminal helical bundle of the holoenzyme [64, 77]. Because the MPN-domain subunits CSN5 and CSN6 are associated with the other subunits by C-terminal helical bundle interactions, it is possible that phosphorylation of CSN subunits

may modulate the positioning of CSN5 relative to the substrate, and potentially CSN5 deneddylase activity.

In my investigation, I observed that MLN4924-treated U-2 OS cells did not affect HDR (Figure 4.2), and based on preliminary findings, appeared to repair DNA DSBs more efficiently by the single-strand annealing (SSA) sub-pathway of homology repair (Figure 4.4). Consistent with neddylation playing a possible role in SSA, MLN4924-treated cells expressing RAD52-GFP, a key protein in SSA, exhibited an extended persistence of RAD52 at DSBs as compared to untreated cells (Figure 4.3). I also observed that RAD52-GFP signal became more unevenly concentrated at later timepoints in MLN4924-treated cells. It is known that changes to chromatin architecture facilitates the DNA damage response by allowing repair factors to access and repair the DSB [299]. Following DNA damage, chromatin regions transiently expand before subsequently re-compacting [300]. The punctate appearance of RAD52-GFP could be from local changes in chromatin compaction. A potential approach to visualize chromatin compaction would be by using a chromatin marker such as a fluorescently-tagged histone protein (e.g. H2B) or a DNA binding dye such as SiR-DNA while performing the protein recruitment studies following laser-induced DNA damage.

It is unclear based on current experiments whether all DSB repair pathway(s) are regulated by neddylation. To address this, additional studies to investigate other DSB repair pathways will need to be done, including non-homologous end-joining (NHEJ) and another homology repair pathway, microhomology-mediated end-joining (MMEJ). Potential reporter assays that are currently available to study NHEJ and MMEJ are the EJ5 assay (to measure total NHEJ activity) [301] and the CRISPR/Cas9-based CRIS-

PITCh assay (to specifically measure MMEJ activity) [302]. It is possible that a lack of neddylation during DDR may promote end-resection; however, a confounding effect would arise from prolonged MLN4924 treatment, and perhaps from prolonged depletion of NEDD8, which would induce 4N (G2) cell accumulation, favouring end-resection-dependent pathways such as HDR and SSA. Additional experiments to factor in cell cycle stage can be performed by direct cell cycle analysis and by using U-2 OS expressing the ES-FUCCI cell cycle reporter system when performing protein recruitment studies after DNA damage. If the SeeSaw 2.0 reporter assay was to be performed in MLN4924-treated cells, I hypothesize that the outcome would favour end-resection-dependent pathways, such as SSA, over end-joining by NHEJ.

5.4 Consequences of Dysregulating Neddylation

Regulating CRL activity alone through neddylation can affect many cellular pathways. It is not surprising that dysregulated neddylation can compromise the organism and lead to disease. For example, in the process of infecting animal cells including those of humans, enteropathogenic *E. coli* and *Burkholderia pseudomallei* secrete Cif (Cycle inhibiting factor) and CHBP, respectively [303, 304]. The secreted proteins deamidate NEDD8, leading to G1/S and G2/M checkpoint activation and apoptosis [303, 305, 306]. Mounting evidence also suggests that the dysregulation of neddylation can contribute to cancer development, as discussed in the next section.

5.4.1 Neddylation and the CSN in Cancer Development

Several characteristics define cancer cells, which include the loss of normal cell cycle control and genome instability [307]. There is mounting evidence to show that cancer cells have altered neddylation states. For example, pancreatic and hepatocellular carcinoma tumors with elevated global neddylation levels and increased NAE1 protein expression have been connected to worse patient survival [308, 309]. CSN subunits also appear to show oncogenic potential. In some human cancers, elevated expression levels of CSN5 and CSN6 are correlated with cancer progression and poor prognosis [226, 262, 310, 311, 312]. A situation arises where a tumour could have both elevated expression of neddylation pathway proteins as well as elevated expression of CSN proteins. Why that is the case will require further investigations into the mechanism, but it is speculated that either the cell compensates for the overall increase in neddylation by upregulating deneddylation, or that the CSN performs secondary roles that are indirectly or independent of cullin deneddylation. As an example, CSN5 is upregulated in hepatocellular carcinomas, which has been purported to promote the targeting of p57 for degradation [313]; however, loss of CSN5 can lead to the stabilization of p57 which can inhibit hepatocellular carcinoma cell growth [314]. This would be contrary to the idea that loss of CSN5 deneddylation would stabilize neddylated CUL1-SKP2, allowing CUL1-SKP2 to ubiquitylate p57 and promote its subsequent degradation [163].

Inhibiting neddylation has shown promise in reducing tumour load under laboratory conditions [315], and researchers have begun using the inhibitor MLN4924 in human clinical trials. The findings presented in this study help to provide a rationale for combination therapies that combine neddylation pathway inhibitors and conventional

chemotherapy. The finding that MLN4924 can induce mitotic defects in cells suggests that inhibition of neddylation could synergize with specific chemotherapies that target proliferating cancer cells, such as microtubule poisons vincristine and taxanes [316]. The finding that inhibiting neddylation may increase homology-directed repair (HDR) and promote RAD52-mediated SSA DNA repair is promising for combining MLN4924 with DNA damaging/break-inducing agents such as platinum-derived compounds for treating tumours that are deficient in HDR. Other studies have shown that BRCA2-deficient tumor cells can employ RAD52 to partially rescue HDR [317]. Treatment of cells with MLN4924 in this context could be combined with a RAD52 inhibitor [318] to more effectively inhibit tumor growth. In support of combination therapies utilizing MLN4924 and anti-mitotic agents and/or DNA damaging agents, a recent clinical trial has demonstrated that MLN4924 has shown efficacy against solid tumors when combined with the taxane paclitaxel and DNA damaging agent carboplatin [319].

5.5 Concluding Remarks

There is growing evidence, and acceptance, that post-translational modifications of proteins (e.g. neddylation) are carefully regulated and are subjected to positive and negative control. The finely-tuned interplay between NEDD8, cullin ubiquitin ligases and the CSN is just one example of an emerging regulatory unit that protects the complex biological systems of cell division and the DNA damage response. The findings in this study extend our knowledge of the role of neddylation in cytokinesis and DNA repair, which may one day be translated into developing more effective cancer therapies.

REFERENCES

1. Chung D, Dellaire G. The Role of the COP9 Signalosome and Neddylation in DNA Damage Signaling and Repair. Biomolecules. 2015 Sep 30;5(4):2388-416. doi: 10.3390/biom5042388. PubMed PMID: 26437438; PubMed Central PMCID: PMCPMC4693240.

2. Lecker SH, Goldberg AL, Mitch WE. Protein degradation by the ubiquitin-proteasome pathway in normal and disease states. J Am Soc Nephrol. 2006 Jul;17(7):1807-19. doi: 10.1681/ASN.2006010083. PubMed PMID: 16738015.

3. Jacobson AD, Zhang NY, Xu P, et al. The lysine 48 and lysine 63 ubiquitin conjugates are processed differently by the 26 s proteasome. J Biol Chem. 2009 Dec 18;284(51):35485-94. doi: 10.1074/jbc.M109.052928. PubMed PMID: 19858201; PubMed Central PMCID: PMCPMC2790978.

4. Jin L, Williamson A, Banerjee S, et al. Mechanism of ubiquitin-chain formation by the human anaphase-promoting complex. Cell. 2008 May 16;133(4):653-65. doi: 10.1016/j.cell.2008.04.012. PubMed PMID: 18485873; PubMed Central PMCID: PMCPMC2696189.

5. Chen ZJ, Sun LJ. Nonproteolytic functions of ubiquitin in cell signaling. Mol Cell. 2009 Feb 13;33(3):275-86. doi: 10.1016/j.molcel.2009.01.014. PubMed PMID: 19217402.

6. Deshaies RJ, Joazeiro CA. RING domain E3 ubiquitin ligases. Annu Rev Biochem. 2009;78:399-434. doi: 10.1146/annurev.biochem.78.101807.093809. PubMed PMID: 19489725.

7. Hochstrasser M. Origin and function of ubiquitin-like proteins. Nature. 2009 Mar 26;458(7237):422-9. doi: 10.1038/nature07958. PubMed PMID: 19325621; PubMed Central PMCID: PMCPMC2819001.

8. van der Veen AG, Ploegh HL. Ubiquitin-like proteins. Annu Rev Biochem. 2012;81:323-57. doi: 10.1146/annurev-biochem-093010-153308. PubMed PMID: 22404627.

9. Kumar S, Tomooka Y, Noda M. Identification of a set of genes with developmentally down-regulated expression in the mouse brain. Biochem Biophys Res Commun. 1992 Jun 30;185(3):1155-61. PubMed PMID: 1378265.

10. Kumar S, Yoshida Y, Noda M. Cloning of a cDNA which encodes a novel ubiquitin-like protein. Biochem Biophys Res Commun. 1993 Aug 31;195(1):393-9. doi: 10.1006/bbrc.1993.2056. PubMed PMID: 8395831.

11. Kamitani T, Kito K, Nguyen HP, et al. Characterization of NEDD8, a developmentally down-regulated ubiquitin-like protein. J Biol Chem. 1997 Nov 7;272(45):28557-62. PubMed PMID: 9353319.

12. Whitby FG, Xia G, Pickart CM, et al. Crystal structure of the human ubiquitin-like protein NEDD8 and interactions with ubiquitin pathway enzymes. J Biol Chem. 1998 Dec 25;273(52):34983-91. PubMed PMID: 9857030.

13. Chan Y, Yoon J, Wu JT, et al. DEN1 deneddylates non-cullin proteins in vivo. J Cell Sci. 2008 Oct 1;121(Pt 19):3218-23. doi: 10.1242/jcs.030445. PubMed PMID: 18782863.

14. Mendoza HM, Shen LN, Botting C, et al. NEDP1, a highly conserved cysteine protease that deNEDDylates Cullins. J Biol Chem. 2003 Jul 11;278(28):25637-43. doi: 10.1074/jbc.M212948200. PubMed PMID: 12730221.

15. Wu K, Yamoah K, Dolios G, et al. DEN1 is a dual function protease capable of processing the C terminus of Nedd8 and deconjugating hyper-neddylated CUL1. J Biol Chem. 2003 Aug 1;278(31):28882-91. doi: 10.1074/jbc.M302888200. PubMed PMID: 12759363.

16. Wada H, Kito K, Caskey LS, et al. Cleavage of the C-terminus of NEDD8 by UCH-L3. Biochem Biophys Res Commun. 1998 Oct 29;251(3):688-92. doi: 10.1006/bbrc.1998.9532. PubMed PMID: 9790970.

17. Walden H, Podgorski MS, Huang DT, et al. The structure of the APPBP1-UBA3-NEDD8-ATP complex reveals the basis for selective ubiquitin-like protein activation by an E1. Mol Cell. 2003 Dec;12(6):1427-37. PubMed PMID: 14690597.

18. Bohnsack RN, Haas AL. Conservation in the mechanism of Nedd8 activation by the human AppBp1-Uba3 heterodimer. J Biol Chem. 2003 Jul 18;278(29):26823-30. doi: 10.1074/jbc.M303177200. PubMed PMID: 12740388.

19. Gong L, Yeh ET. Identification of the activating and conjugating enzymes of the NEDD8 conjugation pathway. J Biol Chem. 1999 Apr 23;274(17):12036-42. PubMed PMID: 10207026.

20. Osaka F, Kawasaki H, Aida N, et al. A new NEDD8-ligating system for cullin-4A. Genes Dev. 1998 Aug 1;12(15):2263-8. PubMed PMID: 9694792; PubMed Central PMCID: PMCPMC317039.

21. Watson IR, Irwin MS, Ohh M. NEDD8 pathways in cancer, Sine Quibus Non. Cancer Cell. 2011 Feb 15;19(2):168-76. doi: 10.1016/j.ccr.2011.01.002. PubMed PMID: 21316600.

22. Petroski MD, Deshaies RJ. Function and regulation of cullin-RING ubiquitin ligases. Nat Rev Mol Cell Biol. 2005 Jan;6(1):9-20. doi: 10.1038/nrm1547. PubMed PMID: 15688063.

23. Huang DT, Ayrault O, Hunt HW, et al. E2-RING expansion of the NEDD8 cascade confers specificity to cullin modification. Mol Cell. 2009 Feb 27;33(4):483-95. doi: 10.1016/j.molcel.2009.01.011. PubMed PMID: 19250909; PubMed Central PMCID: PMCPMC2725360.

24. Scott DC, Monda JK, Grace CR, et al. A dual E3 mechanism for Rub1 ligation to Cdc53. Mol Cell. 2010 Sep 10;39(5):784-96. doi: 10.1016/j.molcel.2010.08.030. PubMed PMID: 20832729; PubMed Central PMCID: PMCPMC3001161.

25. Kamura T, Conrad MN, Yan Q, et al. The Rbx1 subunit of SCF and VHL E3 ubiquitin ligase activates Rub1 modification of cullins Cdc53 and Cul2. Genes Dev. 1999 Nov 15;13(22):2928-33. PubMed PMID: 10579999; PubMed Central PMCID: PMCPMC317157.

26. Ma T, Chen Y, Zhang F, et al. RNF111-dependent neddylation activates DNA damage-induced ubiquitination. Mol Cell. 2013 Mar 7;49(5):897-907. doi: 10.1016/j.molcel.2013.01.006. PubMed PMID: 23394999; PubMed Central PMCID: PMCPMC3595365.

27. Kurz T, Chou YC, Willems AR, et al. Dcn1 functions as a scaffold-type E3 ligase for cullin neddylation. Mol Cell. 2008 Jan 18;29(1):23-35. doi: 10.1016/j.molcel.2007.12.012. PubMed PMID: 18206966.

28. Kurz T, Ozlu N, Rudolf F, et al. The conserved protein DCN-1/Dcn1p is required for cullin neddylation in C. elegans and S. cerevisiae. Nature. 2005 Jun 30;435(7046):1257-61. doi: 10.1038/nature03662. PubMed PMID: 15988528.

29. Kim AY, Bommelje CC, Lee BE, et al. SCCRO (DCUN1D1) is an essential component of the E3 complex for neddylation. J Biol Chem. 2008 Nov 28;283(48):33211-20. doi: 10.1074/jbc.M804440200. PubMed PMID: 18826954; PubMed Central PMCID: PMCPMC2586271.

30. Meyer-Schaller N, Chou YC, Sumara I, et al. The human Dcn1-like protein DCNL3 promotes Cul3 neddylation at membranes. Proc Natl Acad Sci U S A. 2009 Jul 28;106(30):12365-70. doi: 10.1073/pnas.0812528106. PubMed PMID: 19617556; PubMed Central PMCID: PMCPMC2718329.

31. Monda JK, Scott DC, Miller DJ, et al. Structural conservation of distinctive N-terminal acetylation-dependent interactions across a family of mammalian NEDD8 ligation enzymes. Structure. 2013 Jan 8;21(1):42-53. doi: 10.1016/j.str.2012.10.013. PubMed PMID: 23201271; PubMed Central PMCID: PMCPMC3786212.

32. Huang G, Kaufman AJ, Ramanathan Y, et al. SCCRO (DCUN1D1) promotes nuclear translocation and assembly of the neddylation E3 complex. J Biol Chem. 2011 Mar 25;286(12):10297-304. doi: 10.1074/jbc.M110.203729. PubMed PMID: 21247897; PubMed Central PMCID: PMCPMC3060484.

33. Huang G, Stock C, Bommelje CC, et al. SCCRO3 (DCUN1D3) antagonizes the neddylation and oncogenic activity of SCCRO (DCUN1D1). J Biol Chem. 2014 Dec 12;289(50):34728-42. doi: 10.1074/jbc.M114.585505. PubMed PMID: 25349211; PubMed Central PMCID: PMCPMC4263876.

34. Xirodimas DP, Saville MK, Bourdon JC, et al. Mdm2-mediated NEDD8 conjugation of p53 inhibits its transcriptional activity. Cell. 2004 Jul 9;118(1):83-97. doi: 10.1016/j.cell.2004.06.016. PubMed PMID: 15242646.

35. Zuo W, Huang F, Chiang YJ, et al. c-Cbl-mediated neddylation antagonizes ubiquitination and degradation of the TGF-beta type II receptor. Mol Cell. 2013 Feb 7;49(3):499-510. doi: 10.1016/j.molcel.2012.12.002. PubMed PMID: 23290524.

36. Oved S, Mosesson Y, Zwang Y, et al. Conjugation to Nedd8 instigates ubiquitylation and down-regulation of activated receptor tyrosine kinases. J Biol Chem. 2006 Aug 4;281(31):21640-51. doi: 10.1074/jbc.M513034200. PubMed PMID: 16735510.

37. Rabut G, Le Dez G, Verma R, et al. The TFIIH subunit Tfb3 regulates cullin neddylation. Mol Cell. 2011 Aug 5;43(3):488-95. doi: 10.1016/j.molcel.2011.05.032. PubMed PMID: 21816351; PubMed Central PMCID: PMCPMC3186349.

38. Noguchi K, Okumura F, Takahashi N, et al. TRIM40 promotes neddylation of IKKgamma and is downregulated in gastrointestinal cancers. Carcinogenesis. 2011 Jul;32(7):995-1004. doi: 10.1093/carcin/bgr068. PubMed PMID: 21474709.

39. Xie P, Zhang M, He S, et al. The covalent modifier Nedd8 is critical for the activation of Smurf1 ubiquitin ligase in tumorigenesis. Nat Commun. 2014 May 13;5:3733. doi: 10.1038/ncomms4733. PubMed PMID: 24821572.

40. Jones J, Wu K, Yang Y, et al. A targeted proteomic analysis of the ubiquitin-like modifier nedd8 and associated proteins. J Proteome Res. 2008 Mar;7(3):1274-87. doi: 10.1021/pr700749v. PubMed PMID: 18247557; PubMed Central PMCID: PMCPMC2676899.

41. Cope GA, Suh GS, Aravind L, et al. Role of predicted metalloprotease motif of Jab1/Csn5 in cleavage of Nedd8 from Cul1. Science. 2002 Oct 18;298(5593):608-11. doi: 10.1126/science.1075901. PubMed PMID: 12183637.

42. Gan-Erdene T, Nagamalleswari K, Yin L, et al. Identification and characterization of DEN1, a deneddylase of the ULP family. J Biol Chem. 2003 Aug 1;278(31):28892-900. doi: 10.1074/jbc.M302890200. PubMed PMID: 12759362.

43. Mergner J, Heinzlmeir S, Kuster B, et al. DENEDDYLASE1 deconjugates NEDD8 from non-cullin protein substrates in Arabidopsis thaliana. Plant Cell. 2015 Mar;27(3):741-53. doi: 10.1105/tpc.114.135996. PubMed PMID: 25783028; PubMed Central PMCID: PMCPMC4558671.

44. Christmann M, Schmaler T, Gordon C, et al. Control of multicellular development by the physically interacting deneddylases DEN1/DenA and COP9 signalosome. PLoS Genet. 2013;9(2):e1003275. doi: 10.1371/journal.pgen.1003275. PubMed PMID: 23408908; PubMed Central PMCID: PMCPMC3567183.

45. Ferro A, Carvalho AL, Teixeira-Castro A, et al. NEDD8: a new ataxin-3 interactor. Biochim Biophys Acta. 2007 Nov;1773(11):1619-27. doi: 10.1016/j.bbamcr.2007.07.012. PubMed PMID: 17935801.

46. Wei N, Chamovitz DA, Deng XW. Arabidopsis COP9 is a component of a novel signaling complex mediating light control of development. Cell. 1994 Jul 15;78(1):117-24. PubMed PMID: 8033203.

47. Seeger M, Kraft R, Ferrell K, et al. A novel protein complex involved in signal transduction possessing similarities to 26S proteasome subunits. FASEB J. 1998 Apr;12(6):469-78. PubMed PMID: 9535219.

48. Freilich S, Oron E, Kapp Y, et al. The COP9 signalosome is essential for development of Drosophila melanogaster. Curr Biol. 1999 Oct 21;9(20):1187-90. doi: 10.1016/S0960-9822(00)80023-8. PubMed PMID: 10531038.

49. Wei N, Deng XW. Characterization and purification of the mammalian COP9 complex, a conserved nuclear regulator initially identified as a repressor of photomorphogenesis in higher plants. Photochem Photobiol. 1998 Aug;68(2):237-41. PubMed PMID: 9723217.

50. Mundt KE, Porte J, Murray JM, et al. The COP9/signalosome complex is conserved in fission yeast and has a role in S phase. Curr Biol. 1999 Dec 2;9(23):1427-30. PubMed PMID: 10607571.

51. Maytal-Kivity V, Pick E, Piran R, et al. The COP9 signalosome-like complex in S. cerevisiae and links to other PCI complexes. Int J Biochem Cell Biol. 2003 May;35(5):706-15. PubMed PMID: 12672462.

52. Rajan KE, Rajkumar R, Liao CC, et al. Light-induced COP9 signalosome expression in the Indian false vampire bat Megaderma lyra. J Physiol Sci. 2010 Jan;60(1):43-9. doi: 10.1007/s12576-009-0064-4. PubMed PMID: 19787423.

53. Wee S, Hetfeld B, Dubiel W, et al. Conservation of the COP9/signalosome in budding yeast. BMC Genet. 2002 Aug 20;3:15. PubMed PMID: 12186635; PubMed Central PMCID: PMCPMC126249.

54. Lima JF, Malavazi I, von Zeska Kress Fagundes MR, et al. The csnD/csnE signalosome genes are involved in the Aspergillus nidulans DNA damage response. Genetics. 2005 Nov;171(3):1003-15. doi: 10.1534/genetics.105.041376. PubMed PMID: 16079239; PubMed Central PMCID: PMCPMC1456808.

55. Wei N, Serino G, Deng XW. The COP9 signalosome: more than a protease. Trends Biochem Sci. 2008 Dec;33(12):592-600. doi: 10.1016/j.tibs.2008.09.004. PubMed PMID: 18926707.

56. Oron E, Mannervik M, Rencus S, et al. COP9 signalosome subunits 4 and 5 regulate multiple pleiotropic pathways in Drosophila melanogaster. Development. 2002 Oct;129(19):4399-409. PubMed PMID: 12223399.

57. Lykke-Andersen K, Schaefer L, Menon S, et al. Disruption of the COP9 signalosome Csn2 subunit in mice causes deficient cell proliferation, accumulation of p53 and cyclin E, and early embryonic death. Mol Cell Biol. 2003 Oct;23(19):6790-7. PubMed PMID: 12972599; PubMed Central PMCID: PMCPMC193936.

58. Rosel D, Kimmel AR. The COP9 signalosome regulates cell proliferation of Dictyostelium discoideum. Eur J Cell Biol. 2006 Sep;85(9-10):1023-34. doi: 10.1016/j.ejcb.2006.04.006. PubMed PMID: 16781008.

59. Panattoni M, Maiorino L, Lukacs A, et al. The COP9 signalosome is a repressor of replicative stress responses and polyploidization in the regenerating liver. Hepatology. 2014 Jun;59(6):2331-43. doi: 10.1002/hep.27028. PubMed PMID: 24452456.

60. Lyapina S, Cope G, Shevchenko A, et al. Promotion of NEDD-CUL1 conjugate cleavage by COP9 signalosome. Science. 2001 May 18;292(5520):1382-5. doi: 10.1126/science.1059780. PubMed PMID: 11337588.

61. Henke W, Ferrell K, Bech-Otschir D, et al. Comparison of human COP9 signalsome and 26S proteasome lid'. Mol Biol Rep. 1999 Apr;26(1-2):29-34. PubMed PMID: 10363643.

62. Uhle S, Medalia O, Waldron R, et al. Protein kinase CK2 and protein kinase D are associated with the COP9 signalosome. EMBO J. 2003 Mar 17;22(6):1302-12. doi: 10.1093/emboj/cdg127. PubMed PMID: 12628923; PubMed Central PMCID: PMCPMC151059.

63. Huang X, Wagner E, Dumdey R, et al. Phosphorylation by COP9 Signalosome-Associated CK2 Promotes Degradation of p27 during the G1 Cell Cycle Phase. Israel Journal of Chemistry. 2006;46(2):231-238. doi: doi:10.1560/9219-25WN-YU1K-GDVV.

64. Meir M, Galanty Y, Kashani L, et al. The COP9 signalosome is vital for timely repair of DNA double-strand breaks. Nucleic Acids Res. 2015 May 19;43(9):4517-30. doi: 10.1093/nar/gkv270. PubMed PMID: 25855810; PubMed Central PMCID: PMCPMC4482063.

65. Sun Y, Wilson MP, Majerus PW. Inositol 1,3,4-trisphosphate 5/6-kinase associates with the COP9 signalosome by binding to CSN1. J Biol Chem. 2002 Nov 29;277(48):45759-64. doi: 10.1074/jbc.M208709200. PubMed PMID: 12324474.

66. Glickman MH, Rubin DM, Coux O, et al. A subcomplex of the proteasome regulatory particle required for ubiquitin-conjugate degradation and related to the COP9-signalosome and eIF3. Cell. 1998 Sep 4;94(5):615-23. PubMed PMID: 9741626.

67. Kwok SF, Staub JM, Deng XW. Characterization of two subunits of Arabidopsis 19S proteasome regulatory complex and its possible interaction with the COP9 complex. J Mol Biol. 1999 Jan 8;285(1):85-95. doi: 10.1006/jmbi.1998.2315. PubMed PMID: 9878390.

68. Yahalom A, Kim TH, Winter E, et al. Arabidopsis eIF3e (INT-6) associates with both eIF3c and the COP9 signalosome subunit CSN7. J Biol Chem. 2001 Jan 5;276(1):334-40. doi: 10.1074/jbc.M006721200. PubMed PMID: 11029466.

69. Claret FX, Hibi M, Dhut S, et al. A new group of conserved coactivators that increase the specificity of AP-1 transcription factors. Nature. 1996 Oct 3;383(6599):453-7. doi: 10.1038/383453a0. PubMed PMID: 8837781.

70. Olma MH, Roy M, Le Bihan T, et al. An interaction network of the mammalian COP9 signalosome identifies Dda1 as a core subunit of multiple Cul4-based E3 ligases. J Cell Sci. 2009 Apr 1;122(Pt 7):1035-44. doi: 10.1242/jcs.043539. PubMed PMID: 19295130; PubMed Central PMCID: PMCPMC2720933.

71. Kapelari B, Bech-Otschir D, Hegerl R, et al. Electron microscopy and subunit-subunit interaction studies reveal a first architecture of COP9 signalosome. J Mol Biol. 2000 Jul 28;300(5):1169-78. doi: 10.1006/jmbi.2000.3912. PubMed PMID: 10903862.

72. Sharon M, Mao H, Boeri Erba E, et al. Symmetrical modularity of the COP9 signalosome complex suggests its multifunctionality. Structure. 2009 Jan 14;17(1):31-40. doi: 10.1016/j.str.2008.10.012. PubMed PMID: 19141280.

73. Enchev RI, Schreiber A, Beuron F, et al. Structural insights into the COP9 signalosome and its common architecture with the 26S proteasome lid and eIF3. Structure. 2010 Mar 14;18(4):518-27. doi: 10.1016/j.str.2010.02.008. PubMed PMID: 20399188.

74. Kotiguda GG, Weinberg D, Dessau M, et al. The organization of a CSN5-containing subcomplex of the COP9 signalosome. J Biol Chem. 2012 Dec 7;287(50):42031-41. doi: 10.1074/jbc.M112.387977. PubMed PMID: 23086934; PubMed Central PMCID: PMCPMC3516749.

75. Lee JH, Yi L, Li J, et al. Crystal structure and versatile functional roles of the COP9 signalosome subunit 1. Proc Natl Acad Sci U S A. 2013 Jul 16;110(29):11845-50. doi: 10.1073/pnas.1302418110. PubMed PMID: 23818606; PubMed Central PMCID: PMCPMC3718139.

76. Rockel B, Schmaler T, Huang X, et al. Electron microscopy and in vitro deneddylation reveal similar architectures and biochemistry of isolated human and Flag-mouse COP9 signalosome complexes. Biochem Biophys Res Commun. 2014 Jul 25;450(2):991-7. doi: 10.1016/j.bbrc.2014.06.093. PubMed PMID: 24973710.

77. Lingaraju GM, Bunker RD, Cavadini S, et al. Crystal structure of the human COP9 signalosome. Nature. 2014 Aug 14;512(7513):161-5. doi: 10.1038/nature13566. PubMed PMID: 25043011.

78. Birol M, Enchev RI, Padilla A, et al. Structural and biochemical characterization of the Cop9 signalosome CSN5/CSN6 heterodimer. PLoS One. 2014;9(8):e105688. doi: 10.1371/journal.pone.0105688. PubMed PMID: 25144743; PubMed Central PMCID: PMCPMC4140821.

79. Echalier A, Pan Y, Birol M, et al. Insights into the regulation of the human COP9 signalosome catalytic subunit, CSN5/Jab1. Proc Natl Acad Sci U S A. 2013 Jan 22;110(4):1273-8. doi: 10.1073/pnas.1209345110. PubMed PMID: 23288897; PubMed Central PMCID: PMCPMC3557056.

80. Fuzesi-Levi MG, Ben-Nissan G, Bianchi E, et al. Dynamic regulation of the COP9 signalosome in response to DNA damage. Mol Cell Biol. 2014 Mar;34(6):1066-76. doi: 10.1128/MCB.01598-13. PubMed PMID: 24421388; PubMed Central PMCID: PMCPMC3958043.

81. Yoshida A, Yoneda-Kato N, Kato JY. CSN5 specifically interacts with CDK2 and controls senescence in a cytoplasmic cyclin E-mediated manner. Sci Rep. 2013;3:1054. doi: 10.1038/srep01054. PubMed PMID: 23316279; PubMed Central PMCID: PMCPMC3542532.

82. Liu C, Guo LQ, Menon S, et al. COP9 signalosome subunit Csn8 is involved in maintaining proper duration of the G1 phase. J Biol Chem. 2013 Jul 12;288(28):20443-52. doi: 10.1074/jbc.M113.468959. PubMed PMID: 23689509; PubMed Central PMCID: PMCPMC3711310.

83. Mundt KE, Liu C, Carr AM. Deletion mutants in COP9/signalosome subunits in fission yeast Schizosaccharomyces pombe display distinct phenotypes. Mol Biol Cell. 2002 Feb;13(2):493-502. doi: 10.1091/mbc.01-10-0521. PubMed PMID: 11854407; PubMed Central PMCID: PMCPMC65644.

84. Chamovitz DA, Wei N, Osterlund MT, et al. The COP9 complex, a novel multisubunit nuclear regulator involved in light control of a plant developmental switch. Cell. 1996 Jul 12;86(1):115-21. PubMed PMID: 8689678.

85. Huang J, Yuan H, Lu C, et al. Jab1 mediates protein degradation of the Rad9-Rad1-Hus1 checkpoint complex. J Mol Biol. 2007 Aug 10;371(2):514-27. doi: 10.1016/j.jmb.2007.05.095. PubMed PMID: 17583730; PubMed Central PMCID: PMCPMC2712929.

86. Hunter C, Evans J, Valencik ML. Subunit 3 of the COP9 signalosome is poised to facilitate communication between the extracellular matrix and the nucleus through the muscle-specific beta1D integrin. Cell Commun Adhes. 2008 Sep;15(3):247-60. doi: 10.1080/15419060802198660. PubMed PMID: 18979294.

87. Wang J, Barnes RO, West NR, et al. Jab1 is a target of EGFR signaling in ERalpha-negative breast cancer. Breast Cancer Res. 2008;10(3):R51. doi: 10.1186/bcr2105. PubMed PMID: 18534028; PubMed Central PMCID: PMCPMC2481501.

88. Groisman R, Polanowska J, Kuraoka I, et al. The ubiquitin ligase activity in the DDB2 and CSA complexes is differentially regulated by the COP9 signalosome in response to DNA damage. Cell. 2003 May 2;113(3):357-67. PubMed PMID: 12732143.

89. Huang X, Langelotz C, Hetfeld-Pechoc BK, et al. The COP9 signalosome mediates beta-catenin degradation by deneddylation and blocks adenomatous polyposis coli destruction via USP15. J Mol Biol. 2009 Aug 28;391(4):691-702. doi: 10.1016/j.jmb.2009.06.066. PubMed PMID: 19576224.

90. Feist M, Huang X, Muller JM, et al. Can hyperthermic intraperitoneal chemotherapy efficiency be improved by blocking the DNA repair factor COP9 signalosome? Int J Colorectal Dis. 2014 Jun;29(6):673-80. doi: 10.1007/s00384-014-1861-7. PubMed PMID: 24728517.

91. Shiloh Y. The ATM-mediated DNA-damage response: taking shape. Trends Biochem Sci. 2006 Jul;31(7):402-10. doi: 10.1016/j.tibs.2006.05.004. PubMed PMID: 16774833.

92. Olsen JV, Vermeulen M, Santamaria A, et al. Quantitative phosphoproteomics reveals widespread full phosphorylation site occupancy during mitosis. Sci Signal. 2010 Jan 12;3(104):ra3. doi: 10.1126/scisignal.2000475. PubMed PMID: 20068231.

93. Matsuoka S, Ballif BA, Smogorzewska A, et al. ATM and ATR substrate analysis reveals extensive protein networks responsive to DNA damage. Science. 2007 May 25;316(5828):1160-6. doi: 10.1126/science.1140321. PubMed PMID: 17525332.

94. Xue Y, Chen J, Choi HH, et al. HER2-Akt signaling in regulating COP9 signalsome subunit 6 and p53. Cell Cycle. 2012 Nov 15;11(22):4181-90. doi: 10.4161/cc.22413. PubMed PMID: 23095642; PubMed Central PMCID: PMCPMC3524214.

95. Hjerpe R, Thomas Y, Kurz T. NEDD8 overexpression results in neddylation of ubiquitin substrates by the ubiquitin pathway. J Mol Biol. 2012 Aug 3;421(1):27-9. doi: 10.1016/j.jmb.2012.05.013. PubMed PMID: 22608973.

96. Coleman KE, Bekes M, Chapman JR, et al. SENP8 limits aberrant neddylation of NEDD8 pathway components to promote cullin-RING ubiquitin ligase function. Elife. 2017 May 5;6. doi: 10.7554/eLife.24325. PubMed PMID: 28475037; PubMed Central PMCID: PMCPMC5419743.

97. Lydeard JR, Schulman BA, Harper JW. Building and remodelling Cullin-RING E3 ubiquitin ligases. EMBO Rep. 2013 Dec;14(12):1050-61. doi: 10.1038/embor.2013.173. PubMed PMID: 24232186; PubMed Central PMCID: PMCPMC3849489.

98. Hori T, Osaka F, Chiba T, et al. Covalent modification of all members of human cullin family proteins by NEDD8. Oncogene. 1999 Nov 18;18(48):6829-34. doi: 10.1038/sj.onc.1203093. PubMed PMID: 10597293.

99. Pan ZQ, Kentsis A, Dias DC, et al. Nedd8 on cullin: building an expressway to protein destruction. Oncogene. 2004 Mar 15;23(11):1985-97. doi: 10.1038/sj.onc.1207414. PubMed PMID: 15021886.

100. Duda DM, Borg LA, Scott DC, et al. Structural insights into NEDD8 activation of cullin-RING ligases: conformational control of conjugation. Cell. 2008 Sep 19;134(6):995-1006. doi: 10.1016/j.cell.2008.07.022. PubMed PMID: 18805092; PubMed Central PMCID: PMCPMC2628631.

101. Brownell JE, Sintchak MD, Gavin JM, et al. Substrate-assisted inhibition of ubiquitin-like protein-activating enzymes: the NEDD8 E1 inhibitor MLN4924 forms a NEDD8-AMP mimetic in situ. Mol Cell. 2010 Jan 15;37(1):102-11. doi: 10.1016/j.molcel.2009.12.024. PubMed PMID: 20129059.

102. Soucy TA, Smith PG, Milhollen MA, et al. An inhibitor of NEDD8-activating enzyme as a new approach to treat cancer. Nature. 2009 Apr 9;458(7239):732-6. doi: 10.1038/nature07884. PubMed PMID: 19360080.

103. Enchev RI, Scott DC, da Fonseca PC, et al. Structural basis for a reciprocal regulation between SCF and CSN. Cell Rep. 2012 Sep 27;2(3):616-27. doi: 10.1016/j.celrep.2012.08.019. PubMed PMID: 22959436; PubMed Central PMCID: PMCPMC3703508.

104. Liu J, Furukawa M, Matsumoto T, et al. NEDD8 modification of CUL1 dissociates p120(CAND1), an inhibitor of CUL1-SKP1 binding and SCF ligases. Mol Cell. 2002 Dec;10(6):1511-8. PubMed PMID: 12504025.

105. Schmidt MW, McQuary PR, Wee S, et al. F-box-directed CRL complex assembly and regulation by the CSN and CAND1. Mol Cell. 2009 Sep 11;35(5):586-97. doi: 10.1016/j.molcel.2009.07.024. PubMed PMID: 19748355; PubMed Central PMCID: PMCPMC2779159.

106. Pierce NW, Lee JE, Liu X, et al. Cand1 promotes assembly of new SCF complexes through dynamic exchange of F box proteins. Cell. 2013 Mar 28;153(1):206-15. doi: 10.1016/j.cell.2013.02.024. PubMed PMID: 23453757; PubMed Central PMCID: PMCPMC3656483.

107. Bennett EJ, Rush J, Gygi SP, et al. Dynamics of cullin-RING ubiquitin ligase network revealed by systematic quantitative proteomics. Cell. 2010 Dec 10;143(6):951-65. doi: 10.1016/j.cell.2010.11.017. PubMed PMID: 21145461; PubMed Central PMCID: PMCPMC3008586.

108. Zemla A, Thomas Y, Kedziora S, et al. CSN- and CAND1-dependent remodelling of the budding yeast SCF complex. Nat Commun. 2013;4:1641. doi: 10.1038/ncomms2628. PubMed PMID: 23535662.

109. Wu S, Zhu W, Nhan T, et al. CAND1 controls in vivo dynamics of the cullin 1-RING ubiquitin ligase repertoire. Nat Commun. 2013;4:1642. doi: 10.1038/ncomms2636. PubMed PMID: 23535663; PubMed Central PMCID: PMCPMC3637025.

110. Fischer ES, Scrima A, Bohm K, et al. The molecular basis of CRL4DDB2/CSA ubiquitin ligase architecture, targeting, and activation. Cell. 2011 Nov 23;147(5):1024-39. doi: 10.1016/j.cell.2011.10.035. PubMed PMID: 22118460.

111. Emberley ED, Mosadeghi R, Deshaies RJ. Deconjugation of Nedd8 from Cul1 is directly regulated by Skp1-F-box and substrate, and the COP9 signalosome inhibits deneddylated SCF by a noncatalytic mechanism. J Biol Chem. 2012 Aug 24;287(35):29679-89. doi: 10.1074/jbc.M112.352484. PubMed PMID: 22767593; PubMed Central PMCID: PMCPMC3436198.

112. Zhou C, Wee S, Rhee E, et al. Fission yeast COP9/signalosome suppresses cullin activity through recruitment of the deubiquitylating enzyme Ubp12p. Mol Cell. 2003 Apr;11(4):927-38. PubMed PMID: 12718879.

113. Hetfeld BK, Helfrich A, Kapelari B, et al. The zinc finger of the CSN-associated deubiquitinating enzyme USP15 is essential to rescue the E3 ligase Rbx1. Curr Biol. 2005 Jul 12;15(13):1217-21. doi: 10.1016/j.cub.2005.05.059. PubMed PMID: 16005295.

114. Masai H, Matsumoto S, You Z, et al. Eukaryotic chromosome DNA replication: where, when, and how? Annu Rev Biochem. 2010;79:89-130. doi: 10.1146/annurev.biochem.052308.103205. PubMed PMID: 20373915.

115. Rieder CL, Salmon ED. The vertebrate cell kinetochore and its roles during mitosis. Trends Cell Biol. 1998 Aug;8(8):310-8. PubMed PMID: 9704407; PubMed Central PMCID: PMCPMC4774253.

116. Hauf S, Waizenegger IC, Peters JM. Cohesin cleavage by separase required for anaphase and cytokinesis in human cells. Science. 2001 Aug 17;293(5533):1320-3. doi: 10.1126/science.1061376. PubMed PMID: 11509732.

117. Sharp DJ, Rogers GC, Scholey JM. Microtubule motors in mitosis. Nature. 2000 Sep 7;407(6800):41-7. doi: 10.1038/35024000. PubMed PMID: 10993066.

118. Glotzer M. Animal cell cytokinesis. Annu Rev Cell Dev Biol. 2001;17:351-86. doi: 10.1146/annurev.cellbio.17.1.351. PubMed PMID: 11687493.

119. Hu CK, Ozlu N, Coughlin M, et al. Plk1 negatively regulates PRC1 to prevent premature midzone formation before cytokinesis. Mol Biol Cell. 2012 Jul;23(14):2702-11. doi: 10.1091/mbc.E12-01-0058. PubMed PMID: 22621898; PubMed Central PMCID: PMCPMC3395659.

120. Fededa JP, Gerlich DW. Molecular control of animal cell cytokinesis. Nat Cell Biol. 2012 May 2;14(5):440-7. doi: 10.1038/ncb2482. PubMed PMID: 22552143.

121. Zeitlin SG, Sullivan KF. Animal cytokinesis: breaking up is hard to do. Curr Biol. 2001 Jul 10;11(13):R514-6. PubMed PMID: 11470423.

122. Makyio H, Ohgi M, Takei T, et al. Structural basis for Arf6-MKLP1 complex formation on the Flemming body responsible for cytokinesis. EMBO J. 2012 May 30;31(11):2590-603. doi: 10.1038/emboj.2012.89. PubMed PMID: 22522702; PubMed Central PMCID: PMCPMC3365427.

123. Surka MC, Tsang CW, Trimble WS. The mammalian septin MSF localizes with microtubules and is required for completion of cytokinesis. Mol Biol Cell. 2002 Oct;13(10):3532-45. doi: 10.1091/mbc.e02-01-0042. PubMed PMID: 12388755; PubMed Central PMCID: PMCPMC129964.

124. Kinoshita M, Kumar S, Mizoguchi A, et al. Nedd5, a mammalian septin, is a novel cytoskeletal component interacting with actin-based structures. Genes Dev. 1997 Jun 15;11(12):1535-47. PubMed PMID: 9203580.

125. Nagata K, Kawajiri A, Matsui S, et al. Filament formation of MSF-A, a mammalian septin, in human mammary epithelial cells depends on interactions with microtubules. J Biol Chem. 2003 May 16;278(20):18538-43. doi: 10.1074/jbc.M205246200. PubMed PMID: 12626509.

126. Estey MP, Di Ciano-Oliveira C, Froese CD, et al. Distinct roles of septins in cytokinesis: SEPT9 mediates midbody abscission. J Cell Biol. 2010 Nov 15;191(4):741-9. doi: 10.1083/jcb.201006031. PubMed PMID: 21059847; PubMed Central PMCID: PMCPMC2983063.

127. Joo E, Surka MC, Trimble WS. Mammalian SEPT2 is required for scaffolding nonmuscle myosin II and its kinases. Dev Cell. 2007 Nov;13(5):677-90. doi: 10.1016/j.devcel.2007.09.001. PubMed PMID: 17981136.

128. Elia N, Sougrat R, Spurlin TA, et al. Dynamics of endosomal sorting complex required for transport (ESCRT) machinery during cytokinesis and its role in abscission. Proc Natl Acad Sci U S A. 2011 Mar 22;108(12):4846-51. doi: 10.1073/pnas.1102714108. PubMed PMID: 21383202; PubMed Central PMCID: PMCPMC3064317.

129. Carmena M, Wheelock M, Funabiki H, et al. The chromosomal passenger complex (CPC): from easy rider to the godfather of mitosis. Nat Rev Mol Cell Biol. 2012 Dec;13(12):789-803. doi: 10.1038/nrm3474. PubMed PMID: 23175282; PubMed Central PMCID: PMCPMC3729939.

130. Sumara I, Quadroni M, Frei C, et al. A Cul3-based E3 ligase removes Aurora B from mitotic chromosomes, regulating mitotic progression and completion of cytokinesis in human cells. Dev Cell. 2007 Jun;12(6):887-900. doi: 10.1016/j.devcel.2007.03.019. PubMed PMID: 17543862.

131. Maerki S, Olma MH, Staubli T, et al. The Cul3-KLHL21 E3 ubiquitin ligase targets aurora B to midzone microtubules in anaphase and is required for cytokinesis. J Cell Biol. 2009 Dec 14;187(6):791-800. doi: 10.1083/jcb.200906117. PubMed PMID: 19995937; PubMed Central PMCID: PMCPMC2806313.

132. Douglas ME, Davies T, Joseph N, et al. Aurora B and 14-3-3 coordinately regulate clustering of centralspindlin during cytokinesis. Curr Biol. 2010 May 25;20(10):927-33. doi: 10.1016/j.cub.2010.03.055. PubMed PMID: 20451386; PubMed Central PMCID: PMCPMC3348768.

133. Mishima M, Pavicic V, Gruneberg U, et al. Cell cycle regulation of central spindle assembly. Nature. 2004 Aug 19;430(7002):908-13. doi: 10.1038/nature02767. PubMed PMID: 15282614.

134. Zhu C, Bossy-Wetzel E, Jiang W. Recruitment of MKLP1 to the spindle midzone/midbody by INCENP is essential for midbody formation and completion of cytokinesis in human cells. Biochem J. 2005 Jul 15;389(Pt 2):373-81. doi: 10.1042/BJ20050097. PubMed PMID: 15796717; PubMed Central PMCID: PMCPMC1175114.

135. Johnson GL, Lapadat R. Mitogen-activated protein kinase pathways mediated by ERK, JNK, and p38 protein kinases. Science. 2002 Dec 6;298(5600):1911-2. doi: 10.1126/science.1072682. PubMed PMID: 12471242.

136. Lee MG, Nurse P. Complementation used to clone a human homologue of the fission yeast cell cycle control gene cdc2. Nature. 1987 May 7-13;327(6117):31-5. doi: 10.1038/327031a0. PubMed PMID: 3553962.

137. Terada Y, Inoshita S, Nakashima O, et al. Regulation of cyclin D1 expression and cell cycle progression by mitogen-activated protein kinase cascade. Kidney Int. 1999 Oct;56(4):1258-61. doi: 10.1046/j.1523-1755.1999.00704.x. PubMed PMID: 10504469.

138. Sherr CJ, Roberts JM. CDK inhibitors: positive and negative regulators of G1-phase progression. Genes Dev. 1999 Jun 15;13(12):1501-12. PubMed PMID: 10385618.

139. Jeffrey PD, Tong L, Pavletich NP. Structural basis of inhibition of CDK-cyclin complexes by INK4 inhibitors. Genes Dev. 2000 Dec 15;14(24):3115-25. PubMed PMID: 11124804; PubMed Central PMCID: PMCPMC317144.

140. Harbour JW, Dean DC. The Rb/E2F pathway: expanding roles and emerging paradigms. Genes Dev. 2000 Oct 1;14(19):2393-409. PubMed PMID: 11018009.

141. Blomberg I, Hoffmann I. Ectopic expression of Cdc25A accelerates the G(1)/S transition and leads to premature activation of cyclin E- and cyclin A-dependent kinases. Mol Cell Biol. 1999 Sep;19(9):6183-94. PubMed PMID: 10454565; PubMed Central PMCID: PMCPMC84557.

142. Bartek J, Lukas C, Lukas J. Checking on DNA damage in S phase. Nat Rev Mol Cell Biol. 2004 Oct;5(10):792-804. doi: 10.1038/nrm1493. PubMed PMID: 15459660.

143. Osborn AJ, Elledge SJ, Zou L. Checking on the fork: the DNA-replication stress-response pathway. Trends Cell Biol. 2002 Nov;12(11):509-16. PubMed PMID: 12446112.

144. Mitra J, Enders GH. Cyclin A/Cdk2 complexes regulate activation of Cdk1 and Cdc25 phosphatases in human cells. Oncogene. 2004 Apr 22;23(19):3361-7. doi: 10.1038/sj.onc.1207446. PubMed PMID: 14767478; PubMed Central PMCID: PMCPMC1924680.

145. Donzelli M, Draetta GF. Regulating mammalian checkpoints through Cdc25 inactivation. EMBO Rep. 2003 Jul;4(7):671-7. doi: 10.1038/sj.embor.embor887. PubMed PMID: 12835754; PubMed Central PMCID: PMCPMC1326326.

146. Timofeev O, Cizmecioglu O, Settele F, et al. Cdc25 phosphatases are required for timely assembly of CDK1-cyclin B at the G2/M transition. J Biol Chem. 2010 May 28;285(22):16978-90. doi: 10.1074/jbc.M109.096552. PubMed PMID: 20360007; PubMed Central PMCID: PMCPMC2878026.

147. Sur S, Agrawal DK. Phosphatases and kinases regulating CDC25 activity in the cell cycle: clinical implications of CDC25 overexpression and potential treatment strategies. Mol Cell Biochem. 2016 May;416(1-2):33-46. doi: 10.1007/s11010-016-2693-2. PubMed PMID: 27038604; PubMed Central PMCID: PMCPMC4862931.

148. Sanchez Y, Wong C, Thoma RS, et al. Conservation of the Chk1 checkpoint pathway in mammals: linkage of DNA damage to Cdk regulation through Cdc25. Science. 1997 Sep 5;277(5331):1497-501. PubMed PMID: 9278511.

149. Lara-Gonzalez P, Westhorpe FG, Taylor SS. The spindle assembly checkpoint. Curr Biol. 2012 Nov 20;22(22):R966-80. doi: 10.1016/j.cub.2012.10.006. PubMed PMID: 23174302.

150. Mirchenko L, Uhlmann F. Sli15(INCENP) dephosphorylation prevents mitotic checkpoint reengagement due to loss of tension at anaphase onset. Curr Biol. 2010 Aug 10;20(15):1396-401. doi: 10.1016/j.cub.2010.06.023. PubMed PMID: 20619650; PubMed Central PMCID: PMCPMC2964898.

151. Vazquez-Novelle MD, Petronczki M. Relocation of the chromosomal passenger complex prevents mitotic checkpoint engagement at anaphase. Curr Biol. 2010 Aug 10;20(15):1402-7. doi: 10.1016/j.cub.2010.06.036. PubMed PMID: 20619651.

152. Hummer S, Mayer TU. Cdk1 negatively regulates midzone localization of the mitotic kinesin Mklp2 and the chromosomal passenger complex. Curr Biol. 2009 Apr 14;19(7):607-12. doi: 10.1016/j.cub.2009.02.046. PubMed PMID: 19303298.

153. Nasmyth K. Segregating sister genomes: the molecular biology of chromosome separation. Science. 2002 Jul 26;297(5581):559-65. doi: 10.1126/science.1074757. PubMed PMID: 12142526.

154. Irniger S. Cyclin destruction in mitosis: a crucial task of Cdc20. FEBS Lett. 2002 Dec 4;532(1-2):7-11. PubMed PMID: 12459453.

155. Norden C, Mendoza M, Dobbelaere J, et al. The NoCut pathway links completion of cytokinesis to spindle midzone function to prevent chromosome breakage. Cell. 2006 Apr 7;125(1):85-98. doi: 10.1016/j.cell.2006.01.045. PubMed PMID: 16615892.

156. Steigemann P, Wurzenberger C, Schmitz MH, et al. Aurora B-mediated abscission checkpoint protects against tetraploidization. Cell. 2009 Feb 6;136(3):473-84. doi: 10.1016/j.cell.2008.12.020. PubMed PMID: 19203582.

157. Mackay DR, Makise M, Ullman KS. Defects in nuclear pore assembly lead to activation of an Aurora B-mediated abscission checkpoint. J Cell Biol. 2010 Nov 29;191(5):923-31. doi: 10.1083/jcb.201007124. PubMed PMID: 21098116; PubMed Central PMCID: PMCPMC2995170.

158. Capalbo L, Montembault E, Takeda T, et al. The chromosomal passenger complex controls the function of endosomal sorting complex required for transport-III Snf7 proteins during cytokinesis. Open Biol. 2012 May;2(5):120070. doi: 10.1098/rsob.120070. PubMed PMID: 22724069; PubMed Central PMCID: PMCPMC3376741.

159. Carlton JG, Caballe A, Agromayor M, et al. ESCRT-III governs the Aurora B-mediated abscission checkpoint through CHMP4C. Science. 2012 Apr 13;336(6078):220-5. doi: 10.1126/science.1217180. PubMed PMID: 22422861; PubMed Central PMCID: PMCPMC3998087.

160. Skaar JR, Pagano M. Control of cell growth by the SCF and APC/C ubiquitin ligases. Curr Opin Cell Biol. 2009 Dec;21(6):816-24. doi: 10.1016/j.ceb.2009.08.004. PubMed PMID: 19775879; PubMed Central PMCID: PMCPMC2805079.

161. Podust VN, Brownell JE, Gladysheva TB, et al. A Nedd8 conjugation pathway is essential for proteolytic targeting of p27Kip1 by ubiquitination. Proc Natl Acad Sci U S A. 2000 Apr 25;97(9):4579-84. doi: 10.1073/pnas.090465597. PubMed PMID: 10781063; PubMed Central PMCID: PMCPMC18275.

162. Morimoto M, Nishida T, Honda R, et al. Modification of cullin-1 by ubiquitin-like protein Nedd8 enhances the activity of SCF(skp2) toward p27(kip1). Biochem Biophys Res Commun. 2000 Apr 21;270(3):1093-6. doi: 10.1006/bbrc.2000.2576. PubMed PMID: 10772955.

163. Teixeira LK, Reed SI. Ubiquitin ligases and cell cycle control. Annu Rev Biochem. 2013;82:387-414. doi: 10.1146/annurev-biochem-060410-105307. PubMed PMID: 23495935.

164. Higa LA, Yang X, Zheng J, et al. Involvement of CUL4 ubiquitin E3 ligases in regulating CDK inhibitors Dacapo/p27Kip1 and cyclin E degradation. Cell Cycle. 2006 Jan;5(1):71-7. doi: 10.4161/cc.5.1.2266. PubMed PMID: 16322693.

165. Tomoda K, Kubota Y, Kato J. Degradation of the cyclin-dependent-kinase inhibitor p27Kip1 is instigated by Jab1. Nature. 1999 Mar 11;398(6723):160-5. doi: 10.1038/18230. PubMed PMID: 10086358.

166. Chen B, Zhao R, Su CH, et al. CDK inhibitor p57 (Kip2) is negatively regulated by COP9 signalosome subunit 6. Cell Cycle. 2012 Dec 15;11(24):4633-41. doi: 10.4161/cc.22887. PubMed PMID: 23187808; PubMed Central PMCID: PMCPMC3562308.

167. Choi HH, Guma S, Fang L, et al. Regulating the stability and localization of CDK inhibitor p27(Kip1) via CSN6-COP1 axis. Cell Cycle. 2015;14(14):2265-73. doi: 10.1080/15384101.2015.1046655. PubMed PMID: 25945542; PubMed Central PMCID: PMCPMC4613181.

168. Diehl JA, Zindy F, Sherr CJ. Inhibition of cyclin D1 phosphorylation on threonine-286 prevents its rapid degradation via the ubiquitin-proteasome pathway. Genes Dev. 1997 Apr 15;11(8):957-72. PubMed PMID: 9136925.

169. Diehl JA, Cheng M, Roussel MF, et al. Glycogen synthase kinase-3beta regulates cyclin D1 proteolysis and subcellular localization. Genes Dev. 1998 Nov 15;12(22):3499-511. PubMed PMID: 9832503; PubMed Central PMCID: PMCPMC317244.

170. Nakayama K, Nagahama H, Minamishima YA, et al. Targeted disruption of Skp2 results in accumulation of cyclin E and p27(Kip1), polyploidy and centrosome overduplication. EMBO J. 2000 May 2;19(9):2069-81. doi: 10.1093/emboj/19.9.2069. PubMed PMID: 10790373; PubMed Central PMCID: PMCPMC305685.

171. Koepp DM, Harper JW, Elledge SJ. How the cyclin became a cyclin: regulated proteolysis in the cell cycle. Cell. 1999 May 14;97(4):431-4. PubMed PMID: 10338207.

172. Singer JD, Gurian-West M, Clurman B, et al. Cullin-3 targets cyclin E for ubiquitination and controls S phase in mammalian cells. Genes Dev. 1999 Sep 15;13(18):2375-87. PubMed PMID: 10500095; PubMed Central PMCID: PMCPMC317026.

173. Jin J, Arias EE, Chen J, et al. A family of diverse Cul4-Ddb1-interacting proteins includes Cdt2, which is required for S phase destruction of the replication factor Cdt1. Mol Cell. 2006 Sep 1;23(5):709-21. doi: 10.1016/j.molcel.2006.08.010. PubMed PMID: 16949367.

174. Higa LA, Banks D, Wu M, et al. L2DTL/CDT2 interacts with the CUL4/DDB1 complex and PCNA and regulates CDT1 proteolysis in response to DNA damage. Cell Cycle. 2006 Aug;5(15):1675-80. doi: 10.4161/cc.5.15.3149. PubMed PMID: 16861906.

175. Hu J, McCall CM, Ohta T, et al. Targeted ubiquitination of CDT1 by the DDB1-CUL4A-ROC1 ligase in response to DNA damage. Nat Cell Biol. 2004 Oct;6(10):1003-9. doi: 10.1038/ncb1172. PubMed PMID: 15448697.

176. Lovejoy CA, Lock K, Yenamandra A, et al. DDB1 maintains genome integrity through regulation of Cdt1. Mol Cell Biol. 2006 Nov;26(21):7977-90. doi: 10.1128/MCB.00819-06. PubMed PMID: 16940174; PubMed Central PMCID: PMCPMC1636754.

177. Lin JJ, Milhollen MA, Smith PG, et al. NEDD8-targeting drug MLN4924 elicits DNA rereplication by stabilizing Cdt1 in S phase, triggering checkpoint activation, apoptosis, and senescence in cancer cells. Cancer Res. 2010 Dec 15;70(24):10310-20. doi: 10.1158/0008-5472.CAN-10-2062. PubMed PMID: 21159650; PubMed Central PMCID: PMCPMC3059213.

178. Zhong W, Feng H, Santiago FE, et al. CUL-4 ubiquitin ligase maintains genome stability by restraining DNA-replication licensing. Nature. 2003 Jun 19;423(6942):885-9. doi: 10.1038/nature01747. PubMed PMID: 12815436.

179. Busino L, Donzelli M, Chiesa M, et al. Degradation of Cdc25A by beta-TrCP during S phase and in response to DNA damage. Nature. 2003 Nov 6;426(6962):87-91. doi: 10.1038/nature02082. PubMed PMID: 14603323.

180. Jin J, Shirogane T, Xu L, et al. SCFbeta-TRCP links Chk1 signaling to degradation of the Cdc25A protein phosphatase. Genes Dev. 2003 Dec 15;17(24):3062-74. doi: 10.1101/gad.1157503. PubMed PMID: 14681206; PubMed Central PMCID: PMCPMC305258.

181. Watanabe N, Arai H, Nishihara Y, et al. M-phase kinases induce phospho-dependent ubiquitination of somatic Wee1 by SCFbeta-TrCP. Proc Natl Acad Sci U S A. 2004 Mar 30;101(13):4419-24. doi: 10.1073/pnas.0307700101. PubMed PMID: 15070733; PubMed Central PMCID: PMCPMC384762.

182. Margottin-Goguet F, Hsu JY, Loktev A, et al. Prophase destruction of Emi1 by the SCF(betaTrCP/Slimb) ubiquitin ligase activates the anaphase promoting complex to allow progression beyond prometaphase. Dev Cell. 2003 Jun;4(6):813-26. PubMed PMID: 12791267.

183. Hansen DV, Loktev AV, Ban KH, et al. Plk1 regulates activation of the anaphase promoting complex by phosphorylating and triggering SCFbetaTrCP-dependent destruction of the APC Inhibitor Emi1. Mol Biol Cell. 2004 Dec;15(12):5623-34. doi: 10.1091/mbc.e04-07-0598. PubMed PMID: 15469984; PubMed Central PMCID: PMCPMC532041.

184. Guardavaccaro D, Frescas D, Dorrello NV, et al. Control of chromosome stability by the beta-TrCP-REST-Mad2 axis. Nature. 2008 Mar 20;452(7185):365-9. doi: 10.1038/nature06641. PubMed PMID: 18354482; PubMed Central PMCID: PMCPMC2707768.

185. Lin S, Shang Z, Li S, et al. Neddylation inhibitor MLN4924 induces G2 cell cycle arrest, DNA damage and sensitizes esophageal squamous cell carcinoma cells to cisplatin. Oncol Lett. 2018 Feb;15(2):2583-2589. doi: 10.3892/ol.2017.7616. PubMed PMID: 29434977; PubMed Central PMCID: PMCPMC5777299.

186. Mackintosh C, Garcia-Dominguez DJ, Ordonez JL, et al. WEE1 accumulation and deregulation of S-phase proteins mediate MLN4924 potent inhibitory effect on Ewing sarcoma cells. Oncogene. 2013 Mar 14;32(11):1441-51. doi: 10.1038/onc.2012.153. PubMed PMID: 22641220.

187. Arquint C, Cubizolles F, Morand A, et al. The SKP1-Cullin-F-box E3 ligase betaTrCP and CDK2 cooperate to control STIL abundance and centriole number. Open Biol. 2018 Feb;8(2). doi: 10.1098/rsob.170253. PubMed PMID: 29445034; PubMed Central PMCID: PMCPMC5830536.

188. Higa LA, Mihaylov IS, Banks DP, et al. Radiation-mediated proteolysis of CDT1 by CUL4-ROC1 and CSN complexes constitutes a new checkpoint. Nat Cell Biol. 2003 Nov;5(11):1008-15. doi: 10.1038/ncb1061. PubMed PMID: 14578910.

189. Raman M, Havens CG, Walter JC, et al. A genome-wide screen identifies p97 as an essential regulator of DNA damage-dependent CDT1 destruction. Mol Cell. 2011 Oct 7;44(1):72-84. doi: 10.1016/j.molcel.2011.06.036. PubMed PMID: 21981919; PubMed Central PMCID: PMCPMC3190166.

190. Chen BB, Glasser JR, Coon TA, et al. Skp-cullin-F box E3 ligase component FBXL2 ubiquitinates Aurora B to inhibit tumorigenesis. Cell Death Dis. 2013 Aug 8;4:e759. doi: 10.1038/cddis.2013.271. PubMed PMID: 23928698; PubMed Central PMCID: PMCPMC3763433.

191. Sasagawa Y, Urano T, Kohara Y, et al. Caenorhabditis elegans RBX1 is essential for meiosis, mitotic chromosomal condensation and segregation, and cytokinesis. Genes Cells. 2003 Nov;8(11):857-72. PubMed PMID: 14622138.

192. Huang G, Kaufman AJ, Xu K, et al. Squamous cell carcinoma-related oncogene (SCCRO) neddylates Cul3 protein to selectively promote midbody localization and activity of Cul3(KLHL21) protein complex during abscission. J Biol Chem. 2017 Sep 15;292(37):15254-15265. doi: 10.1074/jbc.M117.778530. PubMed PMID: 28620047; PubMed Central PMCID: PMCPMC5602386.

193. David SS, O'Shea VL, Kundu S. Base-excision repair of oxidative DNA damage. Nature. 2007 Jun 21;447(7147):941-50. doi: 10.1038/nature05978. PubMed PMID: 17581577; PubMed Central PMCID: PMCPMC2896554.

194. Jackson SP, Bartek J. The DNA-damage response in human biology and disease. Nature. 2009 Oct 22;461(7267):1071-8. doi: 10.1038/nature08467. PubMed PMID: 19847258; PubMed Central PMCID: PMCPMC2906700.

195. Dellaire G, Bazett-Jones DP. Beyond repair foci: subnuclear domains and the cellular response to DNA damage. Cell Cycle. 2007 Aug 1;6(15):1864-72. doi: 10.4161/cc.6.15.4560. PubMed PMID: 17660715.

196. de Jager M, Dronkert ML, Modesti M, et al. DNA-binding and strand-annealing activities of human Mre11: implications for its roles in DNA double-strand break repair pathways. Nucleic Acids Res. 2001 Mar 15;29(6):1317-25. PubMed PMID: 11238998; PubMed Central PMCID: PMCPMC29748.

197. Paull TT, Gellert M. The 3' to 5' exonuclease activity of Mre 11 facilitates repair of DNA double-strand breaks. Mol Cell. 1998 Jun;1(7):969-79. PubMed PMID: 9651580.

198. Paull TT, Gellert M. Nbs1 potentiates ATP-driven DNA unwinding and endonuclease cleavage by the Mre11/Rad50 complex. Genes Dev. 1999 May 15;13(10):1276-88. PubMed PMID: 10346816; PubMed Central PMCID: PMCPMC316715.

199. Sartori AA, Lukas C, Coates J, et al. Human CtIP promotes DNA end resection. Nature. 2007 Nov 22;450(7169):509-14. doi: 10.1038/nature06337. PubMed PMID: 17965729; PubMed Central PMCID: PMCPMC2409435.

200. Limbo O, Chahwan C, Yamada Y, et al. Ctp1 is a cell-cycle-regulated protein that functions with Mre11 complex to control double-strand break repair by homologous recombination. Mol Cell. 2007 Oct 12;28(1):134-46. doi: 10.1016/j.molcel.2007.09.009. PubMed PMID: 17936710; PubMed Central PMCID: PMCPMC2066204.

201. Lieber MR. The mechanism of double-strand DNA break repair by the nonhomologous DNA end-joining pathway. Annu Rev Biochem. 2010;79:181-211. doi: 10.1146/annurev.biochem.052308.093131. PubMed PMID: 20192759; PubMed Central PMCID: PMCPMC3079308.

202. El-Khamisy SF, Masutani M, Suzuki H, et al. A requirement for PARP-1 for the assembly or stability of XRCC1 nuclear foci at sites of oxidative DNA damage. Nucleic Acids Res. 2003 Oct 1;31(19):5526-33. PubMed PMID: 14500814; PubMed Central PMCID: PMCPMC206461.

203. Mortusewicz O, Rothbauer U, Cardoso MC, et al. Differential recruitment of DNA Ligase I and III to DNA repair sites. Nucleic Acids Res. 2006;34(12):3523-32. doi: 10.1093/nar/gkl492. PubMed PMID: 16855289; PubMed Central PMCID: PMCPMC1524911.

204. Wang M, Wu W, Wu W, et al. PARP-1 and Ku compete for repair of DNA double strand breaks by distinct NHEJ pathways. Nucleic Acids Res. 2006;34(21):6170-82. doi: 10.1093/nar/gkl840. PubMed PMID: 17088286; PubMed Central PMCID: PMCPMC1693894.

205. Escribano-Diaz C, Orthwein A, Fradet-Turcotte A, et al. A cell cycle-dependent regulatory circuit composed of 53BP1-RIF1 and BRCA1-CtIP controls DNA repair pathway choice. Mol Cell. 2013 Mar 7;49(5):872-83. doi: 10.1016/j.molcel.2013.01.001. PubMed PMID: 23333306.

206. Shibata A, Conrad S, Birraux J, et al. Factors determining DNA double-strand break repair pathway choice in G2 phase. EMBO J. 2011 Mar 16;30(6):1079-92. doi: 10.1038/emboj.2011.27. PubMed PMID: 21317870; PubMed Central PMCID: PMCPMC3061033.

207. Lemaitre C, Grabarz A, Tsouroula K, et al. Nuclear position dictates DNA repair pathway choice. Genes Dev. 2014 Nov 15;28(22):2450-63. doi: 10.1101/gad.248369.114. PubMed PMID: 25366693; PubMed Central PMCID: PMCPMC4233239.

208. Ciccia A, Elledge SJ. The DNA damage response: making it safe to play with knives. Mol Cell. 2010 Oct 22;40(2):179-204. doi: 10.1016/j.molcel.2010.09.019. PubMed PMID: 20965415; PubMed Central PMCID: PMCPMC2988877.

209. Uziel T, Lerenthal Y, Moyal L, et al. Requirement of the MRN complex for ATM activation by DNA damage. EMBO J. 2003 Oct 15;22(20):5612-21. doi: 10.1093/emboj/cdg541. PubMed PMID: 14532133; PubMed Central PMCID: PMCPMC213795.

210. Lee JH, Paull TT. ATM activation by DNA double-strand breaks through the Mre11-Rad50-Nbs1 complex. Science. 2005 Apr 22;308(5721):551-4. doi: 10.1126/science.1108297. PubMed PMID: 15790808.

211. Burma S, Chen DJ. Role of DNA-PK in the cellular response to DNA double-strand breaks. DNA Repair (Amst). 2004 Aug-Sep;3(8-9):909-18. doi: 10.1016/j.dnarep.2004.03.021. PubMed PMID: 15279776.

212. Harper JW, Elledge SJ. The DNA damage response: ten years after. Mol Cell. 2007 Dec 14;28(5):739-45. doi: 10.1016/j.molcel.2007.11.015. PubMed PMID: 18082599.

213. Burma S, Chen BP, Murphy M, et al. ATM phosphorylates histone H2AX in response to DNA double-strand breaks. J Biol Chem. 2001 Nov 9;276(45):42462-7. doi: 10.1074/jbc.C100466200. PubMed PMID: 11571274.

214. Stiff T, O'Driscoll M, Rief N, et al. ATM and DNA-PK function redundantly to phosphorylate H2AX after exposure to ionizing radiation. Cancer Res. 2004 Apr 1;64(7):2390-6. PubMed PMID: 15059890.

215. Stucki M, Jackson SP. gammaH2AX and MDC1: anchoring the DNA-damage-response machinery to broken chromosomes. DNA Repair (Amst). 2006 May 10;5(5):534-43. doi: 10.1016/j.dnarep.2006.01.012. PubMed PMID: 16531125.

216. Stracker TH, Usui T, Petrini JH. Taking the time to make important decisions: the checkpoint effector kinases Chk1 and Chk2 and the DNA damage response. DNA Repair (Amst). 2009 Sep 2;8(9):1047-54. doi: 10.1016/j.dnarep.2009.04.012. PubMed PMID: 19473886; PubMed Central PMCID: PMCPMC2725228.

217. Peter M, Le Peuch C, Labbe JC, et al. Initial activation of cyclin-B1-cdc2 kinase requires phosphorylation of cyclin B1. EMBO Rep. 2002 Jun;3(6):551-6. doi: 10.1093/embo-reports/kvf111. PubMed PMID: 12034754; PubMed Central PMCID: PMCPMC1084145.

218. Tibbetts RS, Brumbaugh KM, Williams JM, et al. A role for ATR in the DNA damage-induced phosphorylation of p53. Genes Dev. 1999 Jan 15;13(2):152-7. PubMed PMID: 9925639; PubMed Central PMCID: PMCPMC316393.

219. Cheng Q, Chen J. Mechanism of p53 stabilization by ATM after DNA damage. Cell Cycle. 2010 Feb 1;9(3):472-8. doi: 10.4161/cc.9.3.10556. PubMed PMID: 20081365; PubMed Central PMCID: PMCPMC2977994.

220. Shieh SY, Ahn J, Tamai K, et al. The human homologs of checkpoint kinases Chk1 and Cds1 (Chk2) phosphorylate p53 at multiple DNA damage-inducible sites. Genes Dev. 2000 Feb 1;14(3):289-300. PubMed PMID: 10673501; PubMed Central PMCID: PMCPMC316358.

221. Brugarolas J, Chandrasekaran C, Gordon JI, et al. Radiation-induced cell cycle arrest compromised by p21 deficiency. Nature. 1995 Oct 12;377(6549):552-7. doi: 10.1038/377552a0. PubMed PMID: 7566157.

222. Gillis LD, Leidal AM, Hill R, et al. p21Cip1/WAF1 mediates cyclin B1 degradation in response to DNA damage. Cell Cycle. 2009 Jan 15;8(2):253-6. doi: 10.4161/cc.8.2.7550. PubMed PMID: 19158493.

223. Hermeking H, Benzinger A. 14-3-3 proteins in cell cycle regulation. Semin Cancer Biol. 2006 Jun;16(3):183-92. doi: 10.1016/j.semcancer.2006.03.002. PubMed PMID: 16697662.

224. Bech-Otschir D, Kraft R, Huang X, et al. COP9 signalosome-specific phosphorylation targets p53 to degradation by the ubiquitin system. EMBO J. 2001 Apr 2;20(7):1630-9. doi: 10.1093/emboj/20.7.1630. PubMed PMID: 11285227; PubMed Central PMCID: PMCPMC145508.

225. Oh W, Lee EW, Sung YH, et al. Jab1 induces the cytoplasmic localization and degradation of p53 in coordination with Hdm2. J Biol Chem. 2006 Jun 23;281(25):17457-65. doi: 10.1074/jbc.M601857200. PubMed PMID: 16624822.

226. Zhao R, Yeung SC, Chen J, et al. Subunit 6 of the COP9 signalosome promotes tumorigenesis in mice through stabilization of MDM2 and is upregulated in human cancers. J Clin Invest. 2011 Mar;121(3):851-65. doi: 10.1172/JCI44111. PubMed PMID: 21317535; PubMed Central PMCID: PMCPMC3049400.

227. Zhou BP, Liao Y, Xia W, et al. HER-2/neu induces p53 ubiquitination via Akt-mediated MDM2 phosphorylation. Nat Cell Biol. 2001 Nov;3(11):973-82. doi: 10.1038/ncb1101-973. PubMed PMID: 11715018.

228. Abida WM, Nikolaev A, Zhao W, et al. FBXO11 promotes the Neddylation of p53 and inhibits its transcriptional activity. J Biol Chem. 2007 Jan 19;282(3):1797-804. doi: 10.1074/jbc.M609001200. PubMed PMID: 17098746; PubMed Central PMCID: PMCPMC3690493.

229. Ebina M, Tsuruta F, Katoh MC, et al. Myeloma overexpressed 2 (Myeov2) regulates L11 subnuclear localization through Nedd8 modification. PLoS One. 2013;8(6):e65285. doi: 10.1371/journal.pone.0065285. PubMed PMID: 23776465; PubMed Central PMCID: PMCPMC3680436.

230. Mahata B, Sundqvist A, Xirodimas DP. Recruitment of RPL11 at promoter sites of p53-regulated genes upon nucleolar stress through NEDD8 and in an Mdm2-dependent manner. Oncogene. 2012 Jun 21;31(25):3060-71. doi: 10.1038/onc.2011.482. PubMed PMID: 22081073.

231. Llanos S, Serrano M. Depletion of ribosomal protein L37 occurs in response to DNA damage and activates p53 through the L11/MDM2 pathway. Cell Cycle. 2010 Oct 1;9(19):4005-12. doi: 10.4161/cc.9.19.13299. PubMed PMID: 20935493; PubMed Central PMCID: PMCPMC3615335.

232. Rubbi CP, Milner J. Disruption of the nucleolus mediates stabilization of p53 in response to DNA damage and other stresses. EMBO J. 2003 Nov 17;22(22):6068-77. doi: 10.1093/emboj/cdg579. PubMed PMID: 14609953; PubMed Central PMCID: PMCPMC275437.

233. Nitiss JL. Targeting DNA topoisomerase II in cancer chemotherapy. Nat Rev Cancer. 2009 May;9(5):338-50. doi: 10.1038/nrc2607. PubMed PMID: 19377506; PubMed Central PMCID: PMCPMC2748742.

234. Keeney S. Mechanism and control of meiotic recombination initiation. Curr Top Dev Biol. 2001;52:1-53. PubMed PMID: 11529427.

235. Hanada K, Budzowska M, Modesti M, et al. The structure-specific endonuclease Mus81-Eme1 promotes conversion of interstrand DNA crosslinks into double-strands breaks. EMBO J. 2006 Oct 18;25(20):4921-32. doi: 10.1038/sj.emboj.7601344. PubMed PMID: 17036055; PubMed Central PMCID: PMCPMC1618088.

236. Sollier J, Stork CT, Garcia-Rubio ML, et al. Transcription-coupled nucleotide excision repair factors promote R-loop-induced genome instability. Mol Cell. 2014 Dec 18;56(6):777-85. doi: 10.1016/j.molcel.2014.10.020. PubMed PMID: 25435140; PubMed Central PMCID: PMCPMC4272638.

237. Ran FA, Hsu PD, Wright J, et al. Genome engineering using the CRISPR-Cas9 system. Nat Protoc. 2013 Nov;8(11):2281-2308. doi: 10.1038/nprot.2013.143. PubMed PMID: 24157548; PubMed Central PMCID: PMCPMC3969860.

238. Yun MH, Hiom K. CtIP-BRCA1 modulates the choice of DNA double-strand-break repair pathway throughout the cell cycle. Nature. 2009 May 21;459(7245):460-3. doi: 10.1038/nature07955. PubMed PMID: 19357644; PubMed Central PMCID: PMCPMC2857324.

239. Ira G, Pellicioli A, Balijja A, et al. DNA end resection, homologous recombination and DNA damage checkpoint activation require CDK1. Nature. 2004 Oct 21;431(7011):1011-7. doi: 10.1038/nature02964. PubMed PMID: 15496928; PubMed Central PMCID: PMCPMC4493751.

240. Aylon Y, Liefshitz B, Kupiec M. The CDK regulates repair of double-strand breaks by homologous recombination during the cell cycle. EMBO J. 2004 Dec 8;23(24):4868-75. doi: 10.1038/sj.emboj.7600469. PubMed PMID: 15549137; PubMed Central PMCID: PMCPMC535085.

241. Waters CA, Strande NT, Wyatt DW, et al. Nonhomologous end joining: a good solution for bad ends. DNA Repair (Amst). 2014 May;17:39-51. doi: 10.1016/j.dnarep.2014.02.008. PubMed PMID: 24630899; PubMed Central PMCID: PMCPMC4024359.

242. Karanam K, Kafri R, Loewer A, et al. Quantitative live cell imaging reveals a gradual shift between DNA repair mechanisms and a maximal use of HR in mid S phase. Mol Cell. 2012 Jul 27;47(2):320-9. doi: 10.1016/j.molcel.2012.05.052. PubMed PMID: 22841003; PubMed Central PMCID: PMCPMC3494418.

243. Yu X, Chen J. DNA damage-induced cell cycle checkpoint control requires CtIP, a phosphorylation-dependent binding partner of BRCA1 C-terminal domains. Mol Cell Biol. 2004 Nov;24(21):9478-86. doi: 10.1128/MCB.24.21.9478-9486.2004. PubMed PMID: 15485915; PubMed Central PMCID: PMCPMC522253.

244. Caldecott KW. Single-strand break repair and genetic disease. Nat Rev Genet. 2008 Aug;9(8):619-31. doi: 10.1038/nrg2380. PubMed PMID: 18626472.

245. McVey M, Lee SE. MMEJ repair of double-strand breaks (director's cut): deleted sequences and alternative endings. Trends Genet. 2008 Nov;24(11):529-38. doi: 10.1016/j.tig.2008.08.007. PubMed PMID: 18809224; PubMed Central PMCID: PMCPMC5303623.

246. Audebert M, Salles B, Weinfeld M, et al. Involvement of polynucleotide kinase in a poly(ADP-ribose) polymerase-1-dependent DNA double-strand breaks rejoining pathway. J Mol Biol. 2006 Feb 17;356(2):257-65. doi: 10.1016/j.jmb.2005.11.028. PubMed PMID: 16364363.

247. Mateos-Gomez PA, Gong F, Nair N, et al. Mammalian polymerase theta promotes alternative NHEJ and suppresses recombination. Nature. 2015 Feb 12;518(7538):254-7. doi: 10.1038/nature14157. PubMed PMID: 25642960; PubMed Central PMCID: PMCPMC4718306.

248. Wang H, Rosidi B, Perrault R, et al. DNA ligase III as a candidate component of backup pathways of nonhomologous end joining. Cancer Res. 2005 May 15;65(10):4020-30. doi: 10.1158/0008-5472.CAN-04-3055. PubMed PMID: 15899791.

249. Motycka TA, Bessho T, Post SM, et al. Physical and functional interaction between the XPF/ERCC1 endonuclease and hRad52. J Biol Chem. 2004 Apr 2;279(14):13634-9. doi: 10.1074/jbc.M313779200. PubMed PMID: 14734547.

250. Bhargava R, Onyango DO, Stark JM. Regulation of Single-Strand Annealing and its Role in Genome Maintenance. Trends Genet. 2016 Sep;32(9):566-575. doi: 10.1016/j.tig.2016.06.007. PubMed PMID: 27450436; PubMed Central PMCID: PMCPMC4992407.

251. Johnson RD, Jasin M. Sister chromatid gene conversion is a prominent double-strand break repair pathway in mammalian cells. EMBO J. 2000 Jul 3;19(13):3398-407. doi: 10.1093/emboj/19.13.3398. PubMed PMID: 10880452; PubMed Central PMCID: PMCPMC313931.

252. Jimeno S, Fernandez-Avila MJ, Cruz-Garcia A, et al. Neddylation inhibits CtIP-mediated resection and regulates DNA double strand break repair pathway choice. Nucleic Acids Res. 2015 Jan;43(2):987-99. doi: 10.1093/nar/gku1384. PubMed PMID: 25567988; PubMed Central PMCID: PMCPMC4333419.

253. Shinohara A, Ogawa H, Ogawa T. Rad51 protein involved in repair and recombination in S. cerevisiae is a RecA-like protein. Cell. 1992 May 1;69(3):457-70. PubMed PMID: 1581961.

254. Heyer WD, Ehmsen KT, Liu J. Regulation of homologous recombination in eukaryotes. Annu Rev Genet. 2010;44:113-39. doi: 10.1146/annurev-genet-051710-150955. PubMed PMID: 20690856; PubMed Central PMCID: PMCPMC4114321.

255. Wei D, Li H, Yu J, et al. Radiosensitization of human pancreatic cancer cells by MLN4924, an investigational NEDD8-activating enzyme inhibitor. Cancer Res. 2012 Jan 1;72(1):282-93. doi: 10.1158/0008-5472.CAN-11-2866. PubMed PMID: 22072567; PubMed Central PMCID: PMCPMC3251739.

256. Li T, Guan J, Huang Z, et al. RNF168-mediated H2A neddylation antagonizes ubiquitylation of H2A and regulates DNA damage repair. J Cell Sci. 2014 May 15;127(Pt 10):2238-48. doi: 10.1242/jcs.138891. PubMed PMID: 24634510.

257. Davies OR, Forment JV, Sun M, et al. CtIP tetramer assembly is required for DNA-end resection and repair. Nat Struct Mol Biol. 2015 Feb;22(2):150-157. doi: 10.1038/nsmb.2937. PubMed PMID: 25558984; PubMed Central PMCID: PMCPMC4564947.

258. Poulsen SL, Hansen RK, Wagner SA, et al. RNF111/Arkadia is a SUMO-targeted ubiquitin ligase that facilitates the DNA damage response. J Cell Biol. 2013 Jun 10;201(6):797-807. doi: 10.1083/jcb.201212075. PubMed PMID: 23751493; PubMed Central PMCID: PMCPMC3678163.

259. Erker Y, Neyret-Kahn H, Seeler JS, et al. Arkadia, a novel SUMO-targeted ubiquitin ligase involved in PML degradation. Mol Cell Biol. 2013 Jun;33(11):2163-77. doi: 10.1128/MCB.01019-12. PubMed PMID: 23530056; PubMed Central PMCID: PMCPMC3648077.

260. Brown JS, Lukashchuk N, Sczaniecka-Clift M, et al. Neddylation promotes ubiquitylation and release of Ku from DNA-damage sites. Cell Rep. 2015 May 5;11(5):704-14. doi: 10.1016/j.celrep.2015.03.058. PubMed PMID: 25921528; PubMed Central PMCID: PMCPMC4431666.

261. Tian L, Peng G, Parant JM, et al. Essential roles of Jab1 in cell survival, spontaneous DNA damage and DNA repair. Oncogene. 2010 Nov 18;29(46):6125-37. doi: 10.1038/onc.2010.345. PubMed PMID: 20802511; PubMed Central PMCID: PMCPMC3495558.

262. Pan Y, Zhang Q, Atsaves V, et al. Suppression of Jab1/CSN5 induces radio- and chemo-sensitivity in nasopharyngeal carcinoma through changes to the DNA damage and repair pathways. Oncogene. 2013 May 30;32(22):2756-66. doi: 10.1038/onc.2012.294. PubMed PMID: 22797071; PubMed Central PMCID: PMCPMC3566273.

263. Joseph N, Hutterer A, Poser I, et al. ARF6 GTPase protects the post-mitotic midbody from 14-3-3-mediated disintegration. EMBO J. 2012 May 30;31(11):2604-14. doi: 10.1038/emboj.2012.139. PubMed PMID: 22580824; PubMed Central PMCID: PMCPMC3365424.

264. Bindels DS, Haarbosch L, van Weeren L, et al. mScarlet: a bright monomeric red fluorescent protein for cellular imaging. Nat Methods. 2017 Jan;14(1):53-56. doi: 10.1038/nmeth.4074. PubMed PMID: 27869816.

265. Sladitschek HL, Neveu PA. MXS-Chaining: A Highly Efficient Cloning Platform for Imaging and Flow Cytometry Approaches in Mammalian Systems. PLoS One. 2015;10(4):e0124958. doi: 10.1371/journal.pone.0124958. PubMed PMID: 25909630; PubMed Central PMCID: PMCPMC4409215.

266. Stark JM, Pierce AJ, Oh J, et al. Genetic steps of mammalian homologous repair with distinct mutagenic consequences. Mol Cell Biol. 2004 Nov;24(21):9305-16. doi: 10.1128/MCB.24.21.9305-9316.2004. PubMed PMID: 15485900; PubMed Central PMCID: PMCPMC522275.

267. Shcherbakova DM, Verkhusha VV. Near-infrared fluorescent proteins for multicolor in vivo imaging. Nat Methods. 2013 Aug;10(8):751-4. doi: 10.1038/nmeth.2521. PubMed PMID: 23770755; PubMed Central PMCID: PMCPMC3737237.

268. Pinder J, Salsman J, Dellaire G. Nuclear domain 'knock-in' screen for the evaluation and identification of small molecule enhancers of CRISPR-based genome editing. Nucleic Acids Res. 2015 Oct 30;43(19):9379-92. doi: 10.1093/nar/gkv993. PubMed PMID: 26429972; PubMed Central PMCID: PMCPMC4627099.

269. Sakaue-Sawano A, Kurokawa H, Morimura T, et al. Visualizing spatiotemporal dynamics of multicellular cell-cycle progression. Cell. 2008 Feb 8;132(3):487-98. doi: 10.1016/j.cell.2007.12.033. PubMed PMID: 18267078.

270. Rulina AV, Mittler F, Obeid P, et al. Distinct outcomes of CRL-Nedd8 pathway inhibition reveal cancer cell plasticity. Cell Death Dis. 2016 Dec 1;7(12):e2505. doi: 10.1038/cddis.2016.395. PubMed PMID: 27906189; PubMed Central PMCID: PMCPMC5261022.

271. Conery AR, Harlow E. High-throughput screens in diploid cells identify factors that contribute to the acquisition of chromosomal instability. Proc Natl Acad Sci U S A. 2010 Aug 31;107(35):15455-60. doi: 10.1073/pnas.1010627107. PubMed PMID: 20713694; PubMed Central PMCID: PMCPMC2932617.

272. Freed E, Lacey KR, Huie P, et al. Components of an SCF ubiquitin ligase localize to the centrosome and regulate the centrosome duplication cycle. Genes Dev. 1999 Sep 1;13(17):2242-57. PubMed PMID: 10485847; PubMed Central PMCID: PMCPMC316987.

273. Guse A, Mishima M, Glotzer M. Phosphorylation of ZEN-4/MKLP1 by aurora B regulates completion of cytokinesis. Curr Biol. 2005 Apr 26;15(8):778-86. doi: 10.1016/j.cub.2005.03.041. PubMed PMID: 15854913.

274. Isakson P, Lystad AH, Breen K, et al. TRAF6 mediates ubiquitination of KIF23/MKLP1 and is required for midbody ring degradation by selective autophagy. Autophagy. 2013 Dec;9(12):1955-64. PubMed PMID: 24128730.

275. Zheng CY, Petralia RS, Wang YX, et al. Fluorescence recovery after photobleaching (FRAP) of fluorescence tagged proteins in dendritic spines of cultured hippocampal neurons. J Vis Exp. 2011 Apr 16(50). doi: 10.3791/2568. PubMed PMID: 21525845; PubMed Central PMCID: PMCPMC3339873.

276. Baranes-Bachar K, Levy-Barda A, Oehler J, et al. The Ubiquitin E3/E4 Ligase UBE4A Adjusts Protein Ubiquitylation and Accumulation at Sites of DNA Damage, Facilitating Double-Strand Break Repair. Mol Cell. 2018 Mar 1;69(5):866-878 e7. doi: 10.1016/j.molcel.2018.02.002. PubMed PMID: 29499138.

277. Gomez-Cabello D, Jimeno S, Fernandez-Avila MJ, et al. New tools to study DNA double-strand break repair pathway choice. PLoS One. 2013;8(10):e77206. doi: 10.1371/journal.pone.0077206. PubMed PMID: 24155929; PubMed Central PMCID: PMCPMC3796453.

278. Cong L, Ran FA, Cox D, et al. Multiplex genome engineering using CRISPR/Cas systems. Science. 2013 Feb 15;339(6121):819-23. doi: 10.1126/science.1231143. PubMed PMID: 23287718; PubMed Central PMCID: PMCPMC3795411.

279. Mali P, Yang L, Esvelt KM, et al. RNA-guided human genome engineering via Cas9. Science. 2013 Feb 15;339(6121):823-6. doi: 10.1126/science.1232033. PubMed PMID: 23287722; PubMed Central PMCID: PMCPMC3712628.

280. Lam AJ, St-Pierre F, Gong Y, et al. Improving FRET dynamic range with bright green and red fluorescent proteins. Nat Methods. 2012 Oct;9(10):1005-12. doi: 10.1038/nmeth.2171. PubMed PMID: 22961245; PubMed Central PMCID: PMCPMC3461113.

281. Tong S, Si Y, Yu H, et al. MLN4924 (Pevonedistat), a protein neddylation inhibitor, suppresses proliferation and migration of human clear cell renal cell carcinoma. Sci Rep. 2017 Jul 17;7(1):5599. doi: 10.1038/s41598-017-06098-y. PubMed PMID: 28717191; PubMed Central PMCID: PMCPMC5514088.

282. Luo Z, Yu G, Lee HW, et al. The Nedd8-activating enzyme inhibitor MLN4924 induces autophagy and apoptosis to suppress liver cancer cell growth. Cancer Res. 2012 Jul 1;72(13):3360-71. doi: 10.1158/0008-5472.CAN-12-0388. PubMed PMID: 22562464.

283. Zhang Y, Shi CC, Zhang HP, et al. MLN4924 suppresses neddylation and induces cell cycle arrest, senescence, and apoptosis in human osteosarcoma. Oncotarget. 2016 Jul 19;7(29):45263-45274. doi: 10.18632/oncotarget.9481. PubMed PMID: 27223074; PubMed Central PMCID: PMCPMC5216721.

284. Ruchaud S, Carmena M, Earnshaw WC. Chromosomal passengers: conducting cell division. Nat Rev Mol Cell Biol. 2007 Oct;8(10):798-812. doi: 10.1038/nrm2257. PubMed PMID: 17848966.

285. Pintard L, Kurz T, Glaser S, et al. Neddylation and deneddylation of CUL-3 is required to target MEI-1/Katanin for degradation at the meiosis-to-mitosis transition in C. elegans. Curr Biol. 2003 May 27;13(11):911-21. PubMed PMID: 12781129.

286. Cummings CM, Bentley CA, Perdue SA, et al. The Cul3/Klhdc5 E3 ligase regulates p60/katanin and is required for normal mitosis in mammalian cells. J Biol Chem. 2009 Apr 24;284(17):11663-75. doi: 10.1074/jbc.M809374200. PubMed PMID: 19261606; PubMed Central PMCID: PMCPMC2670170.

287. Pohl C, Jentsch S. Final stages of cytokinesis and midbody ring formation are controlled by BRUCE. Cell. 2008 Mar 7;132(5):832-45. doi: 10.1016/j.cell.2008.01.012. PubMed PMID: 18329369.

288. Peth A, Boettcher JP, Dubiel W. Ubiquitin-dependent proteolysis of the microtubule end-binding protein 1, EB1, is controlled by the COP9 signalosome: possible consequences for microtubule filament stability. J Mol Biol. 2007 Apr 27;368(2):550-63. doi: 10.1016/j.jmb.2007.02.052. PubMed PMID: 17350042.

289. Wang G, Jiang Q, Zhang C. The role of mitotic kinases in coupling the centrosome cycle with the assembly of the mitotic spindle. J Cell Sci. 2014 Oct 1;127(Pt 19):4111-22. doi: 10.1242/jcs.151753. PubMed PMID: 25128564.

290. Popescu NC, DiPaolo JA, Amsbaugh SC. Integration sites of human papillomavirus 18 DNA sequences on HeLa cell chromosomes. Cytogenet Cell Genet. 1987;44(1):58-62. doi: 10.1159/000132342. PubMed PMID: 3028716.

291. Horner SM, DeFilippis RA, Manuelidis L, et al. Repression of the human papillomavirus E6 gene initiates p53-dependent, telomerase-independent senescence and apoptosis in HeLa cervical carcinoma cells. J Virol. 2004 Apr;78(8):4063-73. PubMed PMID: 15047823; PubMed Central PMCID: PMCPMC374296.

292. Pietenpol JA, Stewart ZA. Cell cycle checkpoint signaling: cell cycle arrest versus apoptosis. Toxicology. 2002 Dec 27;181-182:475-81. PubMed PMID: 12505356.

293. Fujiwara T, Bandi M, Nitta M, et al. Cytokinesis failure generating tetraploids promotes tumorigenesis in p53-null cells. Nature. 2005 Oct 13;437(7061):1043-7. doi: 10.1038/nature04217. PubMed PMID: 16222300.

294. Stukenberg PT. Triggering p53 after cytokinesis failure. J Cell Biol. 2004 Jun 7;165(5):607-8. doi: 10.1083/jcb.200405089. PubMed PMID: 15184396; PubMed Central PMCID: PMCPMC2172375.

295. Bodnar AG, Ouellette M, Frolkis M, et al. Extension of life-span by introduction of telomerase into normal human cells. Science. 1998 Jan 16;279(5349):349-52. PubMed PMID: 9454332.

296. Scrima A, Fischer ES, Lingaraju GM, et al. Detecting UV-lesions in the genome: The modular CRL4 ubiquitin ligase does it best! FEBS Lett. 2011 Sep 16;585(18):2818-25. doi: 10.1016/j.febslet.2011.04.064. PubMed PMID: 21550341.

297. Rao F, Xu J, Khan AB, et al. Inositol hexakisphosphate kinase-1 mediates assembly/disassembly of the CRL4-signalosome complex to regulate DNA repair and cell death. Proc Natl Acad Sci U S A. 2014 Nov 11;111(45):16005-10. doi: 10.1073/pnas.1417900111. PubMed PMID: 25349427; PubMed Central PMCID: PMCPMC4234592.

298. Kim SJ, Kim DK, Kang DH. Using UVC Light-Emitting Diodes at Wavelengths of 266 to 279 Nanometers To Inactivate Foodborne Pathogens and Pasteurize Sliced Cheese. Appl Environ Microbiol. 2016 Jan 1;82(1):11-7. doi: 10.1128/AEM.02092-15. PubMed PMID: 26386061; PubMed Central PMCID: PMCPMC4702654.

299. Oberdoerffer P. Stop relaxing: How DNA damage-induced chromatin compaction may affect epigenetic integrity and disease. Mol Cell Oncol. 2015 Jan-Mar;2(1):e970952. doi: 10.4161/23723548.2014.970952. PubMed PMID: 27308388; PubMed Central PMCID: PMCPMC4905243.

300. Burgess RC, Burman B, Kruhlak MJ, et al. Activation of DNA damage response signaling by condensed chromatin. Cell Rep. 2014 Dec 11;9(5):1703-1717. doi: 10.1016/j.celrep.2014.10.060. PubMed PMID: 25464843; PubMed Central PMCID: PMCPMC4267891.

301. Bennardo N, Cheng A, Huang N, et al. Alternative-NHEJ is a mechanistically distinct pathway of mammalian chromosome break repair. PLoS Genet. 2008 Jun 27;4(6):e1000110. doi: 10.1371/journal.pgen.1000110. PubMed PMID: 18584027; PubMed Central PMCID: PMCPMC2430616.

302. Sakuma T, Nakade S, Sakane Y, et al. MMEJ-assisted gene knock-in using TALENs and CRISPR-Cas9 with the PITCh systems. Nat Protoc. 2016 Jan;11(1):118-33. doi: 10.1038/nprot.2015.140. PubMed PMID: 26678082.

303. Crow A, Hughes RK, Taieb F, et al. The molecular basis of ubiquitin-like protein NEDD8 deamidation by the bacterial effector protein Cif. Proc Natl Acad Sci U S A. 2012 Jul 3;109(27):E1830-8. doi: 10.1073/pnas.1112107109. PubMed PMID: 22691497; PubMed Central PMCID: PMCPMC3390873.

304. Cui J, Yao Q, Li S, et al. Glutamine deamidation and dysfunction of ubiquitin/NEDD8 induced by a bacterial effector family. Science. 2010 Sep 3;329(5996):1215-8. doi: 10.1126/science.1193844. PubMed PMID: 20688984; PubMed Central PMCID: PMCPMC3031172.

305. Yao Q, Cui J, Wang J, et al. Structural mechanism of ubiquitin and NEDD8 deamidation catalyzed by bacterial effectors that induce macrophage-specific apoptosis. Proc Natl Acad Sci U S A. 2012 Dec 11;109(50):20395-400. doi: 10.1073/pnas.1210831109. PubMed PMID: 23175788; PubMed Central PMCID: PMCPMC3528514.

306. Jubelin G, Taieb F, Duda DM, et al. Pathogenic bacteria target NEDD8-conjugated cullins to hijack host-cell signaling pathways. PLoS Pathog. 2010 Sep 30;6(9):e1001128. doi: 10.1371/journal.ppat.1001128. PubMed PMID: 20941356; PubMed Central PMCID: PMCPMC2947998.

307. Hanahan D, Weinberg RA. Hallmarks of cancer: the next generation. Cell. 2011 Mar 4;144(5):646-74. doi: 10.1016/j.cell.2011.02.013. PubMed PMID: 21376230.

308. Li H, Zhou W, Li L, et al. Inhibition of Neddylation Modification Sensitizes Pancreatic Cancer Cells to Gemcitabine. Neoplasia. 2017 Jun;19(6):509-518. doi: 10.1016/j.neo.2017.04.003. PubMed PMID: 28535453; PubMed Central PMCID: PMCPMC5440286.

309. Yu J, Huang WL, Xu QG, et al. Overactivated neddylation pathway in human hepatocellular carcinoma. Cancer Med. 2018 May 30. doi: 10.1002/cam4.1578. PubMed PMID: 29846044; PubMed Central PMCID: PMCPMC6051160.

310. Kouvaraki MA, Rassidakis GZ, Tian L, et al. Jun activation domain-binding protein 1 expression in breast cancer inversely correlates with the cell cycle inhibitor p27(Kip1). Cancer Res. 2003 Jun 1;63(11):2977-81. PubMed PMID: 12782606.

311. Rassidakis GZ, Claret FX, Lai R, et al. Expression of p27(Kip1) and c-Jun activation binding protein 1 are inversely correlated in systemic anaplastic large cell lymphoma. Clin Cancer Res. 2003 Mar;9(3):1121-8. PubMed PMID: 12631617.

312. Wang W, Tang M, Zhang L, et al. Clinical implications of CSN6 protein expression and correlation with mutant-type P53 protein in breast cancer. Jpn J Clin Oncol. 2013 Dec;43(12):1170-6. doi: 10.1093/jjco/hyt148. PubMed PMID: 24106298.

313. Hsu MC, Huang CC, Chang HC, et al. Overexpression of Jab1 in hepatocellular carcinoma and its inhibition by peroxisome proliferator-activated receptor{gamma} ligands in vitro and in vivo. Clin Cancer Res. 2008 Jul 1;14(13):4045-52. doi: 10.1158/1078-0432.CCR-07-5040. PubMed PMID: 18593980.

314. Guo H, Jing L, Cheng Y, et al. Down-regulation of the cyclin-dependent kinase inhibitor p57 is mediated by Jab1/Csn5 in hepatocarcinogenesis. Hepatology. 2016 Mar;63(3):898-913. doi: 10.1002/hep.28372. PubMed PMID: 26606000.

315. Soucy TA, Dick LR, Smith PG, et al. The NEDD8 Conjugation Pathway and Its Relevance in Cancer Biology and Therapy. Genes Cancer. 2010 Jul;1(7):708-16. doi: 10.1177/1947601910382898. PubMed PMID: 21779466; PubMed Central PMCID: PMCPMC3092238.

316. Rao CV, Kurkjian CD, Yamada HY. Mitosis-targeting natural products for cancer prevention and therapy. Curr Drug Targets. 2012 Dec;13(14):1820-30. PubMed PMID: 23140292.

317. Huang F, Goyal N, Sullivan K, et al. Targeting BRCA1- and BRCA2-deficient cells with RAD52 small molecule inhibitors. Nucleic Acids Res. 2016 May 19;44(9):4189-99. doi: 10.1093/nar/gkw087. PubMed PMID: 26873923; PubMed Central PMCID: PMCPMC4872086.

318. Sullivan K, Cramer-Morales K, McElroy DL, et al. Identification of a Small Molecule Inhibitor of RAD52 by Structure-Based Selection. PLoS One. 2016;11(1):e0147230. doi: 10.1371/journal.pone.0147230. PubMed PMID: 26784987; PubMed Central PMCID: PMCPMC4718542.

319. Lockhart AC, Bauer TM, Aggarwal C, et al. Phase Ib study of pevonedistat, a NEDD8-activating enzyme inhibitor, in combination with docetaxel, carboplatin and paclitaxel, or gemcitabine, in patients with advanced solid tumors. Invest New Drugs. 2018 May 21. doi: 10.1007/s10637-018-0610-0. PubMed PMID: 29781056.

320. Dohmesen C, Koeppel M, Dobbelstein M. Specific inhibition of Mdm2-mediated neddylation by Tip60. Cell Cycle. 2008 Jan 15;7(2):222-31. doi: 10.4161/cc.7.2.5185. PubMed PMID: 18264029.

321. Singh RK, Iyappan S, Scheffner M. Hetero-oligomerization with MdmX rescues the ubiquitin/Nedd8 ligase activity of RING finger mutants of Mdm2. J Biol Chem. 2007 Apr 13;282(15):10901-7. doi: 10.1074/jbc.M610879200. PubMed PMID: 17301054.

322. Liu G, Xirodimas DP. NUB1 promotes cytoplasmic localization of p53 through cooperation of the NEDD8 and ubiquitin pathways. Oncogene. 2010 Apr 15;29(15):2252-61. doi: 10.1038/onc.2009.494. PubMed PMID: 20101219.

323. Leidecker O, Matic I, Mahata B, et al. The ubiquitin E1 enzyme Ube1 mediates NEDD8 activation under diverse stress conditions. Cell Cycle. 2012 Mar 15;11(6):1142-50. doi: 10.4161/cc.11.6.19559. PubMed PMID: 22370482.

324. Watson IR, Blanch A, Lin DC, et al. Mdm2-mediated NEDD8 modification of TAp73 regulates its transactivation function. J Biol Chem. 2006 Nov 10;281(45):34096-103. doi: 10.1074/jbc.M603654200. PubMed PMID: 16980297.

325. Watson IR, Li BK, Roche O, et al. Chemotherapy induces NEDP1-mediated destabilization of MDM2. Oncogene. 2010 Jan 14;29(2):297-304. doi: 10.1038/onc.2009.314. PubMed PMID: 19784069.

326. Loftus SJ, Liu G, Carr SM, et al. NEDDylation regulates E2F-1-dependent transcription. EMBO Rep. 2012 Sep;13(9):811-8. doi: 10.1038/embor.2012.113. PubMed PMID: 22836579; PubMed Central PMCID: PMCPMC3432805.

327. Aoki I, Higuchi M, Gotoh Y. NEDDylation controls the target specificity of E2F1 and apoptosis induction. Oncogene. 2013 Aug 22;32(34):3954-64. doi: 10.1038/onc.2012.428. PubMed PMID: 23001041.

328. Gao F, Cheng J, Shi T, et al. Neddylation of a breast cancer-associated protein recruits a class III histone deacetylase that represses NFkappaB-dependent transcription. Nat Cell Biol. 2006 Oct;8(10):1171-7. doi: 10.1038/ncb1483. PubMed PMID: 16998474.

329. Takashima O, Tsuruta F, Kigoshi Y, et al. Brap2 regulates temporal control of NF-kappaB localization mediated by inflammatory response. PLoS One. 2013;8(3):e58911. doi: 10.1371/journal.pone.0058911. PubMed PMID: 23554956; PubMed Central PMCID: PMCPMC3598860.

330. Ryu JH, Li SH, Park HS, et al. Hypoxia-inducible factor alpha subunit stabilization by NEDD8 conjugation is reactive oxygen species-dependent. J Biol Chem. 2011 Mar 4;286(9):6963-70. doi: 10.1074/jbc.M110.188706. PubMed PMID: 21193393; PubMed Central PMCID: PMCPMC3044952.

331. Stickle NH, Chung J, Klco JM, et al. pVHL modification by NEDD8 is required for fibronectin matrix assembly and suppression of tumor development. Mol Cell Biol. 2004 Apr;24(8):3251-61. PubMed PMID: 15060148; PubMed Central PMCID: PMCPMC381603.

332. Russell RC, Ohh M. NEDD8 acts as a 'molecular switch' defining the functional selectivity of VHL. EMBO Rep. 2008 May;9(5):486-91. doi: 10.1038/embor.2008.19. PubMed PMID: 18323857; PubMed Central PMCID: PMCPMC2373363.

333. Lee MR, Lee D, Shin SK, et al. Inhibition of APP intracellular domain (AICD) transcriptional activity via covalent conjugation with Nedd8. Biochem Biophys Res Commun. 2008 Feb 22;366(4):976-81. doi: 10.1016/j.bbrc.2007.12.066. PubMed PMID: 18096514.

334. Choo YS, Vogler G, Wang D, et al. Regulation of parkin and PINK1 by neddylation. Hum Mol Genet. 2012 Jun 1;21(11):2514-23. doi: 10.1093/hmg/dds070. PubMed PMID: 22388932; PubMed Central PMCID: PMCPMC3349425.

335. Um JW, Han KA, Im E, et al. Neddylation positively regulates the ubiquitin E3 ligase activity of parkin. J Neurosci Res. 2012 May;90(5):1030-42. doi: 10.1002/jnr.22828. PubMed PMID: 22271254.

336. Broemer M, Tenev T, Rigbolt KT, et al. Systematic in vivo RNAi analysis identifies IAPs as NEDD8-E3 ligases. Mol Cell. 2010 Dec 10;40(5):810-22. doi: 10.1016/j.molcel.2010.11.011. PubMed PMID: 21145488.

337. Sun XX, Wang YG, Xirodimas DP, et al. Perturbation of 60 S ribosomal biogenesis results in ribosomal protein L5- and L11-dependent p53 activation. J Biol Chem. 2010 Aug 13;285(33):25812-21. doi: 10.1074/jbc.M109.098442. PubMed PMID: 20554519; PubMed Central PMCID: PMCPMC2919143.

338. Sundqvist A, Liu G, Mirsaliotis A, et al. Regulation of nucleolar signalling to p53 through NEDDylation of L11. EMBO Rep. 2009 Oct;10(10):1132-9. doi: 10.1038/embor.2009.178. PubMed PMID: 19713960; PubMed Central PMCID: PMCPMC2759733.

339. Zhang J, Bai D, Ma X, et al. hCINAP is a novel regulator of ribosomal protein-HDM2-p53 pathway by controlling NEDDylation of ribosomal protein S14. Oncogene. 2014 Jan 9;33(2):246-54. doi: 10.1038/onc.2012.560. PubMed PMID: 23246961.

340. Embade N, Fernandez-Ramos D, Varela-Rey M, et al. Murine double minute 2 regulates Hu antigen R stability in human liver and colon cancer through NEDDylation. Hepatology. 2012 Apr;55(4):1237-48. doi: 10.1002/hep.24795. PubMed PMID: 22095636; PubMed Central PMCID: PMCPMC3298572.

341. Noh EH, Hwang HS, Hwang HS, et al. Covalent NEDD8 conjugation increases RCAN1 protein stability and potentiates its inhibitory action on calcineurin. PLoS One. 2012;7(10):e48315. doi: 10.1371/journal.pone.0048315. PubMed PMID: 23118980; PubMed Central PMCID: PMCPMC3485183.

APPENDIX I

Table A1. Table of Reported Neddylation Substrates

Target Protein	Biological Function of Target	Effect of Neddylation	E2	E3	Regulation of Neddylation	Neddylated Lysines	Reference
Cullins (CUL1, CUL2, CUL3, CUL4A, CUL4B, CUL5)	RING ubiquitin E3 ligases	Activation of ubiquitin transfer activity	UBC12, UBE2F	RBX1/ RBX2	Promoted by DCUNs, Tfb3 (budding yeast) and ubiquitylation substrates; reversed by CSN	Human CUL1: Lys720 Human CUL2: Lys689 Human CUL3: Lys712 Human CUL4A: Lys705 Human CUL4B: Lys859 Human CUL5: Lys724	[107]
SMURF1	HECT Ubiquitin E3 ligase	Activation of ubiquitin transfer activity	UBC12	SMURF1	Not known	Lys324, Lys495, Lys545, Lys558, Lys559, Lys667 (mass spectrometry)	[39]
TGFβRII	TGF-β signal transduction, inhibition of proliferation	TGFβRII stabilisation, promotes antiproliferative effect of TGF-β	UBC12	c-CBL	c-CBL-mediated neddylation depends on TGFβRII activity; reversed by DEN1	Lys556, Lys557 (mass spectrometry and mutagenesis)	[35]

Target Protein	Biological Function of Target	Effect of Neddylation	E2	E3	Regulation of Neddylation	Neddylated Lysines	Reference
EGFR	Growth factor signal transduction	Enhanced ubiquitylation and subsequent proteasomal degradation	Not known	CBLs (c-CBL, CBL-b, CBL-3)	Stimulated by EGF	Multiple lysines in the tyrosine kinase domain (mutagenesis)	[36]
TP53	Transcription factor	Inhibition of transcription activity, cytoplasmic localisation	Not known	MDM2, MDMX, SCF^{FBXO11}	Reversed by DEN1, inhibited by TIP60, NUB1 decreases TPP53 neddylation	Lys370, Lys372, Lys373 (mutagenesis)	[34, 228, 320, 321, 322, 323]
TP73	Transcription factor	Inhibition of transcription activity, cytoplasmic localisation	Not known	MDM2	Reversed by DEN1	Not known	[324]
MDM2	RING E3 ligase	Stabilisation	Not known	MDM2 (auto-neddylation)	Reversed by DEN1; inhibited by TP60	Not known	[34, 325]

Target Protein	Biological Function of Target	Effect of Neddylation	E2	E3	Regulation of Neddylation	Neddylated Lysines	Reference
E2F (E2F-1, -2,-3, -4 and DP1)	Transcription factor, regulating the G1/S phase cell cycle transition	Down-regulation of transcriptional activity; destabilization	UBC12/ UBE2F	Not known	Reversed by DEN1. SET7/9-mediated methylation promotes neddylation	Mainly Lys residues in the DNA-binding domain (Lys117, Lys120, Lys125, Lys182, Lys183 and Lys 185) (mutagenesis)	[326, 327]
IKKγ (NEMO)	Regulatory subunit of the IKK complex	Inhibition of NF-κB signalling	Not known	TRIM40	Neddylation is higher in normal gastric epithelium than in gastric cancer tissue	Not known	[38]
BCA3 (also known as AKIP1)	Regulator of NF-κB transcription	Inhibition of NF-κB signalling	Not known	Not known	Reversed by DEN1; inhibited by estrogen	All 11 Lys residues (identified by mutagenesis)	[328]
BRAP2	RING E3 regulating the Ras-MAPK pathway; associated with inflammatory dysfunction; suppressor of NF-κB signalling	No effect for inhibition of NF-κB	Not known	Not known	Not known	Lys432 (identified by mutagenesis)	[329]

pTarget protein	Biological Function of Target	Effect of Neddylation	E2	E3	Regulation of Neddylation	Neddylated Lysines	Reference
HIF1α/HIF22α	HIF transcription factor component; survival signaling under hypoxia	Protein stabilisation in both normoxia and hypoxia	Not known	Not known	Not known	PAS-B domain (truncation)	[330]
VHL	CRL2 E3 ligase substrate receptor; regulates HIF1α degradation; positive regulator of fibronectin-mediated extracellular matrix assembly	Prevents CUL2 and fibronectin binding	Not known	Not known	Not known	Lys159, Lys 171, and Lys196. (identified by mutagenesis)	[331, 332]
AICD (APP intracellular domain)	Transcription factor component	Inhibits transcription activity	Not known	Not known	Not known	Lys612 Lys624 Lys649-651 Lys676 Lys688	[333]
Parkin	E3 ubiquitin ligase component; regulator of mitophagy	Increased E3 ligase activity	Not known	Not known	Reversed by DEN1	Lys76 by mass spectrometry in Parkinson's Disease patients; all lysine residues by mutagenesis	[334, 335]

Target Protein	Biological Function of Target	Effect of Neddylation	E2	E3	Regulation of Neddylation	Neddylated Lysines	Reference
PINK1	Protein kinase, activates parkin	Protein stabilization	Possibly UBC12	Not known	Triggered by DNA damage	Not known, possibly multiple residues	[334]
Histone H4	Core nucleosome component; regulates chromatin state and DNA repair	Polyneddylation promotes RNF168 recruitment and facilitates DNA repair	UBC12	RNF111	Reversed by DEN1	N-terminal lysine residues	[26]
drICE	*D. melanogaster* homolog of caspase 7; apoptosis signaling	Inhibits caspase activity	Not known	*Drosophila* IAP1	Reversed by DEN1	All surface lysine residues (identified by mutagenesis)	[336]
RPL11	Ribosomal protein	Protein stabilisation and nucleolar localisation; unneddylated RPL11 binds to MDM2 and activates p53	Not known	MDM2	Reversed by DEN1	All lysine residues (identified by mutagenesis)	[229, 230, 337, 338]

Target Protein	Biological Function of Target	Effect of Neddylation	E2	E3	Regulation of Neddylation	Neddylated Lysines	Reference
RPS14	Ribosomal protein	Protein stabilisation and nucleolar localisation; unneddylated RPL11 binds to MDM2 and activates p53	Not known	MDM2	Reversed by DEN1	Not known	[339]
HuR	mRNA stabilisation; cell differentiation, proliferation	HuR stabilisation; nuclear localisation	Not known	MDM2	Reversed by DEN1	Lys283, Lys313, and Lys326	[340]
RCAN1	Inhibitor of calcineurin signaling	Enhanced stability; increased binding to calcineurin	Not known	Not known	Neddylation observed in mouse embryonic brain but not adult; oxidative stress reduces neddylation	Lys96, Lys104, and Lys170 (identified by mutagenesis)	[341]

Target Protein	Biological Function of Target	Effect of Neddylation	E2	E3	Regulation of Neddylation	Neddylated Lysines	Reference
Ataxin-3	Not known	Not known	Not known	Not known	Nor known	Not known	[45]

APPENDIX II

Table A2.1. Table of PCR primers used to amplify CSN subunit cDNA.

Gene	Sequence
COPS1	F-GGTGCAGAAAGTCAGGACAGA R-CTGCTCTTTAATGGACACCGC
COPS2	F-AAGAAGCTGAGAGTGACGCC R-CTCTCTGGTCATGTTGCCCA
COPS3	F-GGGGAAAACATGGCGTCTG R-CACAGGCTTGGTCCTCTCTG
COPS4	F1-CTGGAGGACCACACTCGTTTTC R1-GCCTCTAGTCTTTCACTTTCGTGG F2-CCACGAAAGTGAAAGACTAGAGGC R2-CACATTTGGAGAGGCATGAAG Perform overlap PCR and amplify using the F1 and R2 primers
COPS5	F-GACGACAACTTCTCCGCTTC R-TTTAGGACACTTCAGAGCACCTT
COPS7A	F-AATTTGCGTCCTTAGAGCGGA R-GGGAGGAAACGACAGTCCTTT
COPS7B	F-ATCATGGACGCTTGACAACCT R-CCTGTTTTGGGATGGCATTGG
COPS8	F-GAGGGACAGTCTGGGGTTTG R-ACTGACAGGCTCCATCCAGA

Table A2.2. Table of PCR primers used to generate 2xNLS (Nuclear Localization sequence).

Primer	Sequence
F1	agaaacgcaaagtgggcacacgaggccgtaaggtcgatctcacctcctg
F2	gcccaagaaaaagcggaaagtgggcacacgtggccccaaaaagaaacgcaaagtgggcac
F3	atcc accggtcgccaccatggcgcccaagaaaaagcggaaagtgg
R	gctttggatcggaggactgc

The 2xSV40-NLS sequence was constructed in three sequential amplification reactions using the next numbered forward primer (in increasing order) and the same reverse primer. The sequence was then inserted into piRFP670-N1 between AgeI and PvuI restriction sites.

Table A2.3. Number of Plated Cells and Media Volume used for Lipofectamine™ 2000 Lipofection.

Cell Line	Vessel Size	# of Cells Plated	Amount of growth media
HeLa	35 mm	$1x10^5$	2 mL
	100 mm	6×10^5	10 mL
U-2 OS	35 mm	$1x10^5$	2 mL
	100 mm	6×10^5	10 mL

Table A2.4. Amount of DNA used for Lipofectamine™ 2000 Lipofection.

Vessel Size	Amount of DNA	Amount of Lipofectamine 2000	Final volume of transfection mix	Amount of growth media
35mm	0.75 μg	1.5 μL	400 μL	1.2 mL
100mm	3.75 μg	7 μL	1000 μL	5 mL

APPENDIX III

Figure A3.1. Cell cycle analysis using propidium iodide on DMSO and MLN4924-treated asynchronous HeLa populations. Representative dot plots and histograms for each treatment as indicated on the left column. Debris and aggregate cells were gated out on the forward scatter (FSC)-height vs FSC-area dot plot (Column 1) and the gated cells were used to generate the propidium iodide (PI)-area vs PI-width dot plot (Column 2). Doublets were gated out of the PI-area vs PI-width plot. Single cells contained in the gate were then displayed on the propidium iodide histogram (Column 3). Gates were manually applied to identify G1, S, G2, and >4N DNA populations.

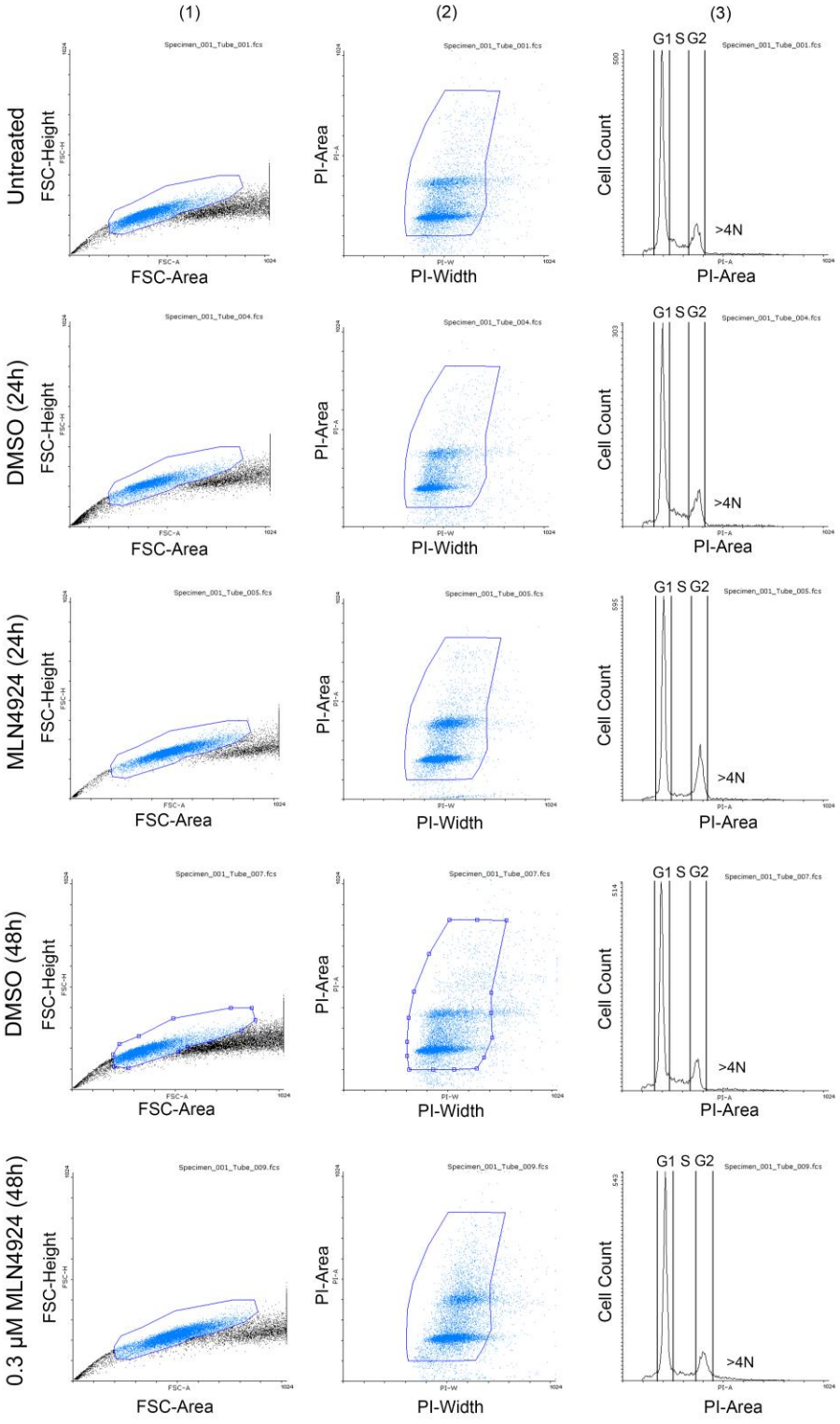
(1)
(2)
(3)
Untreated
DMSO (24h)
MLN4924 (24h)
DMSO (48h)
0.3 µM MLN4924 (48h)
FSC-Height
FSC-Area
PI-Area
PI-Width
Cell Count
G1 S G2
>4N

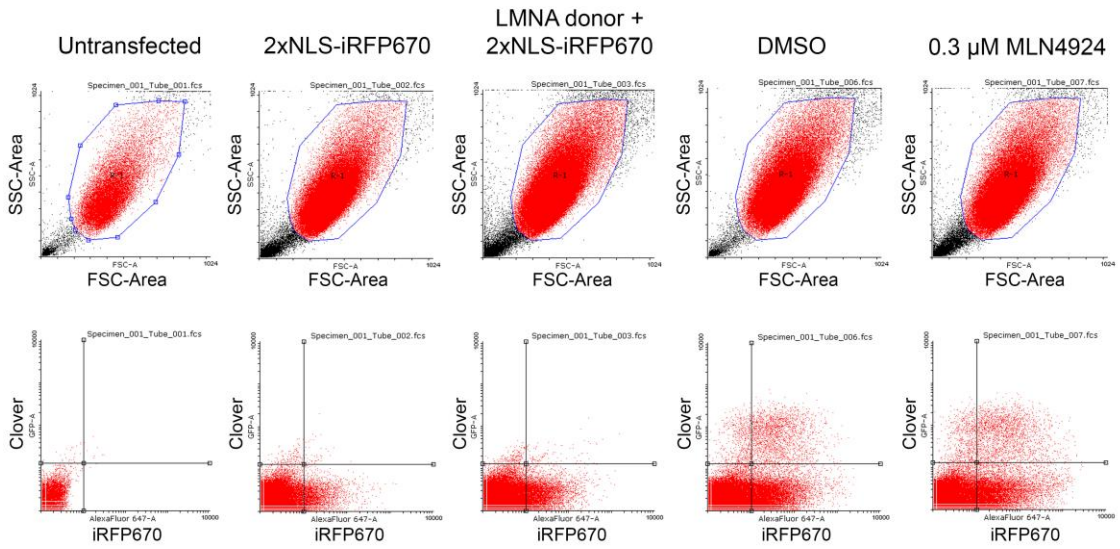

Figure A3.2. Clover-LMNA CRISPR/Cas9 homology-directed repair assay by flow cytometry. Representative dot plots for each transfection and treatment as indicated on the top row. Debris was gated out on the side scatter (SSC)-area vs forward scatter (FSC)-area dot plot and the viable cells were plotted on the Clover vs iRFP670 dot plot. Quadrants were drawn to separate populations that were clover-/iRFP70- (lower left), clover-/iRFP670+ (lower right), clover+/iRFP670- (upper left), and clover+/iRFP670+ (upper right).

APPENDIX IV

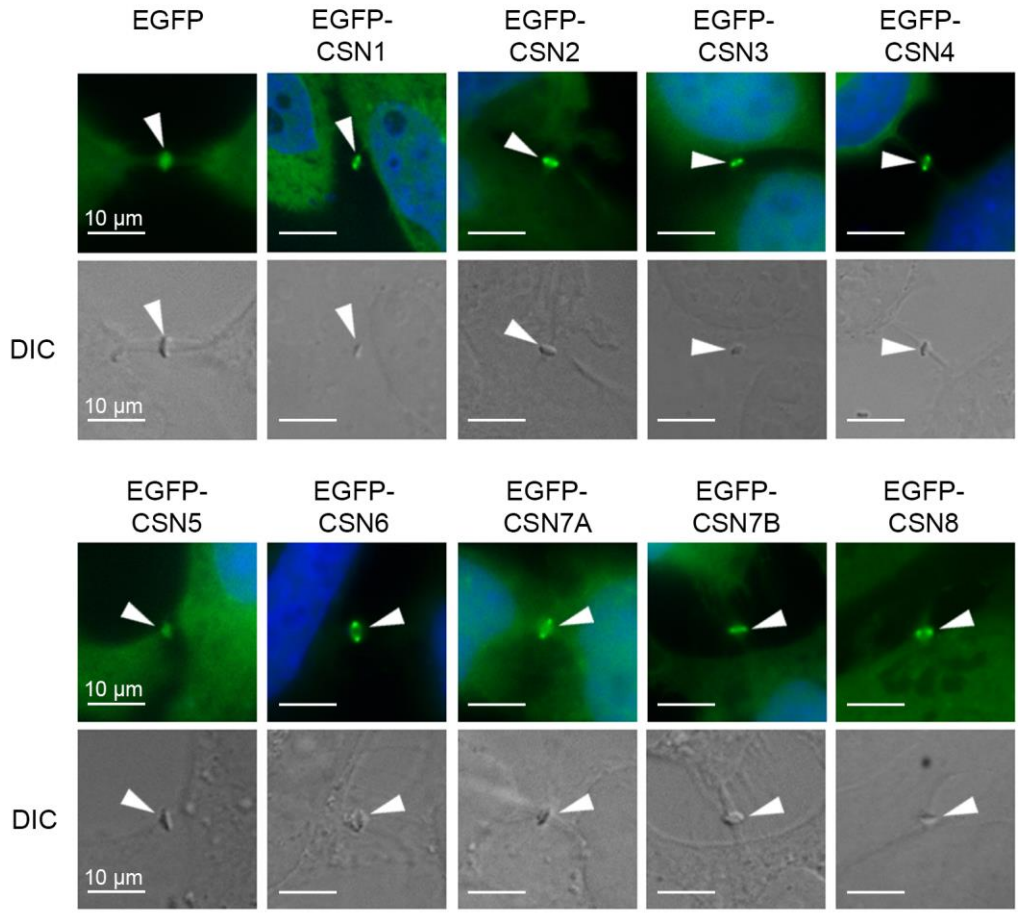

Figure A4. Localization of CSN subunits at the midbody during cytokinesis. Representative fluorescence microscopy images of EGFP and EGFP-tagged human CSN subunits localizing at the midbody in untreated HeLa cells. Midbodies are identified using differential interference contrast (DIC) (indicated by white arrowheads).

APPENDIX V – COPYRIGHT AGREEMENTS

ELSEVIER LICENSE
TERMS AND CONDITIONS

Oct 26, 2018

This Agreement between Mr. Dudley Chung ("You") and Elsevier ("Elsevier") consists of your license details and the terms and conditions provided by Elsevier and Copyright Clearance Center.

License Number	4456681335486
License date	Oct 26, 2018
Licensed Content Publisher	Elsevier
Licensed Content Publication	Molecular Cell
Licensed Content Title	The Ubiquitin E3/E4 Ligase UBE4A Adjusts Protein Ubiquitylation and Accumulation at Sites of DNA Damage, Facilitating Double-Strand Break Repair
Licensed Content Author	Keren Baranes-Bachar,Adva Levy-Barda,Judith Oehler,Dylan A. Reid,Isabel Soria-Bretones,Ty C. Voss,Dudley Chung,Yoon Park,Chao Liu,Jong-Bok Yoon,Wei Li,Graham Dellaire,Tom Misteli,Pablo Huertas,Eli Rothenberg,Kristijan Ramadan,Yael Ziv,Yosef Shiloh
Licensed Content Date	Mar 1, 2018
Licensed Content Volume	69
Licensed Content Issue	5
Licensed Content Pages	20
Start Page	866
End Page	878.e7
Type of Use	reuse in a thesis/dissertation
Portion	figures/tables/illustrations
Number of figures/tables/illustrations	1
Format	both print and electronic
Are you the author of this Elsevier article?	No
Will you be translating?	No
Original figure numbers	Figure 7B
Title of your thesis/dissertation	Evaluating the Role of the COP9 Signalosome and Neddylation during Cytokinesis and in Response to DNA Damage
Expected completion date	Dec 2018
Estimated size (number of pages)	150
Requestor Location	Mr. Dudley Chung Room 11K, Department of Pathology 5850 College Street

	Halifax, NS B3H1X5 Canada Attn: Mr. Dudley Chung
Publisher Tax ID	GB 494 6272 12
Total	0.00 CAD
Terms and Conditions	

INTRODUCTION

1. The publisher for this copyrighted material is Elsevier. By clicking "accept" in connection with completing this licensing transaction, you agree that the following terms and conditions apply to this transaction (along with the Billing and Payment terms and conditions established by Copyright Clearance Center, Inc. ("CCC"), at the time that you opened your Rightslink account and that are available at any time at http://myaccount.copyright.com).

GENERAL TERMS

2. Elsevier hereby grants you permission to reproduce the aforementioned material subject to the terms and conditions indicated.

3. Acknowledgement: If any part of the material to be used (for example, figures) has appeared in our publication with credit or acknowledgement to another source, permission must also be sought from that source. If such permission is not obtained then that material may not be included in your publication/copies. Suitable acknowledgement to the source must be made, either as a footnote or in a reference list at the end of your publication, as follows:

"Reprinted from Publication title, Vol /edition number, Author(s), Title of article / title of chapter, Pages No., Copyright (Year), with permission from Elsevier [OR APPLICABLE SOCIETY COPYRIGHT OWNER]." Also Lancet special credit - "Reprinted from The Lancet, Vol. number, Author(s), Title of article, Pages No., Copyright (Year), with permission from Elsevier."

4. Reproduction of this material is confined to the purpose and/or media for which permission is hereby given.

5. Altering/Modifying Material: Not Permitted. However figures and illustrations may be altered/adapted minimally to serve your work. Any other abbreviations, additions, deletions and/or any other alterations shall be made only with prior written authorization of Elsevier Ltd. (Please contact Elsevier at permissions@elsevier.com). No modifications can be made to any Lancet figures/tables and they must be reproduced in full.

6. If the permission fee for the requested use of our material is waived in this instance, please be advised that your future requests for Elsevier materials may attract a fee.

7. Reservation of Rights: Publisher reserves all rights not specifically granted in the combination of (i) the license details provided by you and accepted in the course of this licensing transaction, (ii) these terms and conditions and (iii) CCC's Billing and Payment terms and conditions.

8. License Contingent Upon Payment: While you may exercise the rights licensed immediately upon issuance of the license at the end of the licensing process for the transaction, provided that you have disclosed complete and accurate details of your proposed use, no license is finally effective unless and until full payment is received from you (either by publisher or by CCC) as provided in CCC's Billing and Payment terms and conditions. If full payment is not received on a timely basis, then any license preliminarily granted shall be deemed automatically revoked and shall be void as if never granted. Further, in the event that you breach any of these terms and conditions or any of CCC's Billing and Payment

terms and conditions, the license is automatically revoked and shall be void as if never granted. Use of materials as described in a revoked license, as well as any use of the materials beyond the scope of an unrevoked license, may constitute copyright infringement and publisher reserves the right to take any and all action to protect its copyright in the materials.
9. Warranties: Publisher makes no representations or warranties with respect to the licensed material.
10. Indemnity: You hereby indemnify and agree to hold harmless publisher and CCC, and their respective officers, directors, employees and agents, from and against any and all claims arising out of your use of the licensed material other than as specifically authorized pursuant to this license.
11. No Transfer of License: This license is personal to you and may not be sublicensed, assigned, or transferred by you to any other person without publisher's written permission.
12. No Amendment Except in Writing: This license may not be amended except in a writing signed by both parties (or, in the case of publisher, by CCC on publisher's behalf).
13. Objection to Contrary Terms: Publisher hereby objects to any terms contained in any purchase order, acknowledgment, check endorsement or other writing prepared by you, which terms are inconsistent with these terms and conditions or CCC's Billing and Payment terms and conditions. These terms and conditions, together with CCC's Billing and Payment terms and conditions (which are incorporated herein), comprise the entire agreement between you and publisher (and CCC) concerning this licensing transaction. In the event of any conflict between your obligations established by these terms and conditions and those established by CCC's Billing and Payment terms and conditions, these terms and conditions shall control.
14. Revocation: Elsevier or Copyright Clearance Center may deny the permissions described in this License at their sole discretion, for any reason or no reason, with a full refund payable to you. Notice of such denial will be made using the contact information provided by you. Failure to receive such notice will not alter or invalidate the denial. In no event will Elsevier or Copyright Clearance Center be responsible or liable for any costs, expenses or damage incurred by you as a result of a denial of your permission request, other than a refund of the amount(s) paid by you to Elsevier and/or Copyright Clearance Center for denied permissions.

LIMITED LICENSE

The following terms and conditions apply only to specific license types:
15. **Translation**: This permission is granted for non-exclusive world **English** rights only unless your license was granted for translation rights. If you licensed translation rights you may only translate this content into the languages you requested. A professional translator must perform all translations and reproduce the content word for word preserving the integrity of the article.
16. **Posting licensed content on any Website**: The following terms and conditions apply as follows: Licensing material from an Elsevier journal: All content posted to the web site must maintain the copyright information line on the bottom of each image; A hyper-text must be included to the Homepage of the journal from which you are licensing at http://www.sciencedirect.com/science/journal/xxxxx or the Elsevier homepage for books at http://www.elsevier.com; Central Storage: This license does not include permission for a scanned version of the material to be stored in a central repository such as that provided by Heron/XanEdu.

Licensing material from an Elsevier book: A hyper-text link must be included to the Elsevier homepage at http://www.elsevier.com . All content posted to the web site must maintain the copyright information line on the bottom of each image.

Posting licensed content on Electronic reserve: In addition to the above the following clauses are applicable: The web site must be password-protected and made available only to bona fide students registered on a relevant course. This permission is granted for 1 year only. You may obtain a new license for future website posting.
17. **For journal authors:** the following clauses are applicable in addition to the above:
Preprints:
A preprint is an author's own write-up of research results and analysis, it has not been peer-reviewed, nor has it had any other value added to it by a publisher (such as formatting, copyright, technical enhancement etc.).
Authors can share their preprints anywhere at any time. Preprints should not be added to or enhanced in any way in order to appear more like, or to substitute for, the final versions of articles however authors can update their preprints on arXiv or RePEc with their Accepted Author Manuscript (see below).
If accepted for publication, we encourage authors to link from the preprint to their formal publication via its DOI. Millions of researchers have access to the formal publications on ScienceDirect, and so links will help users to find, access, cite and use the best available version. Please note that Cell Press, The Lancet and some society-owned have different preprint policies. Information on these policies is available on the journal homepage.
Accepted Author Manuscripts: An accepted author manuscript is the manuscript of an article that has been accepted for publication and which typically includes author-incorporated changes suggested during submission, peer review and editor-author communications.
Authors can share their accepted author manuscript:

- immediately
    - via their non-commercial person homepage or blog
    - by updating a preprint in arXiv or RePEc with the accepted manuscript
    - via their research institute or institutional repository for internal institutional uses or as part of an invitation-only research collaboration work-group
    - directly by providing copies to their students or to research collaborators for their personal use
    - for private scholarly sharing as part of an invitation-only work group on commercial sites with which Elsevier has an agreement
- After the embargo period
    - via non-commercial hosting platforms such as their institutional repository
    - via commercial sites with which Elsevier has an agreement

In all cases accepted manuscripts should:

- link to the formal publication via its DOI
- bear a CC-BY-NC-ND license - this is easy to do
- if aggregated with other manuscripts, for example in a repository or other site, be shared in alignment with our hosting policy not be added to or enhanced in any way to appear more like, or to substitute for, the published journal article.

Published journal article (JPA): A published journal article (PJA) is the definitive final record of published research that appears or will appear in the journal and embodies all value-adding publishing activities including peer review co-ordination, copy-editing, formatting, (if relevant) pagination and online enrichment.
Policies for sharing publishing journal articles differ for subscription and gold open access articles:
Subscription Articles: If you are an author, please share a link to your article rather than the full-text. Millions of researchers have access to the formal publications on ScienceDirect, and so links will help your users to find, access, cite, and use the best available version.
Theses and dissertations which contain embedded PJAs as part of the formal submission can be posted publicly by the awarding institution with DOI links back to the formal publications on ScienceDirect.
If you are affiliated with a library that subscribes to ScienceDirect you have additional private sharing rights for others' research accessed under that agreement. This includes use for classroom teaching and internal training at the institution (including use in course packs and courseware programs), and inclusion of the article for grant funding purposes.
Gold Open Access Articles: May be shared according to the author-selected end-user license and should contain a CrossMark logo, the end user license, and a DOI link to the formal publication on ScienceDirect.
Please refer to Elsevier's posting policy for further information.
18. **For book authors** the following clauses are applicable in addition to the above:
Authors are permitted to place a brief summary of their work online only. You are not allowed to download and post the published electronic version of your chapter, nor may you scan the printed edition to create an electronic version. **Posting to a repository:** Authors are permitted to post a summary of their chapter only in their institution's repository.
19. **Thesis/Dissertation**: If your license is for use in a thesis/dissertation your thesis may be submitted to your institution in either print or electronic form. Should your thesis be published commercially, please reapply for permission. These requirements include permission for the Library and Archives of Canada to supply single copies, on demand, of the complete thesis and include permission for Proquest/UMI to supply single copies, on demand, of the complete thesis. Should your thesis be published commercially, please reapply for permission. Theses and dissertations which contain embedded PJAs as part of the formal submission can be posted publicly by the awarding institution with DOI links back to the formal publications on ScienceDirect.

Elsevier Open Access Terms and Conditions
You can publish open access with Elsevier in hundreds of open access journals or in nearly 2000 established subscription journals that support open access publishing. Permitted third party re-use of these open access articles is defined by the author's choice of Creative Commons user license. See our open access license policy for more information.
Terms & Conditions applicable to all Open Access articles published with Elsevier:
Any reuse of the article must not represent the author as endorsing the adaptation of the article nor should the article be modified in such a way as to damage the author's honour or reputation. If any changes have been made, such changes must be clearly indicated.
The author(s) must be appropriately credited and we ask that you include the end user license and a DOI link to the formal publication on ScienceDirect.
If any part of the material to be used (for example, figures) has appeared in our publication with credit or acknowledgement to another source it is the responsibility of the user to ensure their reuse complies with the terms and conditions determined by the rights holder.